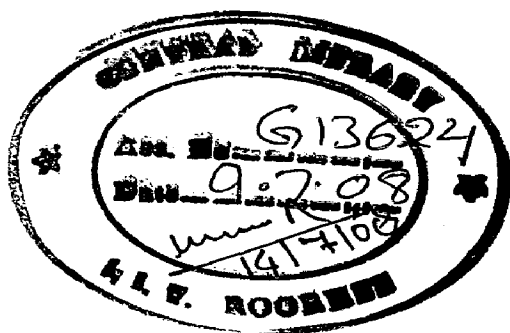# ORGANOSILICON DERIVATIVES OF OXYGEN AND NITROGEN DONOR LIGANDS

A DISSERTATION

Submitted in partial fulfillment of the
requirements for the award of the degree
of
MASTER OF TECHNOLOGY
in
ADVANCED CHEMICAL ANALYSIS

By

SANJAY KUMAR MAURYA

DEPARTMENT OF CHEMISTRY
INDIAN INSTITUTE OF TECHNOLOGY ROORKEE
ROORKEE - 247 667 (INDIA)
JUNE, 2007

CERTIFICATE

I hereby certify that the work entitled "**ORGANOSILICON DERIVATIVES OF OXYGEN AND NITROGEN DONOR LIGANDS**", has been carried out by Sanjay Kumar Maurya, in the department of Chemistry, Indian Institute of Technology Roorkee, India, under my supervision during August-2006 to June-2007. To the best of my knowledge the same has not been submitted elsewhere for the award of degree.

SANJAY KUMAR MAURYA

M.Tech. Final yr.

Department of Chemistry

IIT Roorkee, India

Prof. (Mrs.) MALA NATH

Professor

Department of Chemistry

IIT Roorkee, India

CANDIDATE'S DECLARATION

I hereby declare that the work which is being presented in the project entitled "ORGANOSILICON DERIVATIVES OF OXYGEN AND NITROGEN DONOR LIGANDS", in partial fulfillment of the requirement for the award of the degree of "MASTER OF TECHNOLOGY" submitted in the Department of Chemistry, Indian Institute of Technology Roorkee, is an authentic record of my own work carried out during the period from August-2006 to June- 2007 under the supervision and guidance of **Prof. (Mrs) MALA NATH**, Professor, Department of Chemistry, Indian Institute of Technology Roorkee, Roorkee.

The matter embodied in this project work has not been submitted for the award of any other degree.

Prof. (Mrs) MALA NATH

Professor

Department of Chemistry

I.I.T Roorkee, Roorkee

Date:...29.:6:07

SANJAY KUMAR MAURYA

Candidate's Signature

Date: 29|06| 2007

ACKNOWLEDGEMENT

ABSTRACT

Reactions of chlorotrimethylsilane with long chain fatty acids in 1:1 molar ratio led to the formation of a new series of trimethylsilicon(IV) carboxylates of general formula $Me_3Si(OCOR)$, [where R is different for different acids, viz. palmitic acid, R= $CH_3(CH_2)_{14}$-; stearic acid, R= $CH_3(CH_2)_{16}$-; lauric acid, R= $CH_3(CH_2)_{10}$-; myristric acid, R= $CH_3(CH_2)_{12}$-].

Two Schiff bases, SB and HSal-2-ambz have been synthesized from the condensation of salicyaldehyde with aniline and salicyaldehyde with 2-aminomethylbenzimidazole, respectively.

The reaction of the sodium salt of HSal-2-ambz with chlorotrimethylsilane in a 1:1 stoichiometry and with dichlorodimethylsilane in 2:1 stoichiometry yielded $Me_3Si(sal-2-ambz)$ and $Me_2Si(sal-2-ambz)_2$, respectively.

Dimethyldichlorosilane on reaction with Schiff base (SB) and long chain fatty acid in 1:1:1 ratio gives a new series of mixed complexes of general formula, $Me_2Si(SB)-(OCOR)$ [where R is different for different acids, viz. palmitic acid, R=$CH_3(CH_2)_{14}$- ; stearic acid, R= $CH_3(CH_2)_{16}$-; lauric acid, R= $CH_3(CH_2)_{10}$-; mystric acid, R= $CH_3(CH_2)_{12}$-].

All of the synthesized ligands and organosilicon complexes have been characterized by elemental analysis, IR and UV-visible spectral studies. ^1H and ^{13}C NMR spectral studies of some complexes show appropriate chemical shift corresponds to the proposed geometry of organosilicon complexes.

The residues obtained by the pyrolysis of some of the synthesized complexes have been characterized by XRD and found to be SiO/SiO_2. The surface morphology of the residues has been investigated by SEM and particle sizes determined by SEM and XRD are in the range 68–180 nm.

CONTENTS

3. RESULTS AND DISCUSSION

INTRODUCTION AND LITERATURE REVIEW

INTRODUCTION

1.1 General Introduction

Silicon was discovered as an element in 1823 by Jons Berzelius. The name silicon comes from the Latin *silex, silicis*, the word for "paving stone." It has 14 electrons, 14 neutrons, and an average atomic mass of 28.0855 and located in the periodic table immediately below the carbon in main group 14. It is a solid metalloid at room temperature. In its pure form, silicon melts at 2,570 degrees, and boils at 4,271 degrees Fahrenheit. Silicon is present in the soil and makes up about 25.7% of the earth's crust. It is the second most abundant element, being exceeded only by oxygen. Silicon is not found free in nature, but occurs chiefly as the oxide and as silicates. Sand, quartz, rock crystal, flint, jasper, and opal are some of the forms in which the oxide appears. Granite, hornblende, asbestos, feldspar, clay, mica, etc. are a few of the numerous silicate minerals.

Silicon is tetravalent and usually forms tetrahedral covalent compounds and 5- and 6-coordinated complexes. Unlike carbon, silicon do not form double bonds. There are also some important differences in bond strength: the silicon-silicon bond (230 kJ mol^{-1}) is weak in comparison to the carbon-carbon bond (356 kJ mol^{-1}) whereas the silicon-oxygen bond (368 kJ mol^{-1}) is stronger than the corresponding carbon-oxygen bond (336 kJ mol^{-1}). In general, bonds with electronegative elements are stronger with silicon than with carbon. The bonds between silicon and other atoms are in general longer than the equivalent bonds between carbon and the corresponding atoms. For example, Si–C bond is 1.89Å whereas a typical C–C bond is 1.54Å [1]. The increased bond lengths between silicon and other atoms in comparison to the corresponding systems involving carbon enable hard nucleophiles to react at sterically hindered silicon centres. The most effective nucleophiles for silicon are those which are strongly electronegative and that upon reaction lead to the formation of strong bonds to silicon, and this concept is applicable to oxygen atom. Silicon is able to form single as well as double bonds with oxygen. The latter are stable only under special conditions. In contrast, carbon single and double bonds with oxygen are equally abundant. More detailed differences between silicon and carbon are revealed by means of the ab initio calculation of bond dissociation energies. It is shown that the Si = O double bond is equally as weak as the C–O single bond, and the Si–O single bond is

1

equally as strong as the C = O bond. The most interesting result, however, is the fact that the Si=O bond has a lower bond dissociation energy than the Si—O bond. The extraordinarily strong Si–O bond is generally explained by means of $d\pi$-$p\pi$ interaction [2].

Silicon is one of man's most useful elements. In the form of sand and clay it is used to make concrete and brick; it is a useful refractory material for high-temperature work, and in the form of silicates it is used in making enamels, pottery, etc. Silica, as sand, is a principal ingredient of glass, one of the most inexpensive of materials with excellent mechanical, optical, thermal and electrical properties. Hyperpure silicon can be doped with boron, gallium, phosphorus, or arsenic to produce silicon for use in transistors, solar cells, rectifiers, and other solid-state devices, which are used extensively in the electronics and space-age industries. Silicon also promotes firmness and strength in human tissues. It is a part of the arteries, tendons, skin, connective tissue, and eyes. This is also present with the chondroitin sulfates of cartilage, and it works with calcium to help restore bones. It represents about 0.05 percent of our body weight.

Silicon is the heart of semiconductor industry to date, because it is an important element in semiconductors and high-tech devices: the high-tech region of Silicon valley, California is named after this element. The energy-band gap of silicon is 1.1 eV. This value permits the operation of silicon semiconductors devices at higher temperatures as compare to others like germanium. It is used for diodes, transistors, integrated circuits, memories, infrared detectors and lenses, light-emitting diodes (LED), photosensors, strain gages, solar cells, charge transfer devices, radiation detectors and a variety of other devices. Scientists at IBM have discovered a breakthrough method to stretch silicon, the fundamental material at the heart of microchips that can speed the flow of electrons through transistors increasing semiconductor performance and decreasing power consumption in semiconductors. In the strained silicon, electrons experience less resistance and flow up to 70 percent faster, which can lead to chips that are up to 35 percent faster without having to shrink the size of transistors [3].

As an inherent part of organometallic chemistry, organosilicon chemistry is one of the rapidly developing fields of science. Throughout nature, there are many well known inorganic and polymeric compounds containing silicon; however there are no naturally occurring organosilanes. Numerous applications [4-7] of the organosilicon have been reported in the manufacture of synthetic reagents and intermediates, bioactive molecules, biomedical materials,
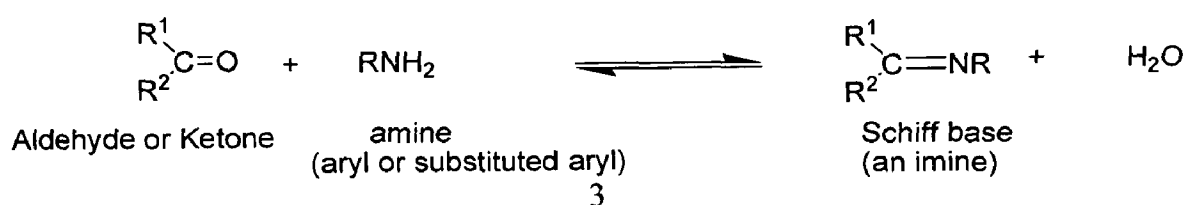
electronic devices, specialty plastics, elastomers, coatings, organosilicon films find extremely diverse applications because of their unique electrical, chemical and surface properties. Potential applications of organosilicon chemically vapour deposited thin films include biocompatible coatings for medical implants [8], semipermeable membranes [9], integrated optical devices [10], dielectric films [11], and abrasion and corrosion resistant coatings [12].

Organosilicon derivatives of amino acids are of interest as potential biocides. They have been found to be active as fungicides and bactericides for seeds and plants. The coordination of organosilicon(IV) moiety with biological molecules results, an exponential increase of industrial, agricultural, domestic and biological applications. Organosilicon(IV) ester formation can be controlled using kinetic conditions (low temperature, strong, sterically demanding base) or thermodynamic conditions (weaker, "equilibrating" base, room or higher temperatures) [13].
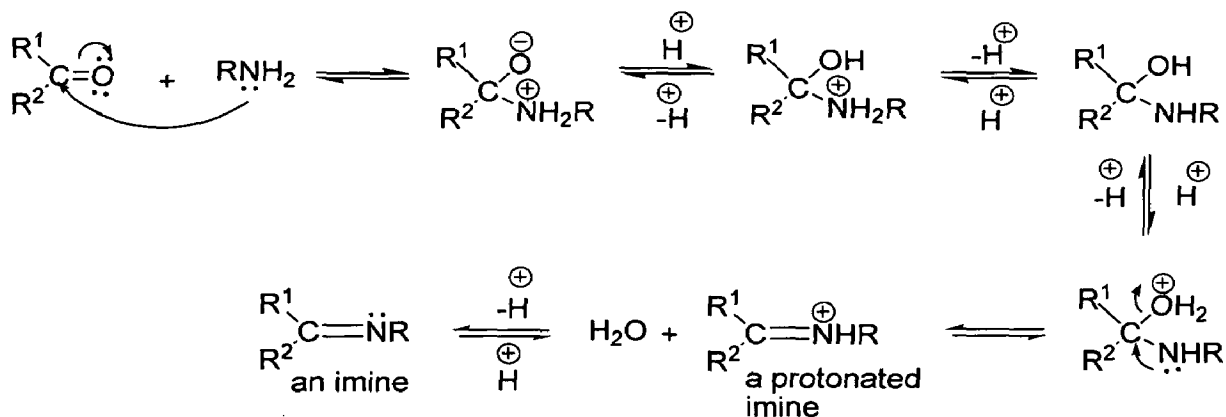
The silicones are a group of organosilicon polymers. They have a wide variety of commercial uses as fluids, oils, elastomers (rubbers) and resins. They have good thermal and oxidative stability, valuable resistance to high and low temperature, excellent water repelling, good dielectric properties, chemical inertness, prolong resistance to uv radiation and weathering. Their strength and inertness are related to high strength of Si–C bond and very high bond energy (502 kJ mol^{-1}) of the Si–O bond of their silica like skeleton of Si–O–Si–O–Si [14]. Silicones can be made as fluids (oils), greases, emulsions, elastomers (rubbers), and resins.

1.2 Schiff bases

Schiff bases are the general condensation product of primary amines and carbonyl compounds. They are represented by formula $RCH=NR^1$, where R and R^1 represent alkyl or aryl substituents. Schiff bases are one of the most important nitrogen donors, which have been used as ligands towards a variety of metal ions. The characteristic group of Schiff base is azomethines group (>C=N). Therefore, these N-substituted imines are often referred as azomethines. Schiff [15] for the first time synthesized a product by the condensation of a carbonyl compounds and primary amine with the elimination of water molecule, therefore, this product is known as 'Schiff's base'. This addition involves nucleophilic attack by the basic nitrogen compound on carbonyl carbon. Therefore, it is necessary to adjust the right pH.

$$\begin{array}{c} R^1 \\ \diagdown \\ C=O \\ \diagup \\ R^2 \end{array} + RNH_2 \rightleftharpoons \begin{array}{c} R^1 \\ \diagdown \\ C=NR \\ \diagup \\ R^2 \end{array} + H_2O$$

Aldehyde or Ketone   amine   Schiff base
(aryl or substituted aryl)   (an imine)

3

Mechanism:

Schiff bases can be prepared by condensation of aromatic aldehydes and aromatic amines. In contract to amines, these imines are stable enough for isolation. However, in some cases, especially with simple alkyl group, they rapidly decompose or polymerize unless there is at least one aryl group on nitrogen or carbon. When there is an aryl group, these compounds are more stable. In general, ketones react more slowly than aldehydes, and higher temperature as well as longer reaction time is required. In addition to this, the equilibrium must often be shifted usually by removal of water either azeotropically by distillation or with a drying agent such as $TiCl_4$. Schiff bases were also synthesized by the reaction of Grignard reagent with aryl cyanide.
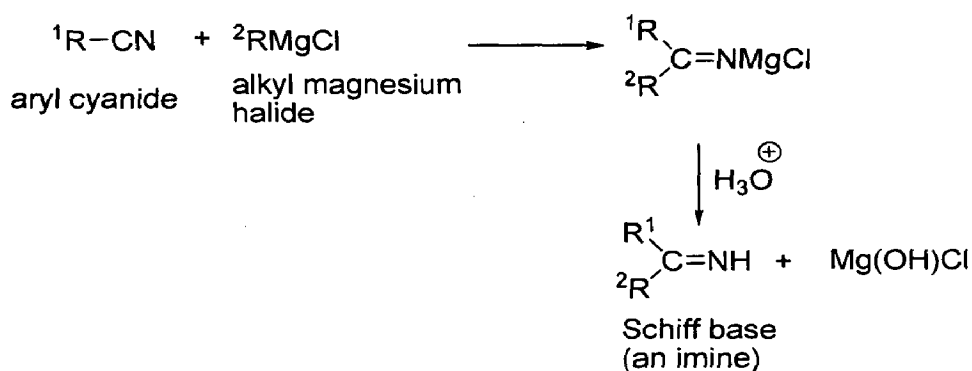

This reaction is discovered by Moureau and Migoniac [16].

Schiff base metal complexes have been studied extensively for years due to the synthetic flexibilities of these ligands and their selectivity as well as sensitivity towards the transition

4

metal ions. The architectural beauty of these coordination complexes arises due to the interesting ligand systems containing different donor sites in heterocyclic rings, e.g., NNO or NNS.

1.3 Basicity of Schiff bases

The ligands having nitrogen as donor atom can donate a lone pair of electrons to the various kinds of Lewis acids and availability of these electrons decreases in the following order;

$$R_3N \quad > \quad \begin{matrix} {}^1R \\ \diagdown \\ {}^2R \diagup \end{matrix} C=NR \quad > \quad RCN$$
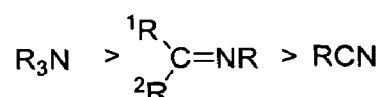
The availability of these electrons is also affected by the substituents present at various positions as R^1 and R^2
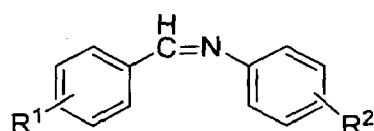
If the electron repelling groups are present the basicity increases due to the accumulation of an excess negative charge, but if, the electron withdrawing groups are present, the opposite effect is observed in the order:

$$Me_3N \quad > \quad OMe \quad > \quad H \quad > \quad Cl \quad > \quad Br \quad > \quad NO_2$$
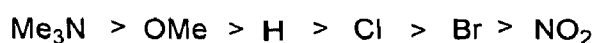
Schiff bases can be hydrolyzed back to the amine and the aldehyde.

1.4 Applications of Organosilicon Compounds, Schiff bases and their Metal Complexes

Organosilicon compounds and metal's Schiff bases complexes have been found to be of great significance. They are important classes of compounds due to the ease of their preparation, different properties, viz. biochemical, industrial and medicinal properties.

1.4.1 As biocides:

Organosilicon compounds have been reported to show nematicidal, insecticidal, antifertility, antifungal antibacterial activities [17]. In the search of better fungicides and bactericides, studies

5

were conducted to assess the growth- inhibiting potential of the various organosilicon complexes against various pathogenic diseases. Dimethylsilicon derivatives of amino acids have been tested *in vitro* against various bacteria, viz. *Escherichia coli, Pseudomonas putida-2252, Aeromonas formicans, Staphylococcus aureus-740,* and *fungi, viz. Aspergillus niger ORS-4* and *Penicillium notatum-1348.* Some Schiff bases derived from acylhydrazine and furanyl and thienyl, and their metal complexes show higher bactericidal activity against *Escherichia coli, Staphylococcus aureus* and *Pseudomonas aeruginosa* [18]. The applications of Schiff bases as anti-cancer compounds have been reviewed by Cho and coworkers [19]. Schiff bases metal complexes have been also found to be active *in vitro* and *in vivo* against *P388 Leukemia* and also exhibit antitumour activity in K.B structures [20]. In 2004, Tumar and coworkers have prepared organosilicon complexes of biologically active Schiff bases of sulpha drugs [21].

1.4.2. As catalyst:

Aromatic Schiff bases and their metal complexes have catalytic property. Schiff bases have catalytic influence on polymerization, oxidation and decomposition. Bis-(furaldehyde) Schiff base Co(II) complexes could activate molecular oxygen, and used as catalyst in the oxidation of cyclohexane [22].

1.4.3. In photography:

Polymeric Schiff bases as well as substituted benzalidenanilines exhibit photoconducting properties [23].

1.4.4. Analytical application:

Some substituted Schiff bases, viz. 1-(8-quinalylamino)propenetrihydrochloride hydrate, are useful analytical reagents. Some hydroxyl azomethine compounds find application as luminescent reagents and as indicators in complexometric titrations. In 1994, several more analytical and pharmacological applications of Schiff bases and their metal complexes are reported [24].

1.4.5. As polymers:

Schiff bases are used as conducting thermoset polymers [25].

1.5 Long Chain Fatty Acids

Fatty acid is a carboxylic acid often with a long unbranched aliphatic tail (chain), which is either saturated or unsaturated. Carboxylic acids as short as butyric acid (4 carbon atoms) are considered to be fatty acids, while fatty acids derived from natural fats and oils may be assumed to have at least 8 carbon atoms, e.g. caprylic acid (octanoic acid). Most of the natural fatty acids have an even number of carbon atoms, because their biosynthesis involves acetyl-CoA, a coenzyme carrying a two-carbon-atom group. Industrially, fatty acids are produced by the hydrolysis of the ester linkages in a fat or biological oil (both of which are triglycerides), with the removal of glycerol. Saturated fatty acids form straight chains and, as a result, can be packed together very tightly, allowing living organisms to store chemical energy very densely. The fatty tissues of animals contain large amounts of long-chain saturated fatty acids. Most commonly occurring saturated fatty acids are:

Butyric $CH_3(CH_2)_2COOH$; Caproic $CH_3(CH_2)_4COOH$; Caprylic $CH_3(CH_2)_6COOH$; Capric $CH_3(CH_2)_8COOH$; Lauric $CH_3(CH_2)_{10}COOH$; Myristic $CH_3(CH_2)_{12}COOH$; Palmitic $CH_3(CH_2)_{14}COOH$; Stearic $CH_3(CH_2)_{16}COOH$ etc.

Unsaturated fatty acids are of similar form, except that one or more alkenyl functional groups exist along the chain. It may be in *cis* or *trans* form. When a chain has many *cis* bonds, it becomes quite curved in its most accessible conformations. For example, oleic acid, with one double bond, has a "kink" in it, while linoleic acid, with two double bonds, has a more pronounced bend. Alpha-linolenic acid, with three double bonds, favors a hooked shape. The effect of this is that in restricted environments, such as when fatty acids are part of a phospholipid in a lipid bilayer, or triglycerides in lipid droplets, cis bonds limit the ability of fatty acids to be closely packed, and therefore could affect the melting temperature of the membrane or of the fat. A *trans* configuration, by contrast, means that the next two carbon atoms are bound to opposite sides of the double bond. As a result, they don't cause the chain to bend much, and their shape is similar to straight saturated fatty acids. The human body can produce all but two of the fatty acids it needs. These two, linoleic acid (LA) and alpha-linolenic acid (LNA), are widely distributed in plant oils. In addition, fish oils contain the longer-chain omega-3 fatty acids eicosapentaenoic acid (EPA) and docosahexaenoic acid (DHA). Since they cannot be made in the body from other substrates and must be supplied in food, they are called essential fatty

acids. In the body, essential fatty acids are primarily used to produce hormone-like substances that regulate a wide range of functions, including blood pressure, blood clotting, blood lipid levels, the immune response, and the inflammation response to injury infection [26].

Low-fat foods have frequently been advocated for people attempting to diet. Some people on diets to lose weight have discovered that they can satisfy their appetite with fewer calories by eating protein and carbohydrate instead of fat. Losing weight not only makes a person look good, it can reduce the danger of getting heart disease, diabetes and cancer [27]. But the health hazards and benefits of fats, carbohydrates and proteins and their effectiveness for diets and dieting depend greatly on the type of fat, carbohydrate and protein. Dietary fat by itself, not just the body fat it produces, can be a health hazard. A recent study has shown that reducing dietary fat from 36% of total calories to 26% of total calories can significantly lower blood pressure within 8 weeks. Saturated fat in the diet can increase the risk of heart disease from atherosclerosis (fatty plaques on blood vessel walls) by raising blood cholesterol. Unsaturated fat is more likely to form free radicals by lipid peroxidation which can lead to cancer and may accelerate aging. Therefore, both saturated and unsaturated fat can have health hazards. But every cell membrane in the body contains fat, and some of those fats cannot be synthesized, making it essential to obtain these fats from diet.

1.6 LITERATURE REVIEW

In the recent years, a considerable amount of work has been done on the synthetic, magnetic and structural properties of transition metal(II) and (III) complexes of bidentate and tridentate Schiff bases. Organosilicon complexes have also received a considerable attention of researchers in the last few years. A comprehensive review of the existing literature on the Schiff bases metal complexes and organosilicon compounds of N and O donors with special references to their synthetic methods, structural and thermal behaviors, and biological applications is presented in following pages.

Khandar *et al.* [28] synthesized Ni(II) complexes of 16-membered mixed-donor macrocyclic Schiff base ligand, potentially hexadentate, bearing two pentadate alcohol function. The complexes have been characterized by IR, UV-visible, magnetic susceptibility and elemental analysis.

Studies on some salicylaldehyde Schiff base derivatives and their complexes with Cr(III), Mn(II), Fe(III), Ni(II) and Cu(II) have been carried by Abdel-Latif and coworkers [29]. The thermal dehydration and decomposition of these complexes have been studied kinetically using the integral method applying the Coats–Redfern equation. It was found that the thermal decomposition of the complexes follow second order kinetics. The thermodynamic parameters of the decomposition are also reported.

Dyers and coworkers [30] synthesized a new series of Schiff base formula of ligand complexes of Cu and Ni. They synthesized new series of salen metal complexes possess bulky groups in the periphery of the ligands. Copper complex is square planar in configuration. The complexes have been characterized by IR, UV-visible, magnetic susceptibility and elemental analysis.

AL-Razaq and coworkers [31] synthesized new complexes of Schiff bases derived from 2-hydroxy- or 2-methoxy benzaldehyde and phenyl 3-aminophenyl ketone or 2-amino-3-hydroxypyridine (L1, L2, L3 and L4, resp.), by reacting with the organosilicon(IV) chlorides, $RnSiCl_{4-n}$ (R = Me or Ph, n = 1–3) to yield complexes of the general formulas [R_nSiCl_3-n(L1-H)], [R_nSiCl_4-n(L2)], n = 1–3; [R_nSiCl_2-n(L3-2H)], n = 1, 2; [Me_2PhSi-(L3-H)] and [R_nSiCl_3-n(L4-H)], n = 1–3. These complexes have been characterized physichemically and spectroscopically. The suggested structures of the complexes were confirmed by computing the steric energy and the physical properties of each complex.

Cu complexes with 3, 5-halogen substituted Schiff base ligands have been synthesized by Takashiro Akitsu et al. [32] and characterized by crystal structure, IR, UV-visible, thermally induced structural phase transition and adsorption spectra. All the complexes exhibit a structural phase transition on heating them in the solid state · regardless of their structures at room temperature.

Gupta and Kirkan [33] synthesized two types of Cu(II) and Ni(II) complexes of Schiff bases, viz. benzophenoneanthronylhydrazone (LI), benzophenonesalicyoylhydrazone (L2) and bidentate heterocyclic base [1,10 phenanthroline (phen)] with stoichiometry ML_2, and characterized by elemental analysis, IR, UV-visible, and magnetic susceptibility measurement.

Complexation behavior of Schiff bases toward transition metal ions has been studied by Ben Saber et al. [34]. The complexes have been investigated by several techniques using elemental analyses (C, H, N), molar conductance measurements, infrared and electronic spectra. The

elemental analysis data suggest the stoichiometry to be 1:1 [M: L]. The molar conductance measurements reveal the presence of non-electrolytic neutral complexes.

Singh and Nagpal [35] synthesized some novel ecofriendly fungicides and bactericides of indole-2,3-dione derivatives, having important pharmacodynamic significance. The ligands used are prepared by the condensation of 1,3-dihydro-3-[2-(phenyl)-2-oxoethylidene]-2H-indol-2-one, 1,3-dihydro-3-[2-(4-nitrophenyl)-2-oxoethylidene]-2H-indol-2-one and 1,3-dihydro-3-[2-(4-nitro-3-methylphenyl)-2-oxoethylidene]-2H-indol-2-one with hydrazinecarboxamide and hydrazinecarbothioamide. These imines, on interaction with diorganosilicon(IV) chlorides, yield complexes having Si–O or Si–S and Si–N bonds. The structure of these compounds were elucidated by elemental microanalyses and spectral [(UV), (IR), (^{1}H, ^{13}C and ^{29}Si NMR)] studies which unerringly point to a trigonal bipyramidal and octahedral geometries for unimolar and bimolar reactions, respectively. The potency of the synthesized compounds was assessed by growth inhibiting potential of the complexes against variety of fungal and bacterial strains and male albino rats. The results of these biological studies were compared with the standard fungicide, Bavistin 1,3-Dihydro-3-[2-(4-nitrophenyl)-2-oxoethylidene]-2H-indol-2-one-hydrazincarbothioamide and its diphenylsilicon(IV) complexes have comparable antimicrobial activity and are less toxic to male albino rats than Bavistin.

Synthesis, characteristic spectral studies, and *in vitro* antimicrobial activity of organosilicon(IV) derivatives of N-benzoylamino acids have been done by Nath and Goyal [36]. These complexes have been characterized by elemental analysis, magnetic susceptibility, conductivity measurement, IR and multinuclear magnetic resonance studies.

Khan and coworkers [37] have studied Organosilicon(IV) complexes of biologically active Schiff bases of sulphadrugs. The complexes have been characterized by crystal structure, IR, UV-visible.

Complexes of silicon, manganese and tin of salicylanilide sulphathiazole [sic] having nematicidal, insecticidal, antifertility, antifungal and antibacterial activities have been synthesized by Jain *et al.* [38]. The structures of the compounds were elucidated by IR, ^{1}H NMR, ^{13}C NMR, ^{29}Si NMR, ^{119}Sn NMR, and ESR studies, which suggest a trigonal bipyramidal geometry around Si(IV) and Sn(IV), and tetrahedral geometry around Mn(II).

Chaviara and coworkers [39] prepared Cu(II) complexes of Schiff bases derived from heterocyclic aldehyde and 2-amino-5-methyl-thiazole, and studied their antiproliferative and

antibacterial characteristics. The complex of the type Cu(dienXXY$_2$) exhibits increased activity both in cancer cell and in bacteria compared to the starting material.

Omar and coworkers [40] synthesized metal complexes with Schiff bases derived from 2-thiophene carboxaldehyde and amino benzoic acid and characterized by elemental analysis, IR, UV-visible, ^{1}HMNR, magnetic moment, molar conductance and thermal analysis (TGA). It was found that Ni(II) complex is ionic and is of type 2:1 electrolyte while Cu(II) complex is noneletrolyte. TGA of these chelates show that the hydrated complexes remove water molecule in the first step.

Mn(III)-Schiff base complexes assembled with L-amino acid ethyl ester were synthesized by Liu *et al.* [41]. They were found to be highly effective catalyst for enantioselective epoxidation of conjugated olefins while the corresponding binuclear Mn(III) complexes showed lower enantioselectivity.

Synthesis and spectroscopic properties of Schiff bases derived from 3-hydroxy-4-pyridinecarboxaldehyde have been done by Sanz *et al.* [42]. The ^{1}H, ^{13}C, ^{15}N and ^{17}O NMR data of these compounds are used to discuss the tautomerism. ^{15}N NMR and ^{17}O NMR chemical shifts established the tautomer existing in solution as the hydroxy/imino. From ^{13}C CPMAS NMR confirms that the same tautomer is found in the solid state.

A new polydentate Schiff base [43] derived from the condensation of 2,6-diformyl-4-methylphenol and S-methylhydrazine carbodithionate was reported. The 1:1 metal complexes were formed from the interaction of these Schiff base and metal ions Cu(II), Cr(II) and Co(II). The complexes were characterized by elemental analysis and IR spectroscopy.

Karmakar and coworkers [44] synthesized new dimeric manganese(III) comple [MnL(H$_2$O)]$_2$(ClO$_4$).H$_2$O where [L=N,N'-bis(2-hydroxyacetophenylidene-1,2-diaminopropane]. It was characterized by spectroscopic and single crystal crystallographic techniques. The electrochemical study has also been reported. Low temperature magnetic susceptibility shows a ferromagnetic intra-dimer interaction.

Dravent *et al.* [45] synthesized new porous crystals of Cu(I) complexes with Schiff base containing triazole ligand, (CuL^1$_2$)$_2$(BF$_4$)$_2$0.5THF, where L^1 = N-[(E)-(4-chlorophenyl)-methylidene]-4H-1,2,4-triazole-4-amine, having great ability towards building the porous structures of the crystals.

Rai [46] studied the complexing behaviour of some Schiff bases with Ni(II), Cu(II) and Co(II). Homonuclear metal complexes, [M(HL)X₂], where L = 2-(3',4'-dimethylphenyl)-imino-3-(hydroxyimino)butane , X = halides, nitrates, and chlorates, were synthesized and characterized from elemental analysis, magnetic susceptibility, conductivity measurement, IR and electronic data.

Nath and Goyal synthesized [47] trimethyl- and triphenylsilicon(IV) complexes of the type R_3SiAA [AA = anion of amino acids]. These complexes have been characterized by elemental analysis, magnetic susceptibility, conductivity measurement, IR and multinuclear magnetic resonance studies. On the basis of spectral studies a penta-coordinate distorted trigonal-bipyramidal amino-bridged structure has been suggested for all complexes.

In the same year, Wagler and coworkers [48] synthesized silicon complexes, RSi(salen-Me₂-N,N',O,O') I where R = Ph, Me, CH=CH₂. These complexes have been characterized by elemental analysis, magnetic susceptibility, conductivity measurement, IR and ^{1}H, ^{13}NMR and ^{29}Si NMR spectral studies. On the basis of spectral studies a penta-coordinate trigonal-bipyramidal structure has been suggested for all complexes.
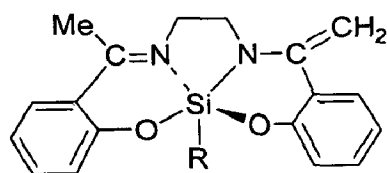
(I)

Nath and Goyal [49] also synthesized fifteen new organosilicon(IV) complexes formulated as $R_3Si[2-HOC_{10}H_6CH:NCH(X)COO]$ and $Me_2Si[2-OC_{10}H_6CH:NCH(X)COO]$ [X = H (H₂L1), CH₂CHMe₂ (H₂L2), CH₂CH₂SMe (H₂L3), Me (H₂L4) and CHMe₂ (H₂L5)] and characterized by ^{1}H and ^{13}C NMR, IR, electronic spectral studies, and elemental analysis. All of the complexes are nonelectrolytes. The spectral studies suggested a distorted trigonal-bipyramidal geometry around the Si atom. Antimicrobial activity screening for all of the complexes was carried out against various bacteria [*Escherichia coli, Aeromonas formicans, Pseudomonas putida-2252*, and *Staphylococcus aureus-740*] and fungi [*Aureobasidium pullulans-1991, Penicillium chrysogenum-1348, Verticillium dahliae-2063*, and *Aspergillus niger ORS-4*]. The complexes showed good activity.

A new series of dimethylsilicon (IV) derivatives of amino acids have been synthesized by Nath and Goyal [50]. Reaction of dichlorodimethylsilane with the sodium salt of amino acids in 1:2 molar ratio led to the formation of dimethylsilicon (IV) complexes of general formula, Me_2SiL_2 [L=anion of amino acids]. The complexes have been characterized from elemental analysis, magnetic susceptibility, conductivity measurement, IR and electronic data.

Sharma, [51] synthesized a new series of $Me_2Si(N \frown O)_2$ type organosilicon (IV) complexes by reactions of diethoxydimethylsilane with Schiff bases derived from the condensation of furfuraldehyde, indole-3-carbaldehyde with alanine, glycine, valine, isoleucine and tryptophan in a 1:2 molar ratio. The complexes are monomeric and non-electrolytic in nature. The coordination behavior of Schiff bases through organosilicon(IV) has been investigated by IR, ^1H, ^{13}C & ^{29}Si NMR spectral studies. Schiff bases and their silicon complexes have also been screened for their antifungal activity. Several of these complexes were quite active in this respect.

New pentacoordinated triorganosilicon(IV) complexes [52] derived from biologically active benzothiazolines, 2-(2-furyl)benzothiazoline, 2-(2-pyridyl)benzothiazoline and 2-(2-thienyl)-benzothiazoline were prepared. The newly synthesized complexes $R_3Si(Bzt)$ (R = Me or Ph; Bzt = 2-alkylideneaminobenzenethiolate) were characterized by elemental analyses, molecular weight determinations and conductometric measurements. A probable trigonal bipyramidal structure for the resulting derivatives is proposed on the basis of electronic, IR, ^1H, ^{13}C NMR and ^{29}Si NMR spectral studies.

Nath and Goyal [53] studied synthesis, spectral and biological studies of organosilicon(IV) complexes of schiff bases derived from amino acids. The new organosilicon(IV) complexes formed of the type $Me_3Si(L/L')$ [where L/L' = anions of the Schiff bases]. The complexes have been characterized by elemental analyses, molar conductance, electronic, IR and multi-NMR (^1H and ^{13}C, ^{29}Si) studies. All the complexes are non-electrolytes. A pentacoordinate, trigonal-bipyramidal geometry is suggested for all of the complexes. The *in vitro* antimicrobial activity of the trimethyl- and triphenylsilicon(IV) complexes has also been screened against bacteria *and fungi.*

Singh and Singh [54] synthesized complexes of tri-, di- and mono-organosilicon(IV) chlorides with the Schiff base N,N'- ethylenebis(salicylideneimine) and characterized by elemental analyses and spectroscopic (IR, ^1H, ^{13}C and ^{29}Si NMR) studies. Molecular weight

13

determination in chloroform revealed the monomeric nature of these complexes. The data supports the binding of oxygen to silicon(IV) with an octahedral geometry as shown in example, (II).
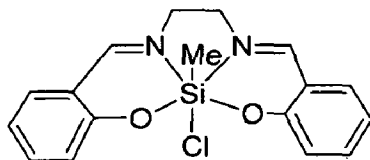
(II)

S. Balwal and coworkers [55] synthesized a new class of penta and hexacoordinate silicon derivatives, $R_2Si(L)Cl$ and R_2SiL_2 (R = Me, Ph) by reacting dimethyldichlorosilane and diphenyldichlorosilane with sodium derivatives of semicarbazone and thiosemicarbazone of a ketone of indole series (LH). The complexes show the herbicidal and pesticidal activity. The structure of products was established by electronic, IR and multi-NMR (^{1}H and ^{13}C, ^{29}Si) studies. X-ray diffraction data confirms the structure of III:
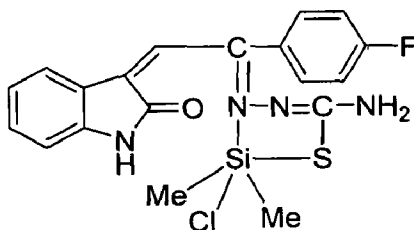
(III)

New complexes, Me_3SiL, $Me_2SiL_nCl_{2-n}$ and $MeSiLnCl_{3-n}$ (LH = benzilmonoxime) were synthesized by reacting organosilicon(IV) chlorides with sodium salt of ligand (prepared in situ) in different molar ratios [56]. These complexes were characterized by elemental analyses, molecular weight determination, conductomeric measurements and spectral (IR, ^{1}H and ^{13}C NMR,^{29}Si) studies.

Nath and Goyal [57] studied synthesis, spectral, and biological behaviour of organosilicon(IV) complexes $Ph_3Si(L)$ [where L = anions of the Schiff bases derived from the condensation of 2-methoxybenzaldehyde or acetophenone with glycine (HL1/HL6), L-leucine (HL2/HL7), L-methionine (HL3/HL8), DL-alanine (HL4/HL9) and L-valine (HL5/HL10)]. These were characterized by elemental analyses, molar conductance, electronic, IR and

multinuclear magnetic resonance (^{1}H and ^{13}C) studies. All the complexes are nonelectrolyte. From the spectral studies a pentacoordinated trigonal bipyramidal geometry is suggested for all the complexes.

Belwal [58] also synthesized diorganotin(IV) and diorganosilicon(IV) derivatives $R_2MCl(L1)$, $R_2MCl(L2)$, $R_2M(L1)_2$ and $R_2M(L2)_2$ (where, R = Ph or Me, M = Sn or Si and L1/L2 = anions of the thiosemicarzone ligands) were synthesized and characterized by elemental analyses, IR, ^{1}H, ^{13}C, ^{29}Si and ^{119}Sn NMR spectroscopy. These data support the binding of O to Sn(IV) and Si(IV) in $R_2MCl(L1)$ and $R_2MCl(L2)$ complexes with a trigonal bipyramidal geometry. However, $R_2M(L1)_2$ and $R_2M(L2)_2$ complexes possess an octahedral geometry. The results of antimicrobial effects of some representative complexes on different species of pathogenic fungi and bacteria also were recorded and discussed.

A few organotin and organosilicon complexes (Me_2SiCl_2L, Me_2SnCl_2L, Ph_3SnClL; L = $RC_6H_4C(O)CH:CHC(O)NHN:C(Me)C_6H_4OH-2$, R = H, 4-Me) of substituted hydrazones were prepared and characterized by their elemental analyses, conductometric measurement and IR and 1H NMR spectral data. The ligand and their complexes were evaluated for fungicidal activity against phytopathogenic fungi, viz. *Alternaria alternata, Colletotrichum capsicum, Fusarium oxysporum* and *Rhizoctonia solani* at 37 ^{0}C and bactericidal activity against *Bacillus subtilis* and *Escherichia coli* at 28 ^{0}C [59].

Saini and Kumar [60] have described the biochemical aspects of some organosilicon and organotin complexes of salicylanilide (sal. anil) and its thiosemicarbazone (sal. anil. TSCZ). The ligand and their organosilicon complexes have been tested *in vitro* against a number of pathogenic fungi *(Alternaria brassicicola, Macrophomina phaseolina, Fusarium oxysporum)* and bacteria *(Xanthomonas campestris, Pseudomonas pisi, Escherichia coli* and *Staphylococcus aureus)* at different concentrations and were found to possess remarkable fugicidal and bactericidal properties.

A few coordination compounds of silicon(IV) synthesized by the interaction of trimethyl- and triphenyl-chlorosilane with nitrogen-sulphur donor ligands. These compounds are monomeric, as indicated by molecular weight determination, and they behave as nonelectrolytes in dry DMF. From the electronic, infrared, ^{1}H, and ^{13}C NMR spectral results, it has been concluded that in these compounds, silicon is penta-coordinated in a trigonal bipyramidal environment. An assessment of biological activity of these compounds has shown that some of

15

them are very active against *P. mirabilis* and others against *S. viridans* bacteria, while all of them show good fungicidal action against *F. oxysporum, A. alternata,* and *A. niger* [61].

Pujar and Siddapa [62] synthesized a series of new Me_2SiL_2 complexes, where L is azo ligands derived from vanillin and different primary amines, and characterized by elemental analyses, conductance measurements, electronic and IR spectral data. The ligands behave as bidentate and coordinate to silicon(IV) through azo nitrogen and phenolic oxygen. The complexes exhibit octahedral geometry.

Saxena and Singh [63] synthesized trimethyl- and triphenylsilicon(IV) complexes with monofunctional bidentate semicarbazones derived by the condensation of 2-acetylfuran, 2-acetylthiophene, 2-acetylpyridine or 2-acetylnaphthalene with semicarbazide hydrochloride. The products, $Me_3Si(L)$ and $Ph_3Si(L)$, were obtained by the 1:1 stoichiometric interactions of trimethylchlorosilane and triphenylchlorosilane with sodium salts of oxygen donor ligands, (HL), in anhydrous methanol. The pentacoordinated environment around silicon(IV) is proposed on the basis of IR, ^1H NMR and ^{13}C NMR spectral studies, molecular weight deteterminations and conductance measurements.

In 1990, Singh and Singh [64] synthesized $Me_2Si[ArC(Me):NN:C(NH_2)O]Cl$ and

$Me_2Si[ArC(Me):NN:C(NH_2)O]_2$ (Ar = furyl, thienyl, naphthyl, pyridyl). On the basis of electronic, IR, ^1H and ^{13}C NMR spectral studies, trigonal bipyramidal and octahedral geometries were suggested for the above complexes respectively. 2-Acetylthiophene semicarbazone and its Si complexes were effective bactericides, fungicides and also acted as sterilizing agents by reducing the production of sperm in male mice.

1.7 FORMULATION OF THE PROBLEM

From the literature survey on organosilicon schiff bases and amino acids of the years, the following points have been emerged out which are required to study:

1. Organosilicon carboxylates of lower acid (up to four carbons) are known but no work has been reported so for, for longer fatty acids.

2. Various organosilicon schiff base complexes are known. Though not a single organosilicon complex is known in which benzimidazole moiety is present as schiff base.

3. Large number of organosilicon complexes derived from various ligand are known. In these complexes donor atoms are from same ligand. Not a single complex is found in which donor atoms are from different ligand.

In the view of above findings, synthesis and characterization of organosilicon derivatives of long chain fatty acid such as lauric acid, myristic acid, stearic acid, palmitic acid; schiff bases derivative, and mixed derivatives of Schiff base and long chain fatty acid have been carried out and reported in this dissertation.

EXPERIMENTAL

EXPERIMENTAL

2.1 Chemicals

The reagents used are summarized in table no.1

Table 1: Reagents, their grades and makes

S.No.	CHEMICALS	GRADE	MAKE
1	Methanol (distilled)	LR (Specially dried with KOH)	Rankem
2	Chloroform (distilled)	LR	Rankem
3	Potassium hydroxide	GPR	Merck
4	Triethyl amine	AR	Rankem
5	Pamitic acid	AR	Fluka, Sigma aldrich
6	Stearic acid	AR	Fluka, Sigma aldrich
7	Lauric acid	AR	Fluka, Sigma aldrich
8	Mystric acid	AR	Fluka, Sigma aldrich
9	Glycine	LR	R.R. Chemicals Inc.
10	Aniline	LR	Lancaster
11	Salicylaldehyde	LR	Lancaster
	Salicylaldehyde	L	
12	Dimethylsilicon dichloride	LR	Merck
13	Trimethylsilicon chloride	LR	Merck
14	o-phenylenediamine	LR	Loba Chem

2.2 Synthesis of Trimethylsilicon Carboxylate

The reaction of trimethylsilicon chloride with high molecular weight organic acid is very slow and attempts were made to synthesize pure trimethylsilicon carboxylates in good yield. Therefore, following different synthetic procedures were carried out in order to optimize the best reaction conditions.

2.2.1 Synthesis of trimethylsilicon palmate by using triethylamine

Palmitic acid (1 m mol, 0.26 gm) was dissolved in methanol (10 ml), taken in a flask and triethyleamine (1 m mol, 0.14ml) in methanol (10 ml) was taken in another flask. To the solution of trimethylsilicon chloride (in excess) in methanol (5 ml) was added the solution of palmitic acid and triethyl amine simultaneously drop wise with stirring under N_2. The reaction mixture was stirred for 40-46 h. The solution was concentrated under vacuum and allowed to cool in freezer. White solid was obtained. In this method the desired product was not obtained in pure phase and largely contaminated with unreacted palmitic acid. Hence this procedure was not used for the synthesis of other trimethylsilicon carboxylates.

2.2.2 Synthesis of trimethylsilicon palmate by using KOH

Trimethylsilicon chloride (1.5 ml in excess) was taken in 5 ml methanol under nitrogen and Potassium hydroxide pellet was added. After 15 minutes stirring, palmitic acid (1 mmol, 0.26 g) in methanol (10 ml) was added and stirred the reaction mixture for 30-40 h. After stirring, the solution was filtered to remove KCl. Then solution was concentrated under vacuum and allowed to cool in freezer. White solid was obtained. Same procedure was repeated with stearic acid, lauric acid, mystric acid.

Reaction:

$$Me_3SiCl + KOH \longrightarrow Me_3SiOH + KCl$$

Trimethylsilicon chloride   Potassium hydroxide   Trimethylsilanol

$$Me_3SiOH + CH_3(CH_2)_{14}COOH \longrightarrow Me_3SiOOC(CH_2)_{14}Me + H_2O$$

Trimethylsilanol   Palmitic acid   Trimethylsiliconpalmate

19
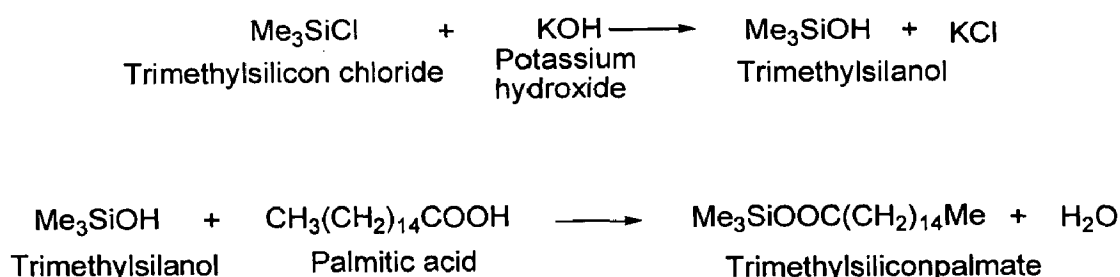
2.2.3 Synthesis of trimethylsilicon-stearate, -laurate and –mystrate.

These compounds were synthesized by interaction of trimethylsilicon chloride (1.5ml in excess) with organic acid (1mmol) in methanol using KOH method as described in the previous section 2.2.2.

Reaction:
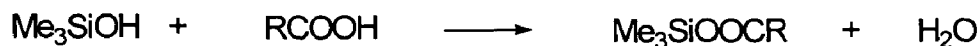
$$Me_3SiOH \quad + \quad RCOOH \quad \longrightarrow \quad Me_3SiOOCR \quad + \quad H_2O$$

$R = CH_3(CH_2)_{16}$ for stearic acid; $R = CH_3(CH_2)_{10}$ for lauric acid; $R = CH_3(CH_2)_{12}$ for myristric acid

After removing the solvent the product was obtained in different state for different acid, viz. trimethylsilicon palmate - white solid; trimethylsilicon stearate-white solid; trimethylsilicon laurate –solid; and trimethylsilicon myristrate – liquid.

2.3 Synthesis of Schiff base and their Complexes

2.3.1 Schiff base from salicylaldehyde and aniline, (SB)

A solution of aniline (1.1 ml, 10 m mole) in methanol (10 ml) has been added to a solution of salicylaldehyde (0.9 ml, 10 m mole) in methanol (10 ml) in round bottom flask. The resulting mixture was refluxed for 5 h and allowed to cool. Yellow solid was filtered, and recrystallised with distilled methanol, and dried under vacuum.

Yield = 90%; Color = yellow; m.p. = 46-48 ^{0}C

Reaction:

Salicyladehyde   Aniline   Schiff base (SB)
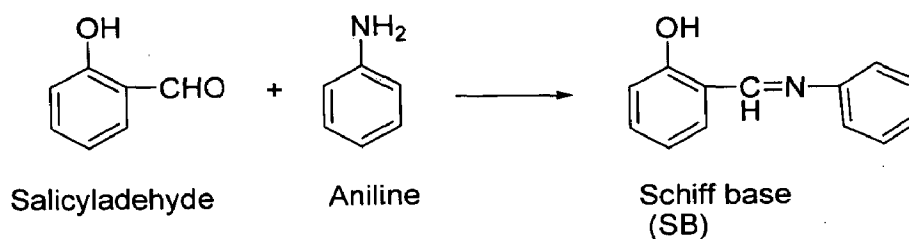
2.3.2.(a) Synthesis of 2-aminomethylbenzimidazole

Glycine (5g, 67 mmole) and o-phenylenediamine (5g, 50 m mole) were dissolved in 75 ml of 4M HCl. The brown solution was refluxed for 4 days and then kept for overnight at room

20

temperature. Blueish crystals had formed. These crystals were filtered off, washed twice with acetone and dried in air.

. **Reaction:**

Glycine + O-phenylenediamine + HCl (Hydrocloric acid) → 2-aminomethylbenzimidazole
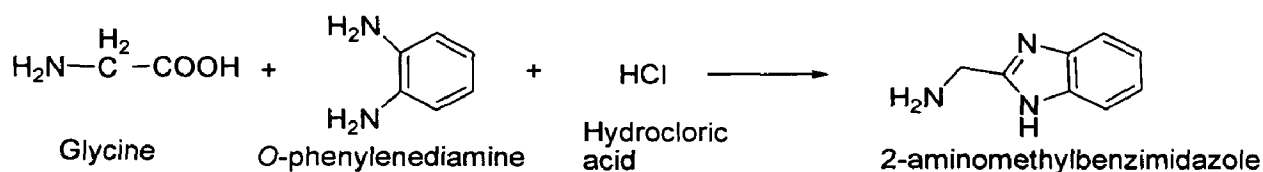
Yield = 3.12 g; Color = light blue; m.p. = 80 °C

2.3.2(b) Synthesis of Schiff base from salicyaldehyde and 2-aminomethylbenzimidazole

2-Aminomethylbenzimidazole (1.1 g, 5 mmol) was dissolved first in the minimum amount of H_2O (15 ml) and to this aqueous K_2CO_3 (0.83 g, 6 mmol) was added to neutralize HCl and then salicylaldehyde (0.61 g, 5 mmol) already mixed in methanol (8 ml) was added slowly with stirring at room temperature. A yellow precipitate started to appear due to formation of ligand. It [Ref. 65] was filtered, washed with H_2O, and then finely with petroleum ether, and then dried in vacuum at room temperature. It was recrystallised with acetonitrile.

Yield = 0.88g, Colour = yellow, m.p. = 150-155 °c

Reaction:

Salicyaldehyde + 2-aminomethylbenzimidazole → (aqu.K_2CO_3) → HSal-2-aminomethylbenzimidazole
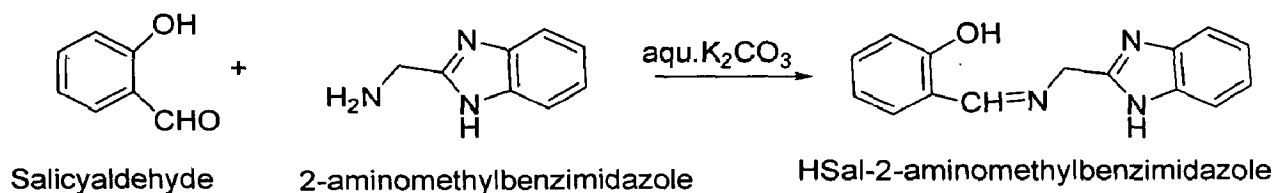
2.3.3 Synthesis of dimethylsilicon complex of HSal-2-aminomethylbenzimidazole

Dissolved HSal-2-aminomethylbenzimidazole (0.5 mmole; 0.1255 g) in minimum amount of methanol and then sodium methoxide (0.5mmole) was added drop by drop. The whole solution was refluxed for 3-4h and then cooled. This cooled solution was added to dichlorodimethylsilane (taken in excess from 1.5 mmole) taken in methanol and then stirred for 3-4h. The resulting solution then dried under vacuum.

21

Reaction:

Sal-2-aminomethylbenzimidazole   Dimethyldichlorosilane   Dimethylsilicon complex of sal-2-ambz

2.3.4 Synthesis of trimethylsilicon complex of HSal-2-aminomethylbenzimidazole

Dissolved HSal-2-aminomethylbenzimidazole (1.5mmole; 0.3765g) in minimum amount of methanol and then sodium methoxide (1.5 mmole) was added drop by drop. The whole solution was refluxed for 3-4 h and then cooled. This cooled solution was added to trimethylchlorosilane (taken in excess from 1.5 mmole) taken in methanol and then stirred for 3-4 h. The resulting solution then dried under vacuum.

Reaction:

Sal-2-aminomethylbenzimidazole   Trimethylchlorosilane   Trimethylsilicon complex of sal-2-ambz
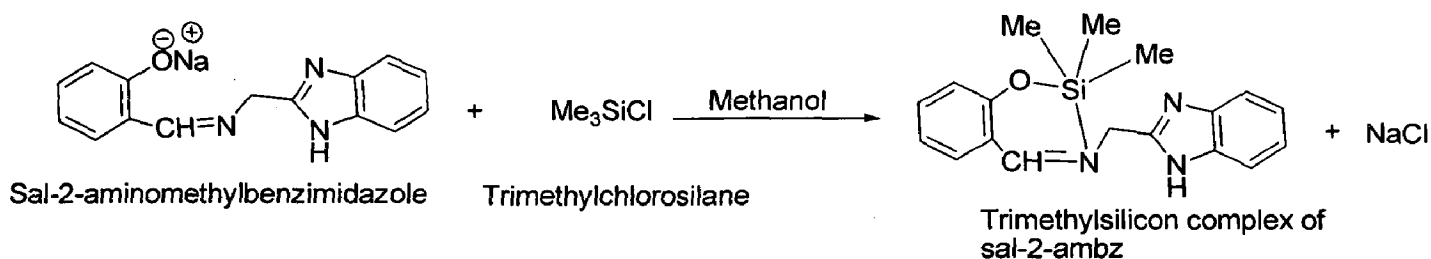
2.4 Synthesis of Dimethylsilicon Complexes of Schiff base and Long Chain Fatty Acid:

Dimethylsilicon dichloride (1.5 ml; in excess) was taken in 5 ml chloroform under nitrogen atmosphere and Potassium hydroxide pellet was added. After 15 minutes stirring, acid (1 mmole) in minimum amount of $CHCl_3$ and Schiff base (1mmole) also in minimum amount of $CHCl_3$was added from different arms of Y-tube drop-drop and stirred the reaction mixture for 30-40 hrs. After stirring, the solution was filtererd to kept out KCl. Then solution was concentrated under vacuum and allowed to cool in freezer. Yellow solid was obtained.

Reaction:

Me$_2$SiCl$_2$ + RCOOH + [o-hydroxybenzylidene-aniline Schiff base] —CH=N— —X + 2KOH ⟶ Dimethylsilicon complex + 2KCl

Dimethyldiclorosilane

Schiff base
Where, X=H, Cl

Dimethylsilicon complex
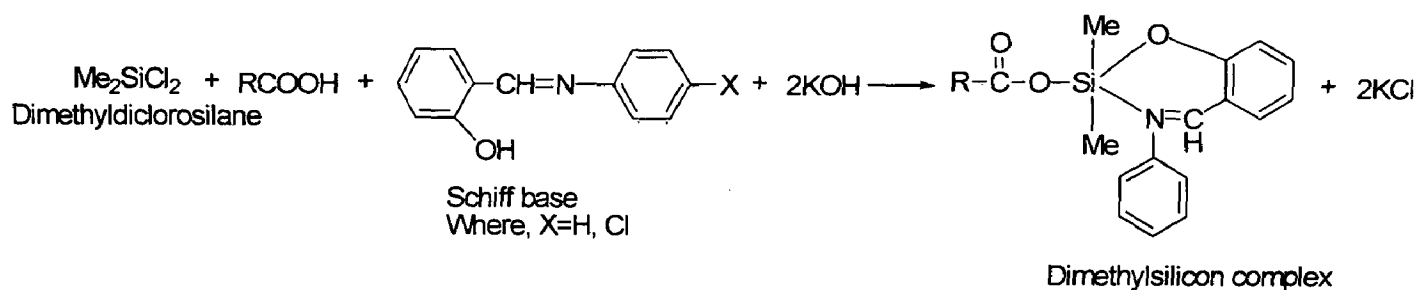
Where, R= $CH_3(CH_2)_{16}$ for Stearic acid; R= $CH_3(CH_2)_{10}$ for Lauric acid; R= $CH_3(CH_2)_{12}$ for Myristric acid.

2.5 Principle of Various Techniques and Specification of Instruments Used for Characterisation of the Complexes

2.5.1 C, H, N analysis

Carbon, hydrogen and nitrogen contents in all of the synthesized compounds were determined by Elementar-vario (III) elemental analyzer. The elemental analysis data of the synthesized complexes and Schiff bases are given in table 2, 7 and 17.

2.5.2 Ultraviolet (UV) and visible spectroscopy

Electronic absorption spectroscopy is a powerful tool in the determination of the chromophores in organic ligands. The spectra in UV-visible region are due the electronic transitions of various kinds e.g. $\sigma \rightarrow \sigma^*$, $n \rightarrow \sigma^*$, $n \rightarrow \pi^*$, $\pi \rightarrow \pi^*$ and d-d transition in case of transition metal complex. The spectra of the synthesized compounds were recorded on UV-VIS 1610PC instrument. Characteristic uv absorption along with their assignments in all the complexes are given in table 3, 8 and 15 respectively.

2.5.3 Infrared spectroscopy

IR spectroscopy is the most powerful technique for determination of various types of functional group.IR spectrum originates from the different modes of vibration and rotation of the molecules. The constituent atoms of the molecules are constantly oscillating about their mean position at definite frequencies, when such an oscillation disturbs the dipole equilibrium of the

molecules, the radiant energy will be absorbed if the frequency corresponds to the oscillation. The region of electromagnetic spectrum in which these molecular vibrations occur is called the infrared region. IR spectra were recorded on a Perkin Elmer FTIR1600 series ($4000 - 500$ cm^{-1}) spectrophotometer. KBr pellet was used for solids and for liquids, Nujol (mineral oil) with salt plates was used. Characteristic IR frequencies along with their assignments in all the complexes are given in table 4, 9 and 16 respectively.

2.5.4 Scanning electron microscope (S.E.M.)

When an electron beam strikes the sample, X-rays, secondary electron, back scattered electron, etc are radiated. Appropriate collection and processing of these radiations give lots of information about the surface, atomic number contents and composition. Secondary electrons as well as back scattered electron are used to form the image. The photographs were recorded by LEO 435VP, at I.I.C., I.IT.R.

2.5.5 X-ray diffraction

When a suitable specimen is exposed to a beam of X-rays at a suitable angle, x-rays appear to be "reflected" and the phenomenon is actually diffraction. The angle of diffraction and intensities of the diffracted beams becomes a measure of the composition of the specimen or lattice spacing of the crystal. Diffraction follows Bragg's law given by: $n\lambda = 2d \sin\theta$; where λ = wave length of X-rays used, d = plane spacing, θ = diffraction angle.

The diffraction data were recorded using Brucker AXS D8 Advance, at I.I.C., I.IT.R.

The respective tables are 12 and 13.

2.5.6 TG/DTG/DTA analysis

These techniques are useful in the determination of composition of complexes. Under TGA (thermogravimetric analysis), there is measurement of weight loss as a function of temperature change while in DTA (differential thermal analysis) difference in temperature between the sample and reference as a function of temperature is measured. Alumina was taken as references. TG/DTG/DTA are recorded on a Perkin Elmar Diamond thermal analyzer, at I.I.C., I.IT.R. These are given in table 6, 11, and 18 respectively.

24

2.5.7 ^{1}H and ^{13}C NMR technique

NMR is most powerful technique, which gives information about the number of magnetically distinct atoms of the type being studied as well as the nature of immediate environment of each type. Characteristic absorption of energy by certain spinning nuclei in a strong magnetic field, when irradiated by a second and weaker field perpendicular to it, permits the identification of atomic configuration of molecules. Absorption occurs when these nuclei undergo transition from one alignment in the applied field to another one. The principle governing ^{13}C are exactly similar to those of ^{1}H spectroscopy. NMR was recordedon a Brucker, 500 MHz NMR instrument, at I.I.C., I.IT.R. These are given in table 5, 10 and 17.

RESULTS AND DISCUSSION

RESULTS AND DISCUSSION

3.1 Trimethylsilicon Carboxylates

3.1.1 Physical characteristics of complexes

Reaction of Me_3SiCl with different organic fatty acids (HPal, HSte, HLau, HMys) in led to formation of carboxylates having general formula Me_3SiL [L= Pal, Ste, Lau, Mys]. The above reaction has been found to be facile and completed with in 30-40 h stirring. The resulting carboxylates have been obtained in good yield (75-80%). $Me_3Si(Pal)$, $Me_3Si(Ste)$, and $Me_3Si(Lau)$ have been obtained in the solid state while $Me_3Si(Mys)$ is a liquid. They have been readily soluble in methanol as well as in chloroform. Satisfactory elemental analyses have been obtained for all the compounds. All of them melt over a high temperature ranging appoximately~ 220^0C. The molar conductance values in the range 27.8- 48.6 $\Omega^{-1}cm^2mol^{-1}$ of $10^{-3}M$ solution of compounds in methanol have indicated their non electrolytic nature. Analytical data and Physical characteristics of trimethylsilicon carboxylates are given in Table 2. $Me_3Si(Pal)$ has some amount of unreacted palmitic acid which after recrystallization has not been completely removed.

Table 2: Analytical data and physical characteristics of trimethylsilicon caboxylate

S.No	Complexes (empirical formula)	m.p (^0C)	Yield (%)	M.wt. (gm)	Color and physical state	%obsd. (calcd.)		Molar conductance ($\Omega^{-1}cm^2mol$)
						C	H	
1	$Me_3Si(Pal)$	220	75	328.61	White solid	64.46 (67.73)	9.89 (11.95)	35.2
2	$Me_3Si(Ste)$	212	76	356.61	White solid	71.43 (72.90)	10.98 (12.16)	27.8
3	$Me_3Si(Lau)$	210	78	272.50	White solid	66.97 (68.02)	10.78 (11.38)	31.5
4	$Me_3Si(Mys)$	-	80	300.38	colorless liquid	-	-	48.6

3.2 Electronic Spectra

The electronic spectra of $Me_3Si(Pal)$, $Me_3Si(Ste)$, $Me_3Si(Lau)$, $Me_3Si(Mys)$ in chloroform exhibit a very intense band at 250 nm, 234 nm, 242 nm, 243 nm, respectively which may be due to $n \rightarrow \pi^*$ transition of the (COO) chromophore. This indicates the complex formation. figure 1—4 respectively shows the $n \rightarrow \pi^*$ transition.

Table 3: Electronic spectral bands of all four organosilicon carboxylates

S.No.	Compounds	Spectral data $n \rightarrow \pi^*$ (nm) of (COO)
1	$Me_3Si(Pal)$	250
2	$Me_3Si(Ste)$	234
3	$Me_3Si(Lau)$	242
4	$Me_3Si(Mys)$	243

3.3 Infrared spectra and mode of bonding

3.3.1 Trimethylsilicon carboxylates

Structural proposals are based on vibrational data, which are collected in Table 4 and given in figure 5–8 respectively for all of the complexes. The IR spectra of complexes are compared with those of the free ligands in order to determine the co-ordination sites that may involve in complexation. There are some guide peaks, in the spectra of the ligand, which are of good help for achieving this goal. The position and the intensities of these peaks are expected to be changed upon coordination. The v_{as} (COO) and v_s (COO) in the trimethylsilicon carboxylates were observed at 1689 ± 51 and 1468 ± 5 cm^{-1}, respectively, indicating that the v_{as} (COO) moved to higher frequencies and the v_s (COO) absorption either remained at the same value or moved to slight higher frequencies than in the parent organic acids. Strong interactions between carboxylate carbonyl and the silicon atom were ruled out on this basis. The band position and also Δv values [v_{as} (COO) — v_s (COO)] were in the range (221-$267 cm^{-1}$), indicating that the

carboxylate groups act as monodentate ester; ionic as well as bridging or chelated (COO) groups, which would give $\Delta v < 200 cm^{-1}$, were thus excluded. The conclusions drawn above were further supported by the presence of new bands in all the complexes at ca. 848 ± 38 and 638 ± 14cm^{-1} which may be assigned as $v_{as}(Si-O)$ and $v_s(Si-O)$ respectively. The IR spectra of trimethylsilicon carboxylates show two bands at 1383 ± 16 and 1255 ± 6 cm^{-1}, which have been assigned to the asymmetric and symmetric deformation modes of the CH_3-Si respectively. A weak to medium intensity band at 804 ± 4cm^{-1} may be due to $v(Si-C)$ modes.

Table 4: Characteristic IR frequencies of acids and organosilicon carboxylates

S.No.	Ligand/ Complexes	v(OH) (cm⁻¹)	v_sym(OCO) v_asym(OCO) (cm⁻¹)	vas(Si—O) v_s(Si—O) (cm⁻¹)	v(Si—C) (cm⁻¹)	v_as(Si—C) v_s(Si—C) (cm⁻¹)
1	HPal	3412br	1703vs 1468s	-	-	-
2	HSte	3421br	1713w 1466m	-	-	
3	HLau	3410br	1701vs 1466s	-	-	-
4	HMys	3425br	1701vs 1468s	-	-	-
5	Me₃Si(Pal)	3431br	1705vs 1473s	825s 620w	805s	1446w 1261s.
6	Me₃Si(Ste)	3414br	1638vs 1471s	886s 624s	806s	1430s 1303m
7	Me₃Si(Lau)	3418br	1638vs 1462s	878w 624m	816m	1368s 1295vs
8	Me₃Si(Mys)	3469br	1740w 1463m	853w 722s	800w	1376vs 1352w
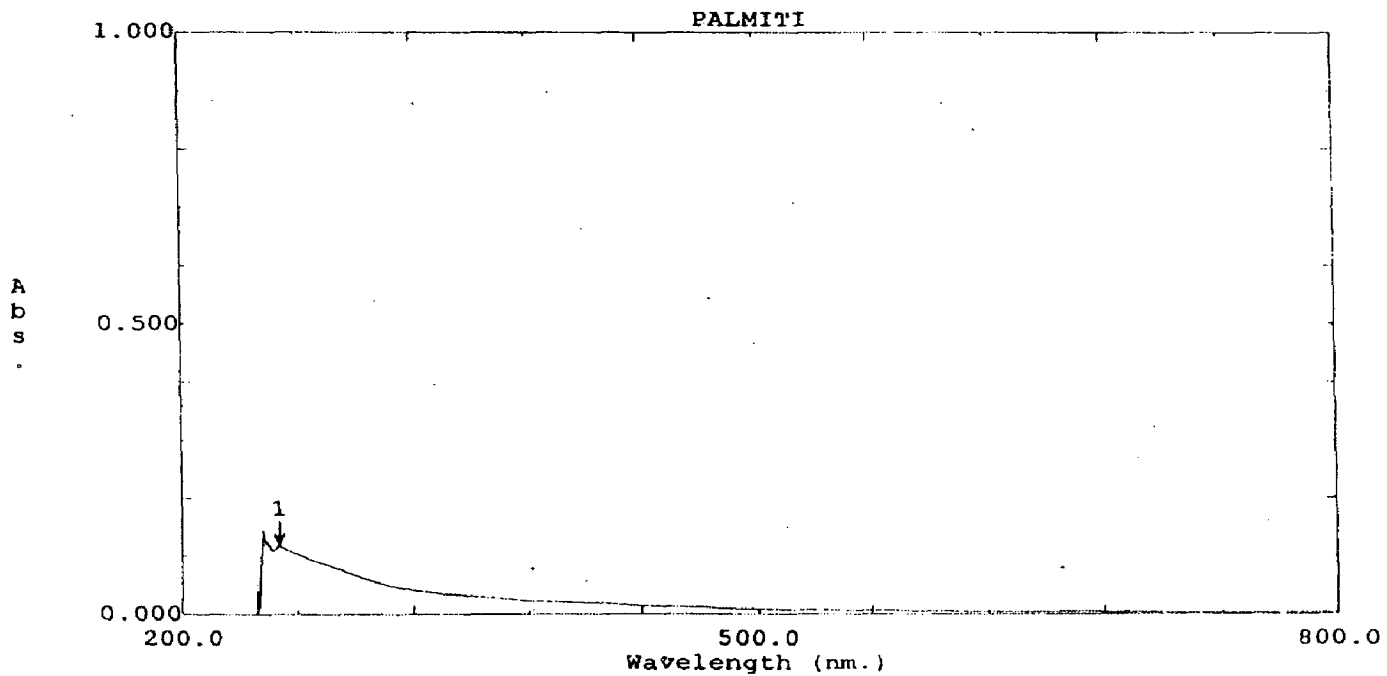
Figure 1: Electronic spectrum of Me₃Si(Pal)
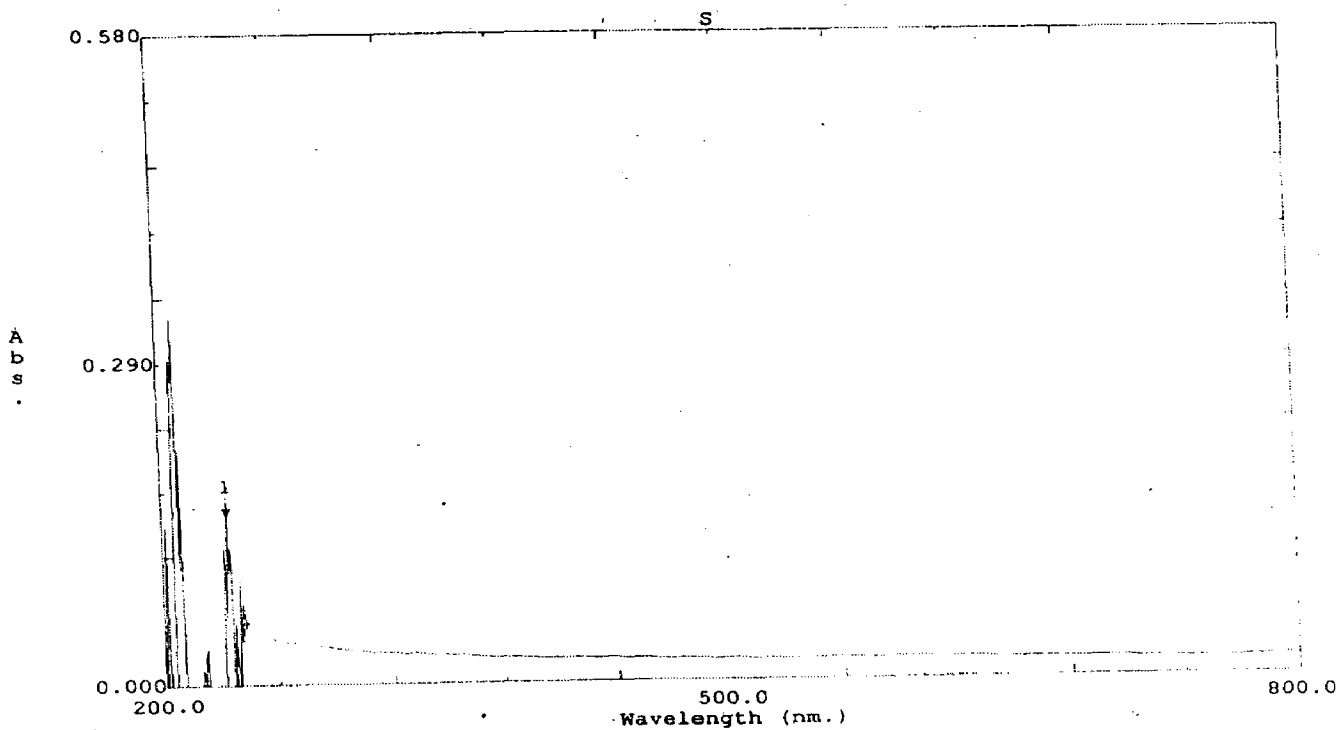
Figure 2: Electronic spectrum of Me₃Si(Ste)

29
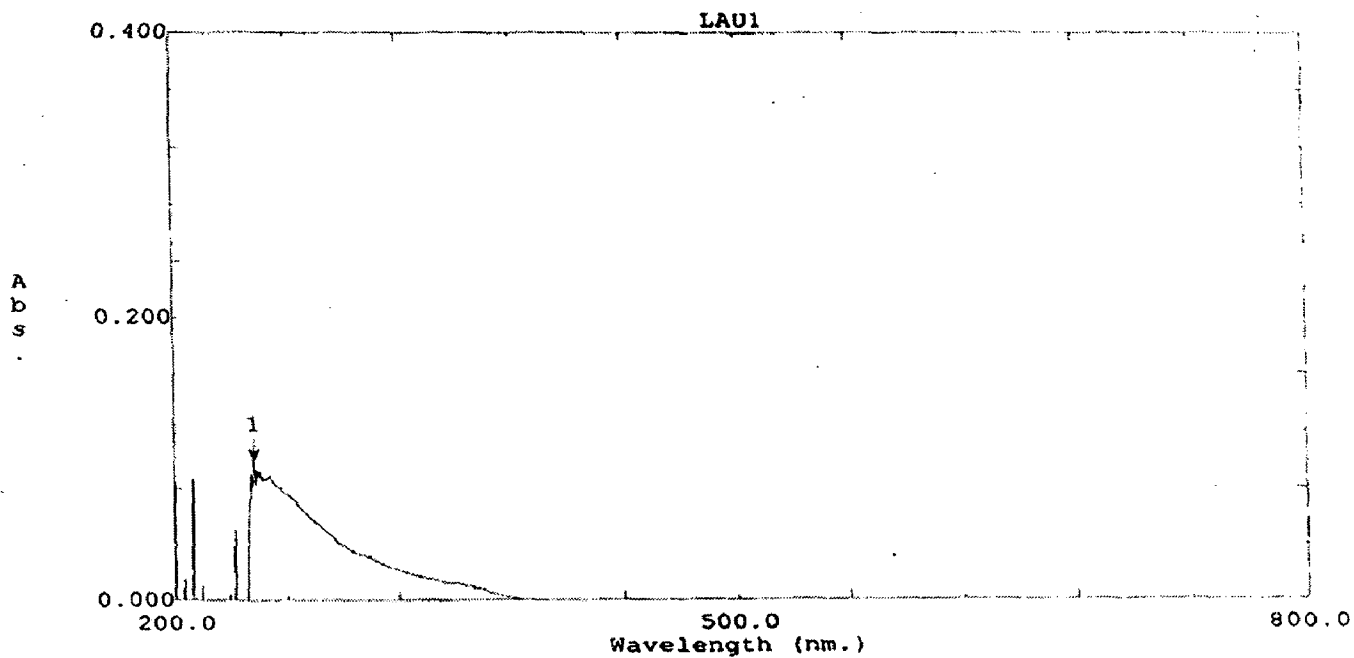
Figure 3: Electronic spectrum of Me₃Si(Lau)
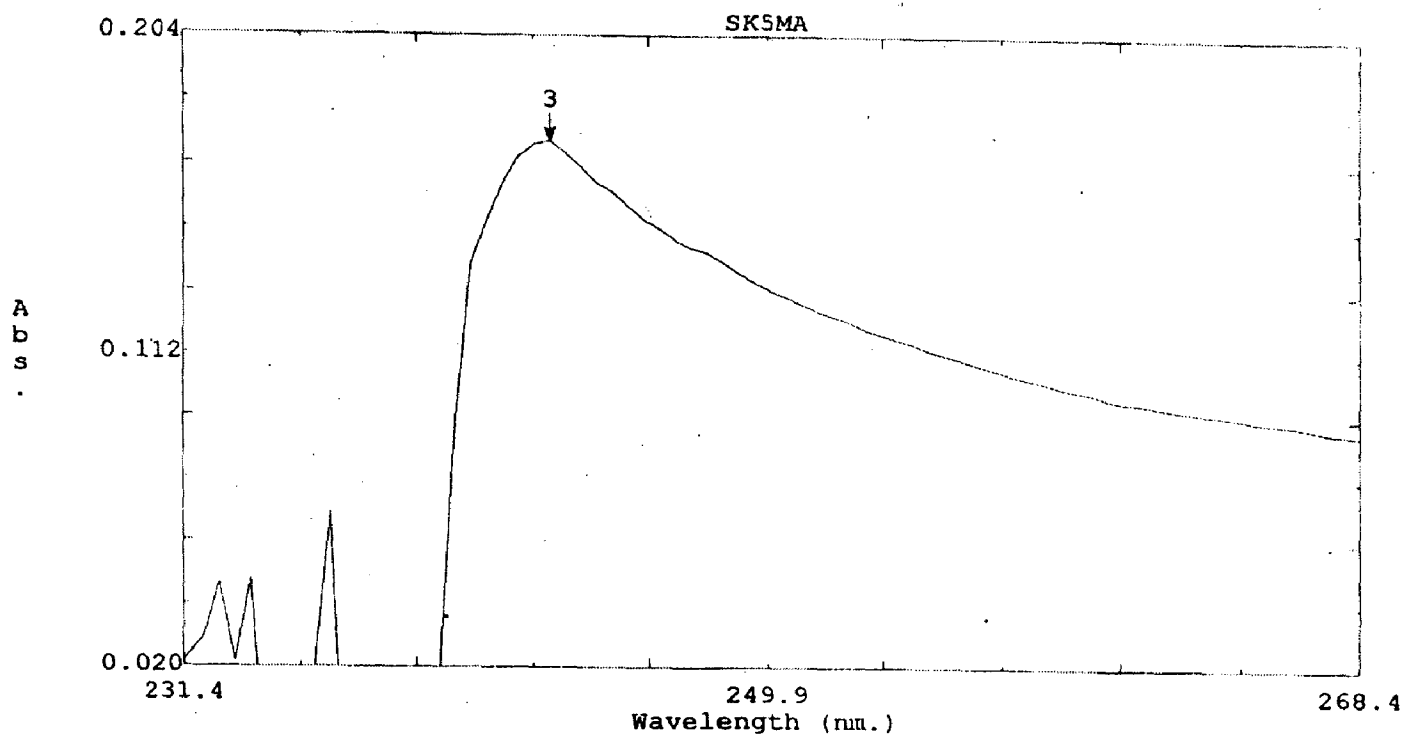
Figure 4: Electronic spectrum of Me₃Si(Mys)
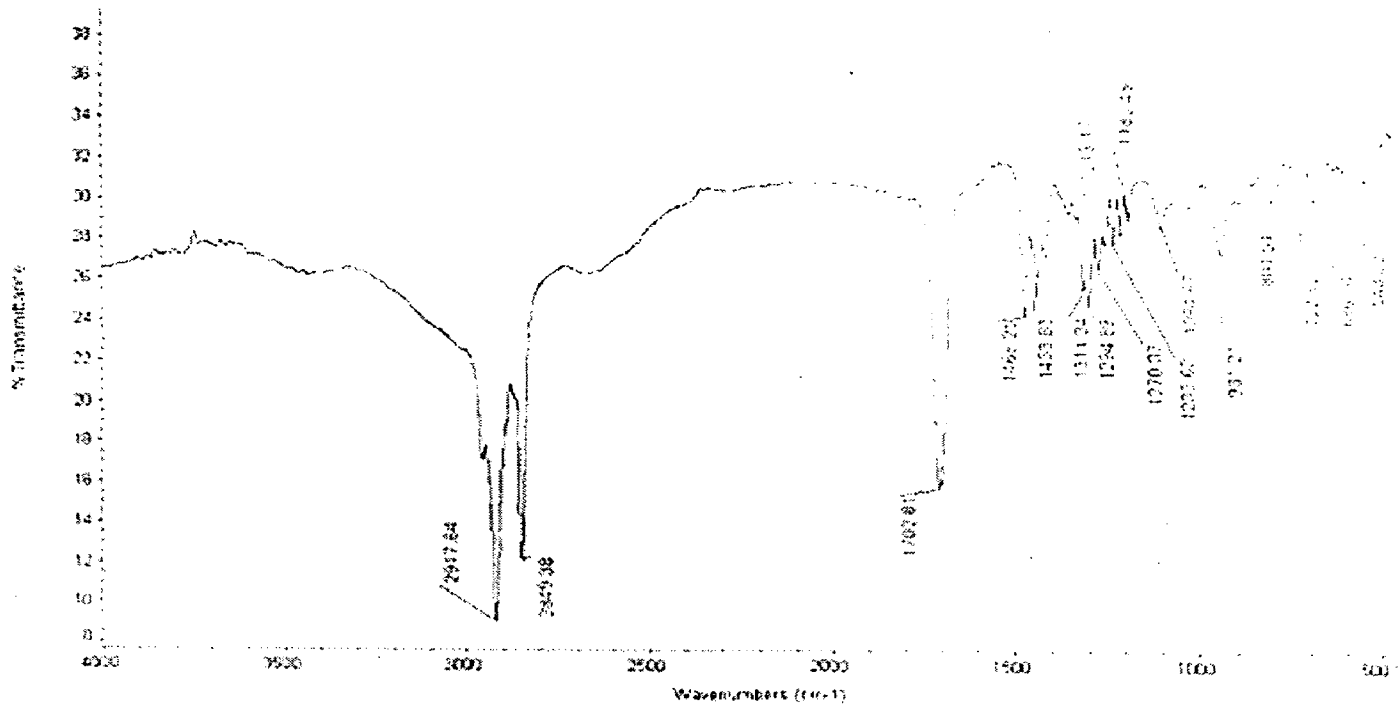
Figure 5: IR spectrum of Me₃Si(Pal)
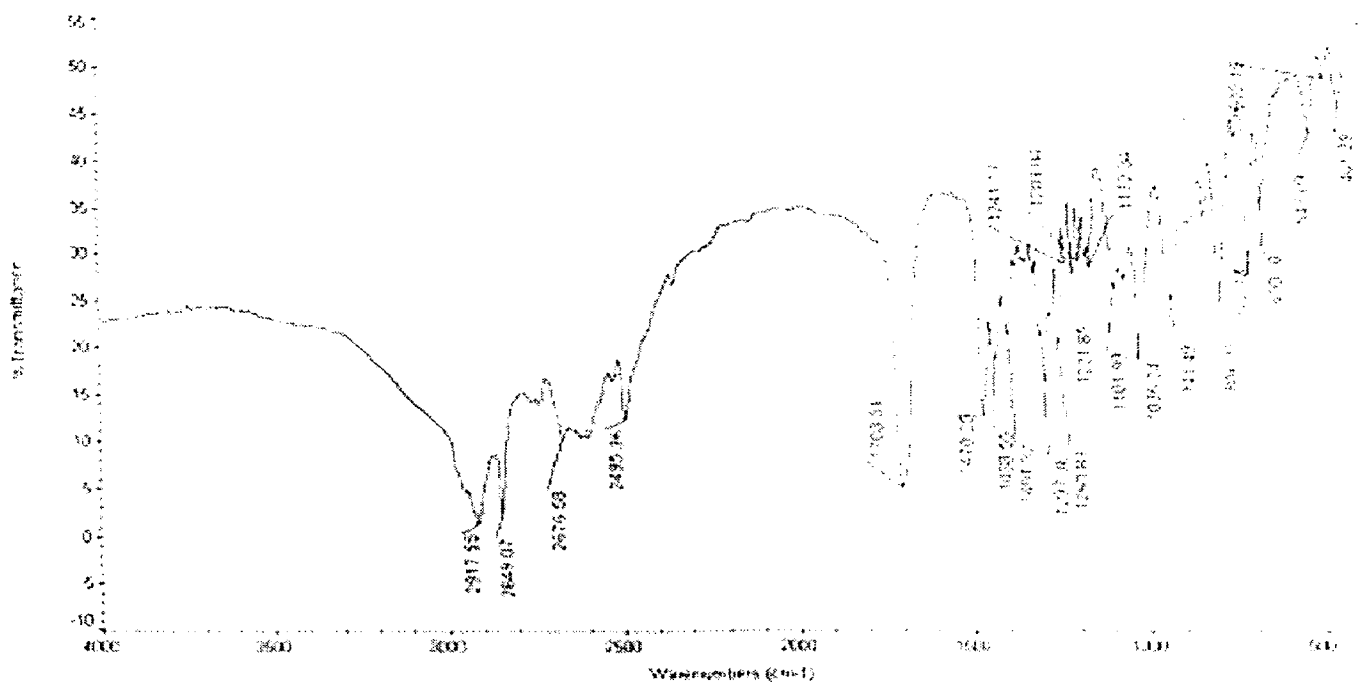
Figure 6: IR spectrum of Me₃Si(Ste)

31
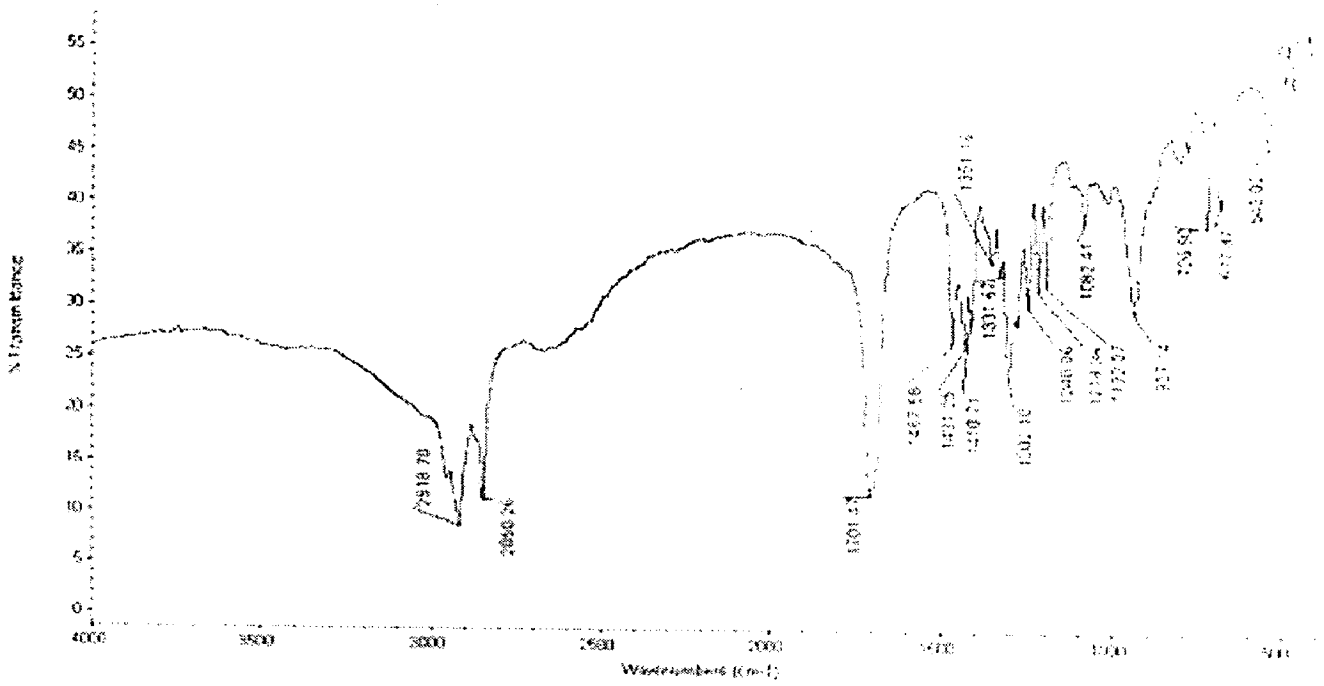
Figure 7: IR spectrum of Me₃Si(Lau)
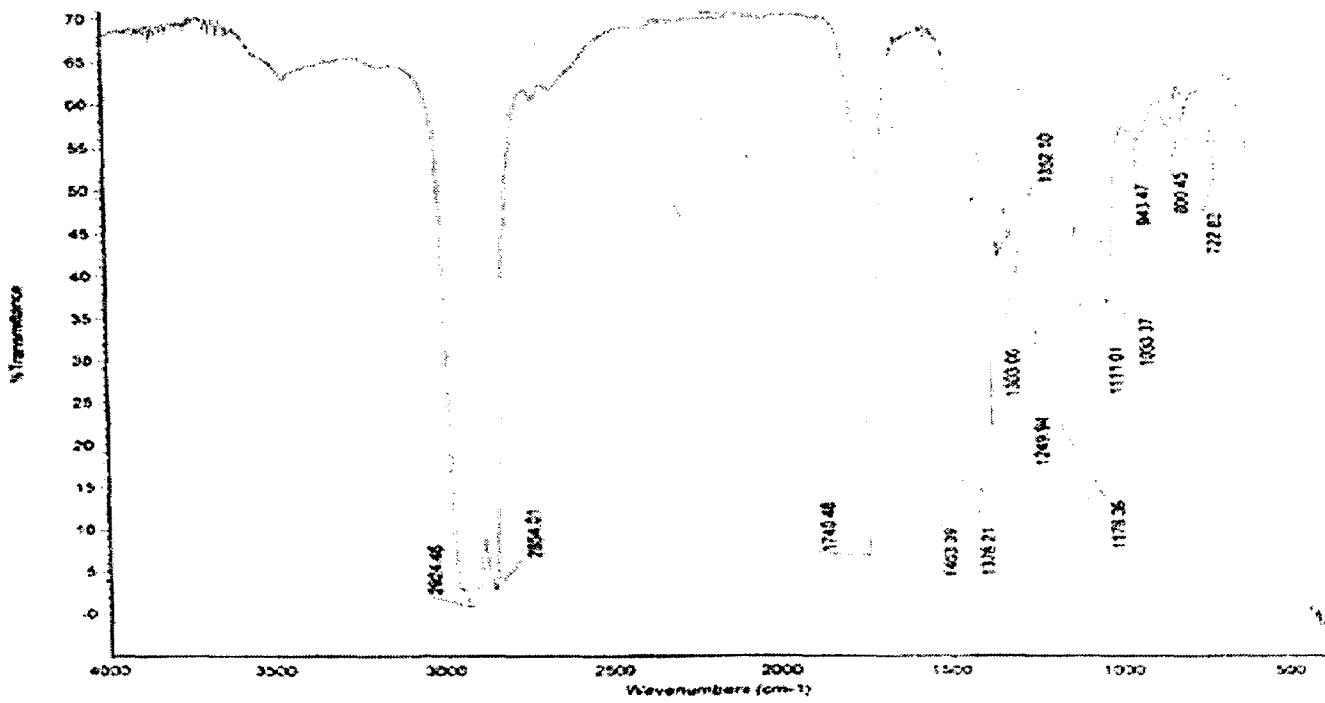
Fig

ure 8: IR spectrum of Me₃Si(Mys)

3.4 ^{1}H and ^{13}C NMR analysis

The expanded form of molecular formula of organosilicon caboxylate is given below and shown in figure 9 (^{1}H) and figure 10 (^{13}C) respectively.

Me$_3$Si(Mys):[C^{14}H$_3$-C^{13}H$_2$-C^{12}H$_2$-C^{11}H$_2$-C^{10}H$_2$-C^{9}H$_2$-C^{8}H$_2$-C^{7}H$_2$-C^{6}H$_2$-C^{5}H$_2$-C^{4}H$_2$-C^{3}H$_2$-C^{2}H$_2$-C^{1}OO]Si-(C*H$_3$)$_3$
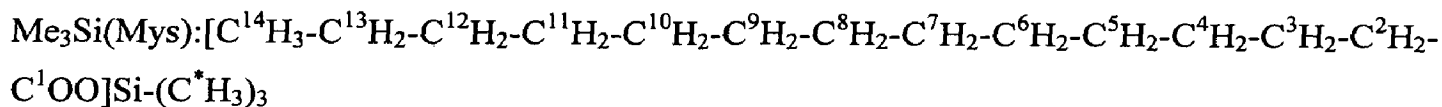
The chemical shift (δ,ppm) of various protons in organosilicon carboxylates, which are sufficiently soluble in MeOD and CDCl$_3$, are given in Table 5.The data supported the formation of trimethylsilicon mystrate. For other complexes, trimethylsilicon stereate, trimethylsilicon laurate, trimethylsilicon palmate, NMR could not be recorded unfortunately because of mechanical problem which persisted for longer time.
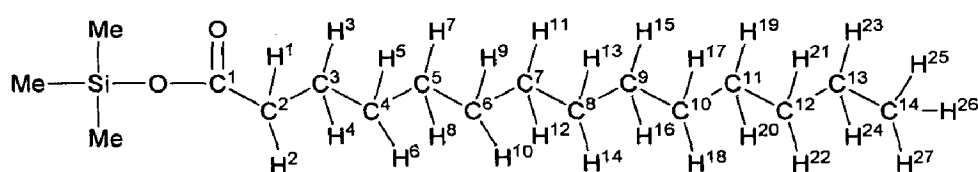
Trimethylsilicon myristate

Table 5: ^{1}H and ^{13}C NMR spectral data

S.No.	Compounds	Analysis	δ(ppm)
1	Me$_3$Si(Mys)	^{1}H	1.62-0.87 (m, 32H) (for H^5-H^{27} & 9 Si-Me protons), 2.78 (br s, 2H) (for H^3 & H^4), 4.12 (br s, 2H) (for H^1 & H^2)
		^{13}C	C^1-173.9; C^2-34; C^3-32;C^4 - C^{11}(29.6-29.1) ; C^{12}-24.9; C^{13}-22.7; C^{14}-14;

On the basis of electronic, IR, ^{1}H/ ^{13}C NMR spectral studies following tetrahedral structure for trimethylsilicon carboxylate has been proposed. The figure is given below:
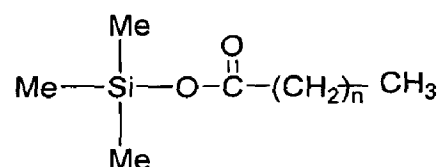
where, n = 10 for lauric acid; n = 12 for myristic acid; n = 14 for palmitic acid; n = 16 for stearic acid
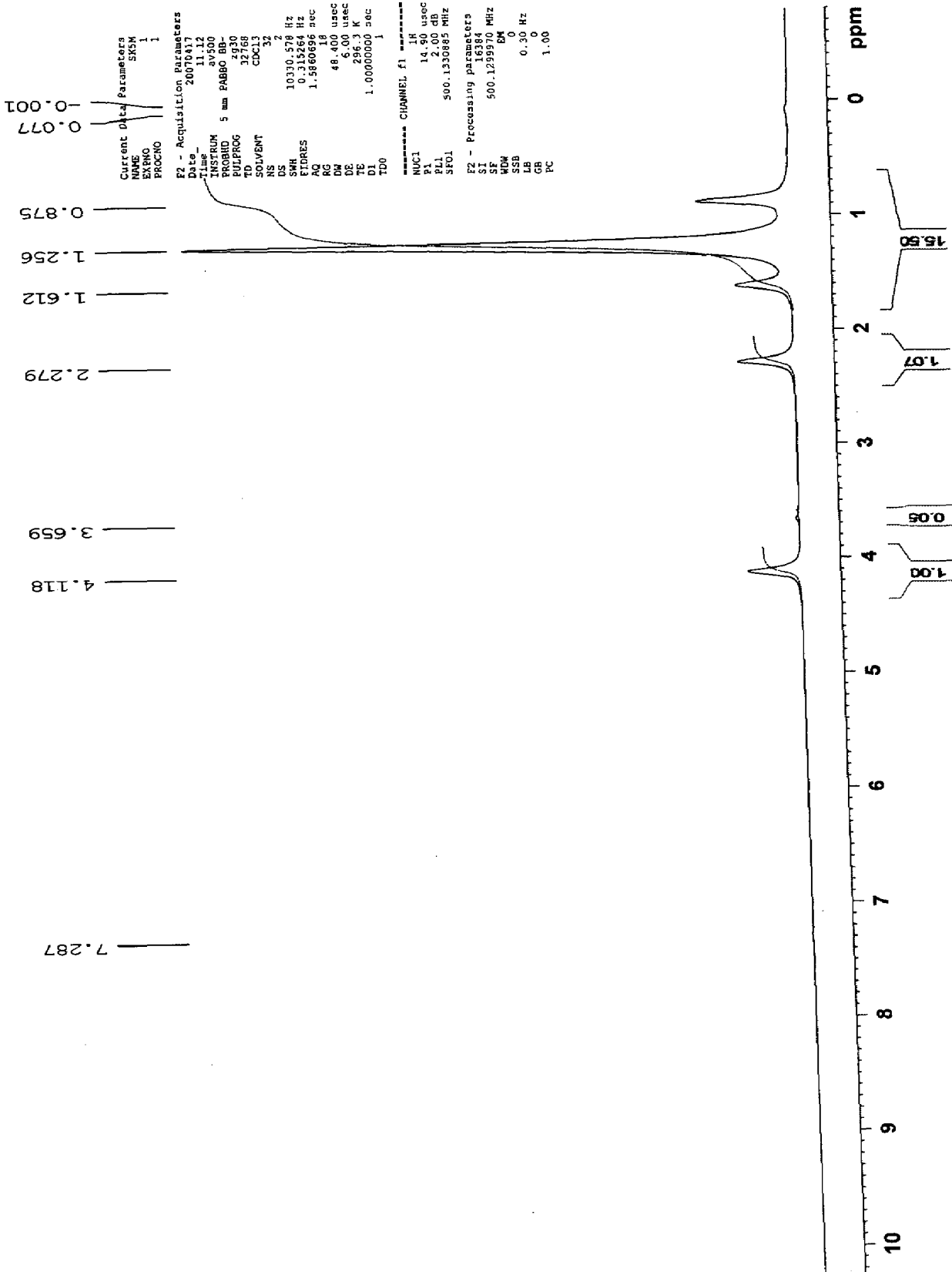
Figure 9: ^{1}H NMR spectrum of Me$_3$Si(Mys)
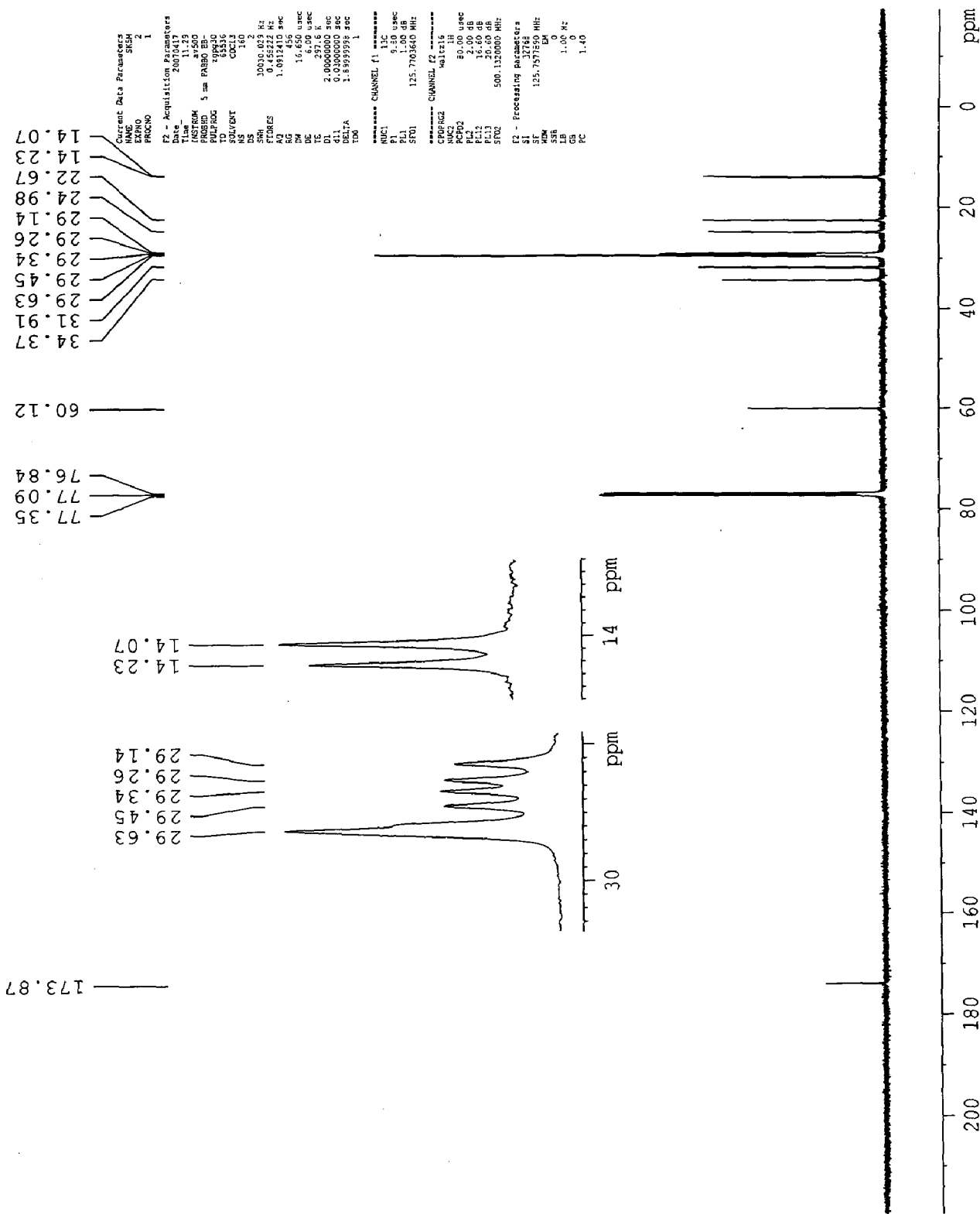
Figure 10: ^{13}C NMR spectrum of Me$_3$Si(Mys)

3.5 TG, DTG and DTA analysis

TG, DTG and DTA data of Me₃Si(Pal), Me₃Si(Ste) and Me₃Si(Lau) are given in table 6 and presented in figure 11–13 respectively.

Me₃Si(Pal) complex, shows one step decomposition in the temperature range from 25–275 °C. Decomposition pattern shows one peak at 245 °C in DTG curve and three peaks in DTA curve. In DTA curve, first endothermic peak · at 64 °C corresponds to m.p. of palmitic acid (contaminated in complex as impurity) second and third exothermic peak at 215 °C and 297 °C (broad) respectively corresponds to decomposition of the complex to give the end product SiO₂ and finally sublimed.

$$\text{Me}_3\text{Si(Pal)} \xrightarrow{\ \ 25\text{-}275\ ^0\text{C}\ \ } \text{SiO}_2 \longrightarrow \text{sublimed}$$
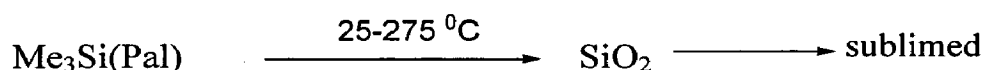
Me₃Si(Ste) complex shows incomplete decomposition because of sticking during the decomposition, still there are some decomposition steps. The first TG curve ranges 26–85 °C. There corresponds an endothermic peak in DTA curve at 58 °C which is m.p. of acid (contaminated in complex as impurity). The second and third temperature range of TG curve (85–119 °C, 119–193 °C) indicates decomposition of two methyl groups, supported by endothermic peak at 99 °C and 128 °C in DTA curve.

Me₃Si(Lau) complex shows one step decomposition. One endothermic peak in DTA at 48 °C corresponds to m.p. of lauric acid (contaminated in complex as impurity), and another peaks at 186 °C and 236 °C respectively corresponds to decomposition of organic acid from the complex and finally sublimation, indicated by exothermic nature of DTA curve at 300 °C and 388 °C respectively and DTG curve at 234 °C.

$$\text{Me}_3\text{Si(Lau)} \xrightarrow{\ \ 100\text{--}247\ ^0\text{C}\ \ } \text{Decomposed and Sublimed}$$
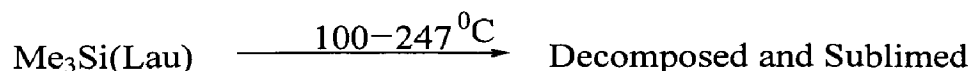
Table 6: TG, DTA and DTG data of organosilicon carboxylates.

S.No.	Compounds	Step	TG Temp. range (°C)	DTG (°C)	DTA (°C)	ΔH (mJ/mg)	Wt. loss(%) obsd.(calcd.)	Species lost
1	Me₃Si(Pal)	I	25-275	245	64 215	197 -225	81.72 (81.37)	$C_{19}H_{37}$
2	Me₃Si(Ste)	I	26-85	58	58	28.1	2.24	H_2O
		II	85-119	94	99	54.6	3.40	CH_3 .
		III	119-193	126	128	42.8	3.19	CH_3
		IV	193-450	203	203	-159	incomplete	-
3	Me₃Si(Lau)	I	100-247	234	186 236	52.5 83.3	-	-

From the above discussion based on TG, DTA and DTG it is clear that Me₃Si(Pal) is more stable than Me₃Si(Lau) though its decomposition starts early.
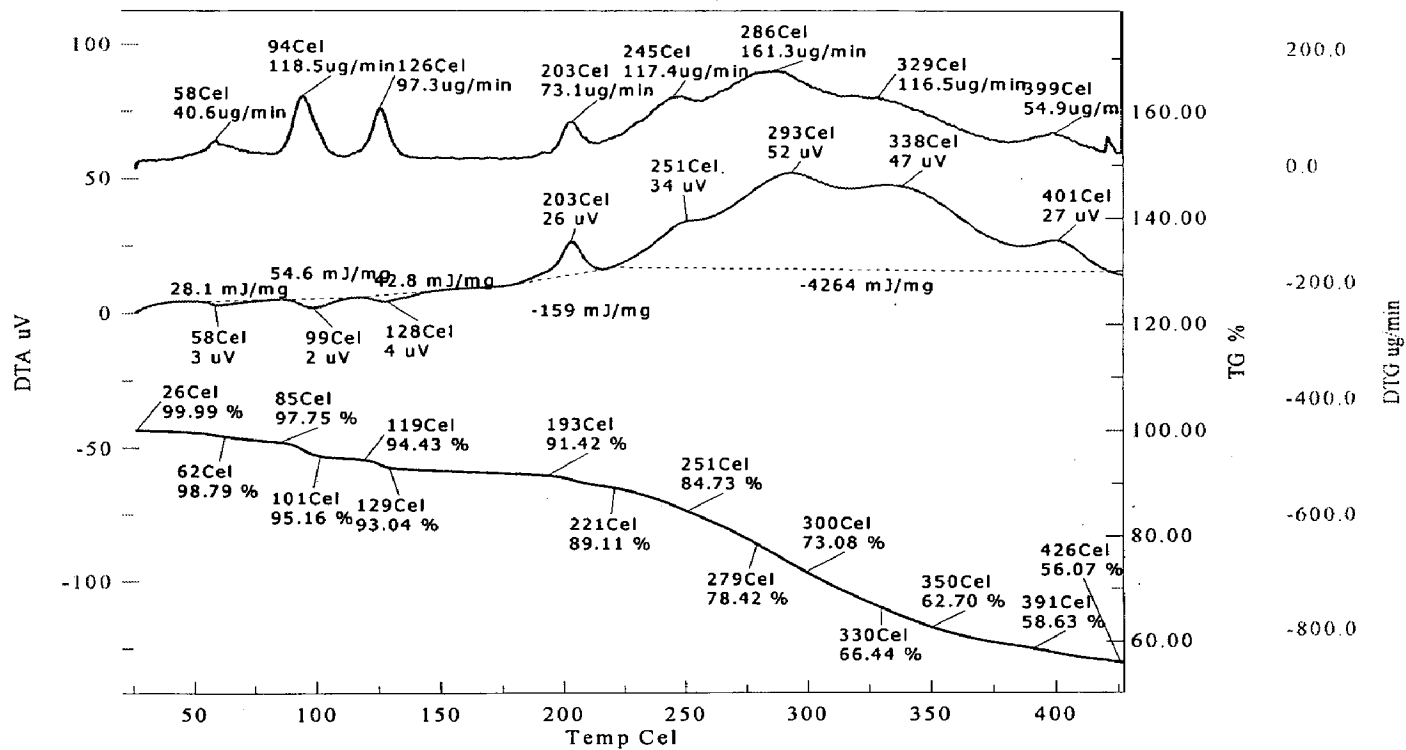
Figure 11: DTA –DTG –TG of Me₃Si(Pal)
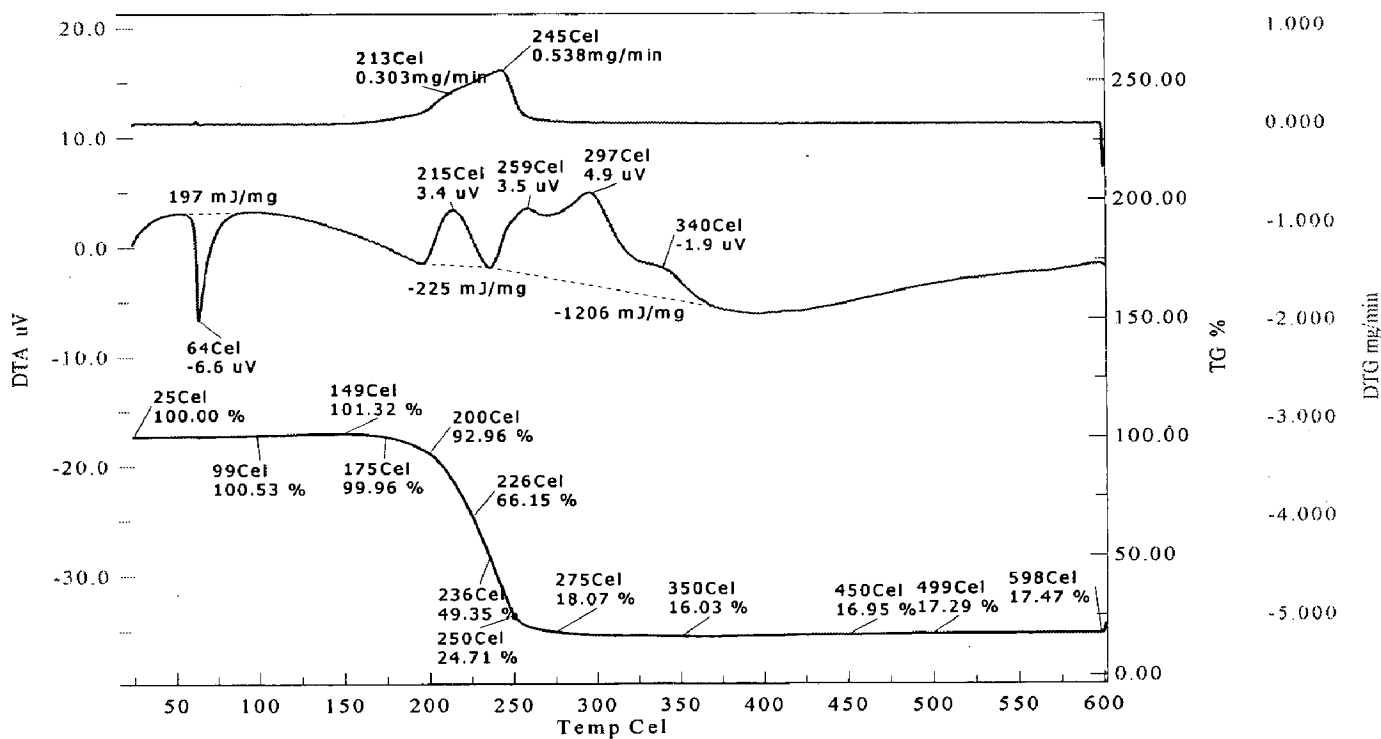
Figure 12: DTA –DTG –TG of Me₃Si(Ste)
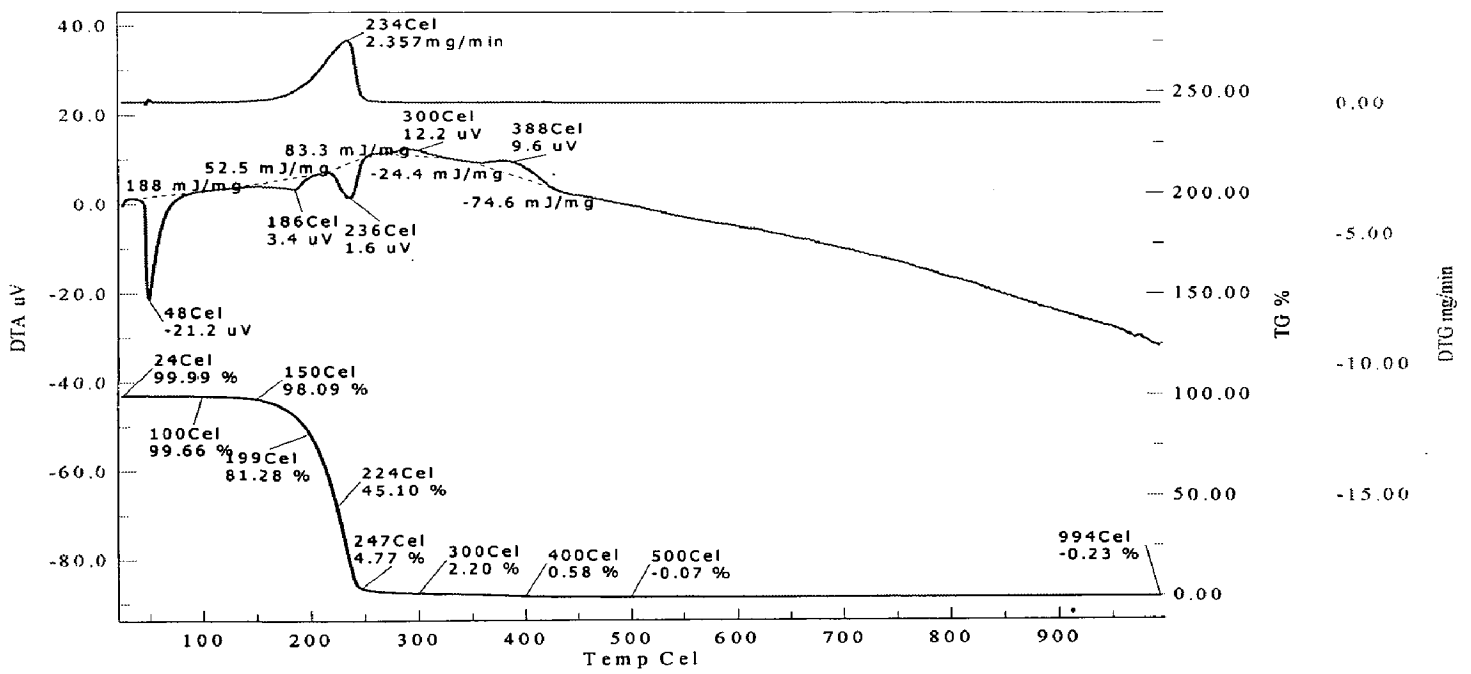
Figure 13: DTA –DTG –TG of Me₃Si(Lau)

3.6. Di- and Tri-methylsilicon Derivatives of Schiff base Derived from HSal-2-ambz

3.6.1 Physical characteristics

The physical characteristics of products are summarized below in the table 7.

Table 7: Analytical data and physical characteristics of trimethylsilicon and dimethylsilicon complexes derived from HSal-2-ambz

S. No	Complexes (empirical formula)	m.p (^{0}C)	Yield (%)	M.wt. (gm)	Color; physical state	%obsd. (calcd.)			Molar conductance ($\Omega^{-1}cm^2mol$)
						C	H	N	
1	Me$_2$Si(sal–2–ambz)$_2$	220	75	558	Dark brawn ; sticky solid	-	-	-	28.2
2.	Me$_3$Si(sal–2–ambz)	210	79	323	Light Brawn; solid	62.2 (66.67)	6.19 (4.10)	8.00 (13)	24.3

3.6.2 Electronic spectra

The electronic spectra of Sal–2–ambz, Me$_2$Si(sal–2–ambz)$_2$, and Me$_3$Si(sal–2–ambz) in methanol (solvent) are represented in fig 14–16 respectively and characteristic bands are given in table 8.

The band at 319 ± 4 nm in all of the compounds is due to n→π* transition arising from (>C=N) group of benzimidazole moiety. The band at 281–282 nm (B - band, n→π*) is due to benzene ring of benzimidazole. The band at 275 nm, in all of the compounds is due to π-π*transition of (>C=N) group of benzimidazole moiety or n→π* of benzene ring. The band observed in the range 244–257 nm is due the n→π* arising from the azomethine group of salicyaldimine. The band at 209–215 nm is due to solvent or benzene (E- band, π→π*). A shift in n→π* transition of azomethine group towards shorter wave length side (blue shift) indicates the coordination of azomethine (>C=N) group.

40

Table 8: Electronic spectral data of Hsal-2-ambz and its di- and tri-methylsilicon complexes

S.No.	Compounds	Transitions λ_{max}(nm); [Abs.]			
		$\pi \rightarrow \pi^*$ of C=N$_{benzi}$ / B-band of C_6H_6	$n \rightarrow \pi^*$ of C=N$_{benzi}$; B-band of C_6H_6	$n \rightarrow \pi^*$ (solvent/benzene)	$n \rightarrow \pi^*$ of C=N$_{azomethine}$
1.	HSal-2-ambz*	275[0.7102]	319[0.2510] 282[0.6257]	209 [1.9862]	257[0.9989]
2.	Me$_2$Si(sal-2-ambz)$_2$	275[1.5179]	327[0.1448] 281[1.4185]	215 [2.1116]	244[1.4161]
3.	Me$_3$Si(sal-2-ambz)	275[0.9064]	321[0.1591] 281[0.8446]	213 [1.8898]	249[0.9119]

ambz* = aminomethylbenzimidazole, sal* = salicylaldehyde

3.6.3 Infrared spectroscopy

Infrared spectra of Sal–2–ambz, Me$_2$Si(sal–2–ambz)$_2$, and Me$_3$Si(sal–2–ambz) are given in figure 17–19 and characteristics frequencies along with their assignments are presented in table 9.

A broad absorption band in the region 3430—3467 cm^{-1} is due to v(N–H) present in all of the compounds. The band at 1636 cm^{-1} is due to azomethine group of salicylaldimine. A downward shift in v(C=N) absorption frequencies (5–7 cm^{-1}) indicates the co-ordination of the azomethine group with Si, which is further confirmed by the presence of a new absorption band in the region 520—580 cm^{-1} due to Si←N bond, in both the complexes.

The band at 886 cm^{-1} is assigned to v_{as}(Si–O) and a band in the region 620–628 cm^{-1} is due to v_s(Si–O). Further, v_{as} (Si–C) and v_s(Si–C) frequencies are observed at 1422 ± 2 cm^{-1} and in the region 1220–1266 cm^{-1}, respectively.

Table 9. Characteristic infrared frequencies (cm^{-1}) and their assignments in Hsal-2-ambz and its di- and tri-methylsilicon complexes

S. No.	compounds	$\nu(OH)$	$\nu(C{\equiv}N)$	$\nu(N{-}H)$	$\nu(Si{-}N)$	ν_{as} (Si–O) ν_{as}(Si–O)	$\nu(Si{-}C)$	ν_{as}(Si –C) ν_s(Si–C)
1.	HSal-2-ambz	3125br	1636s	3430br				
2.	Me$_3$Si(sal-2- ambz)	3467br	1629s	3467br	580w	886s 621s	772m	1424s 1220s
3.	Me$_2$Si(sal-2- ambz)$_2$	3466br	1631s	3466br	520w	886w 628s	800m	1422m 1266s
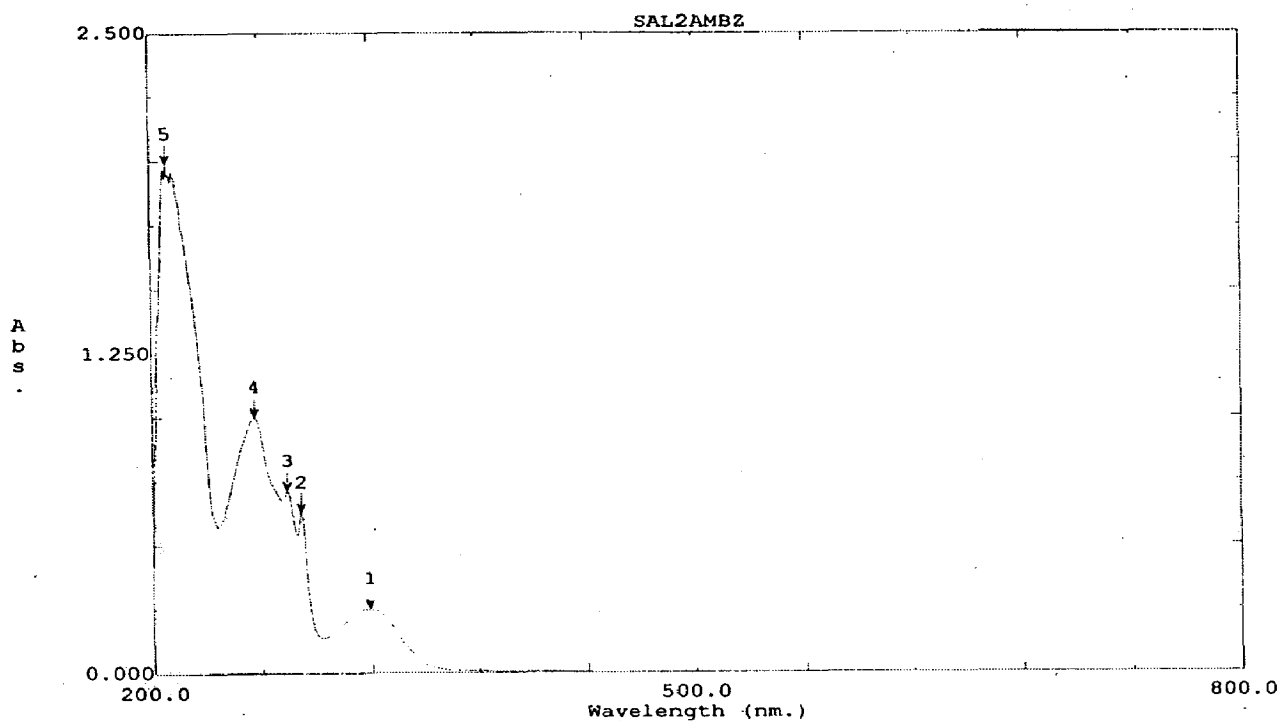
Figure 14: Electronic spectrum of HSal-2-ambz
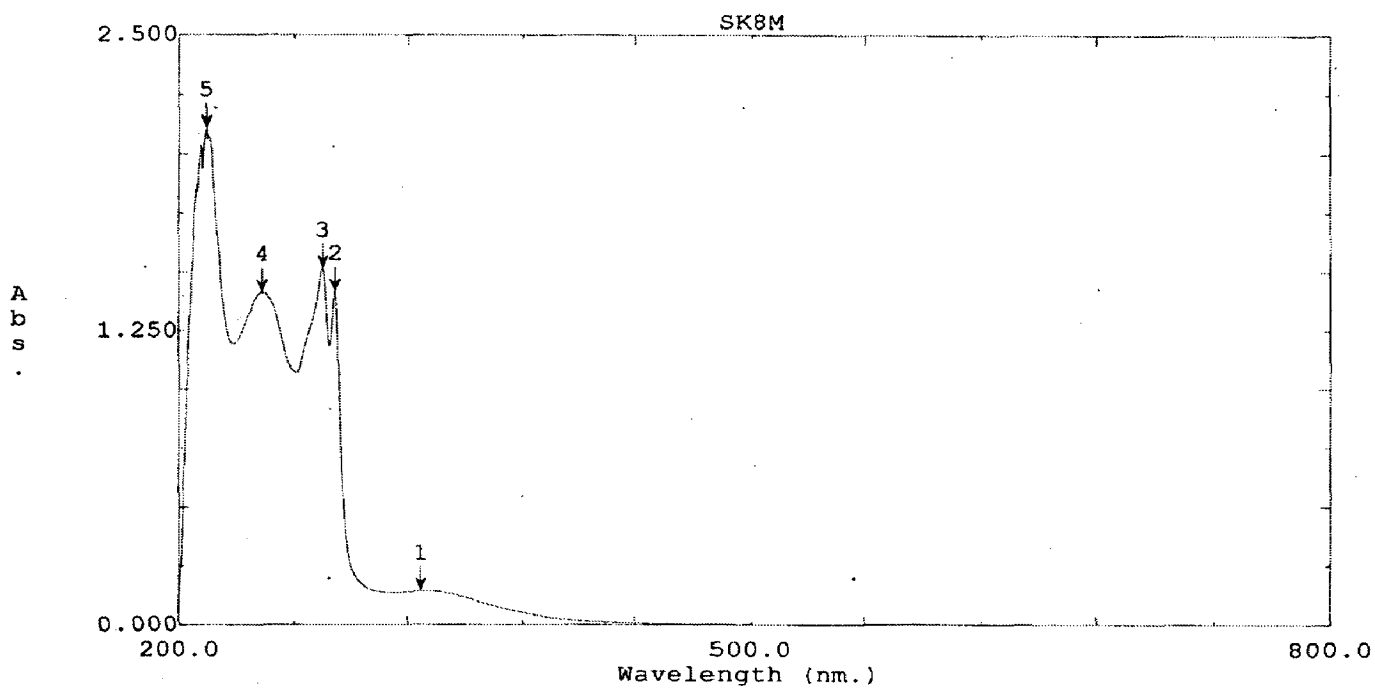
Figure 15: Electronic spectrum of Me₂Si(sal-2-ambz)₂

43
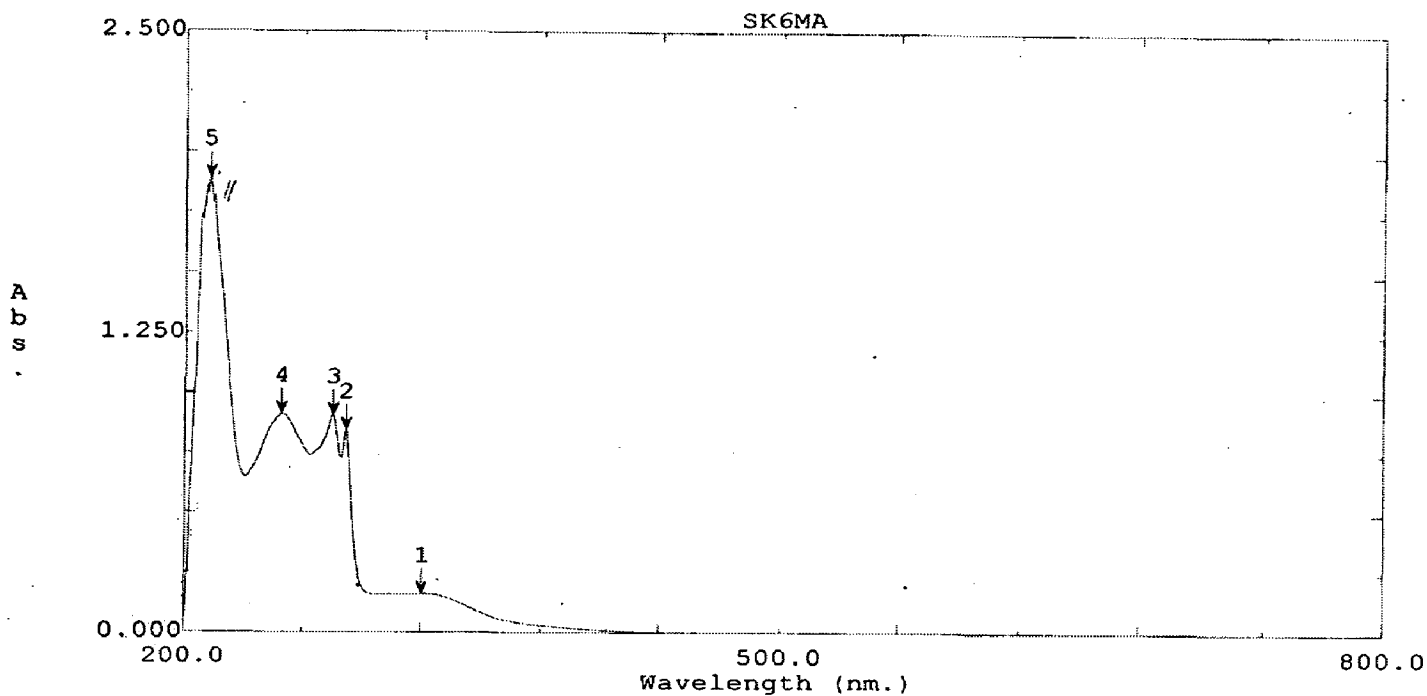
Figure 16: Electronic spectrum of Me₃Si(sal-2-ambz)
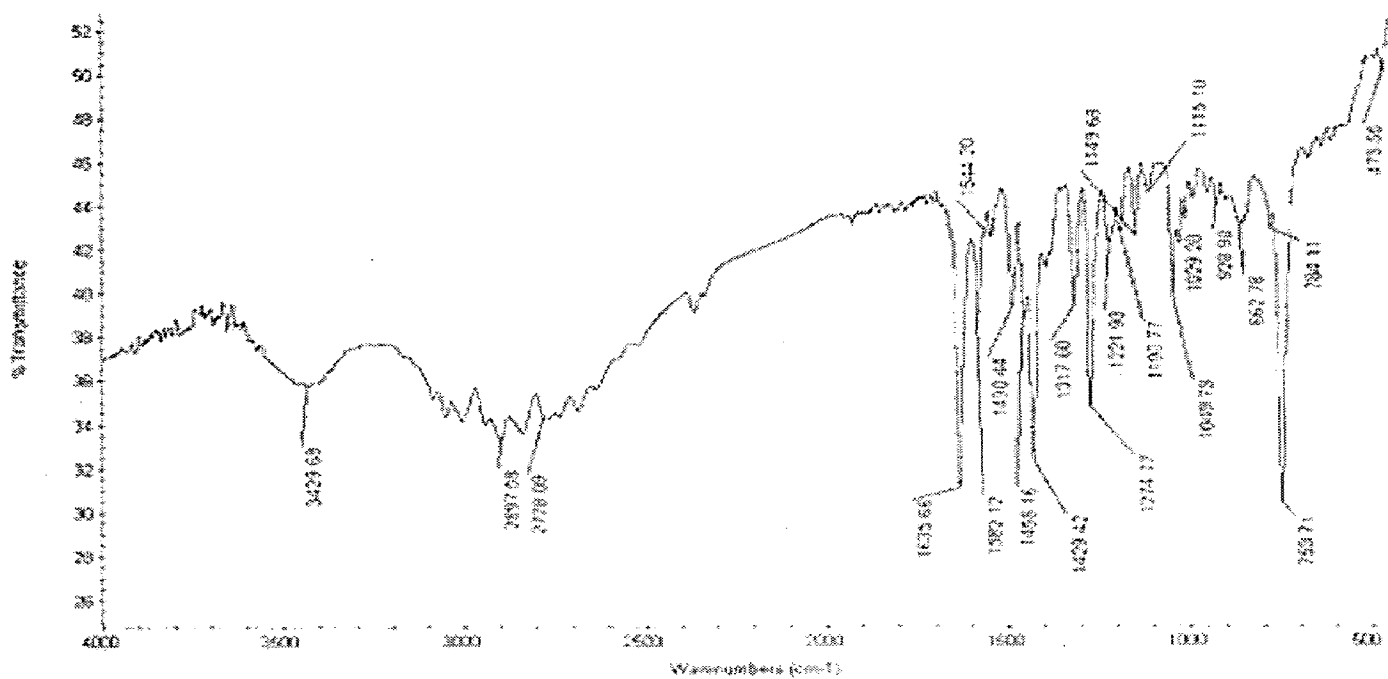
Figure 17: IR spectrum of HSal-2-ambz
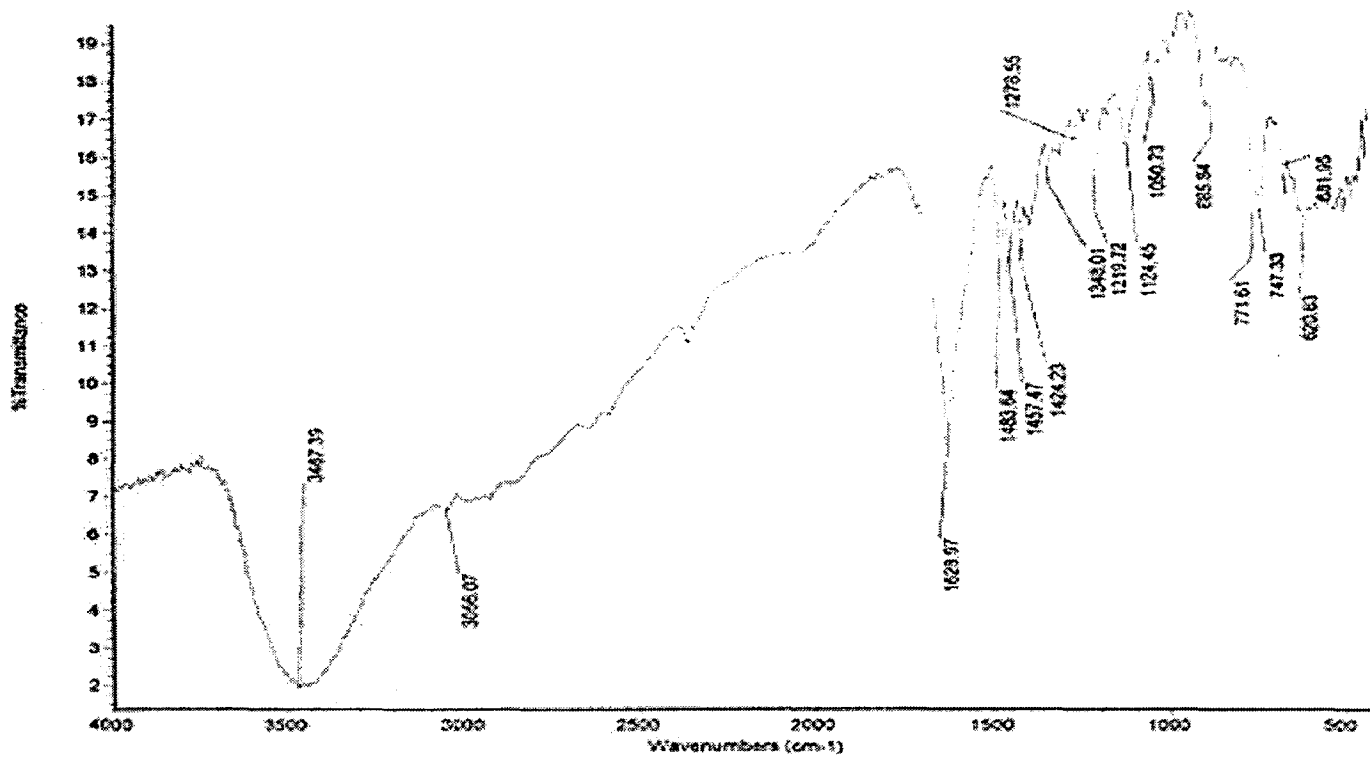
Figure 18: IR spectrum of Me₃Si(sal-2- ambz)
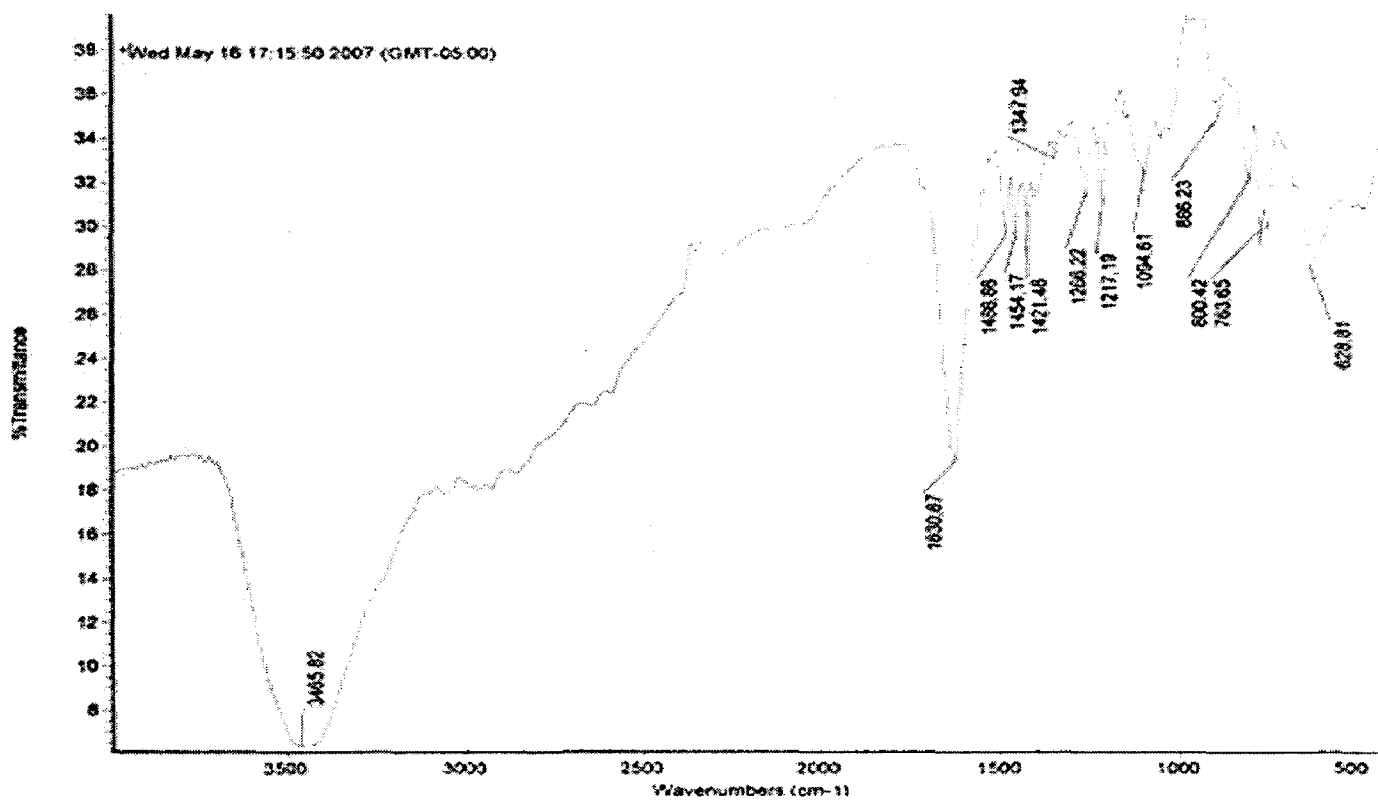
Figure 19: IR spectrum of Me₂Si(sal-2- ambz)₂

45

3.6.4 ^{1}H and ^{13}C NMR Spectra

The chemical shift (δ ppm) for various protons and carbons are listed in the table 10 below and given in figure 20 and 21 respectively.
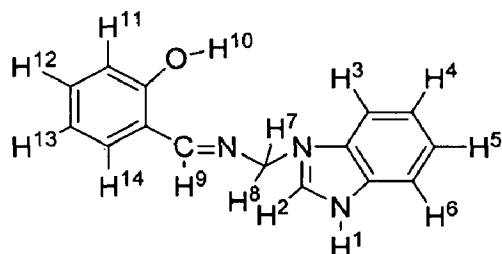
Figure: HSal–2–ambz (expanded form)

Table 10: ^{1}H and ^{13}C values for HSal-2-ambz

S.No.	Compounds	Analysis	δ(ppm)
1	HSal–2–ambz	^{1}H	8.66 (s, 1H) (for H^9), 7.54-6.87 (m, 9H) (for H^2-H^6, H^{11}-H^{14}), 5.02 (s, 2H) (for H^7 & H^8)
		^{13}C	168.50, 151.49, 132.50, 131.85, 118.66, 116.30, 56.26.

46
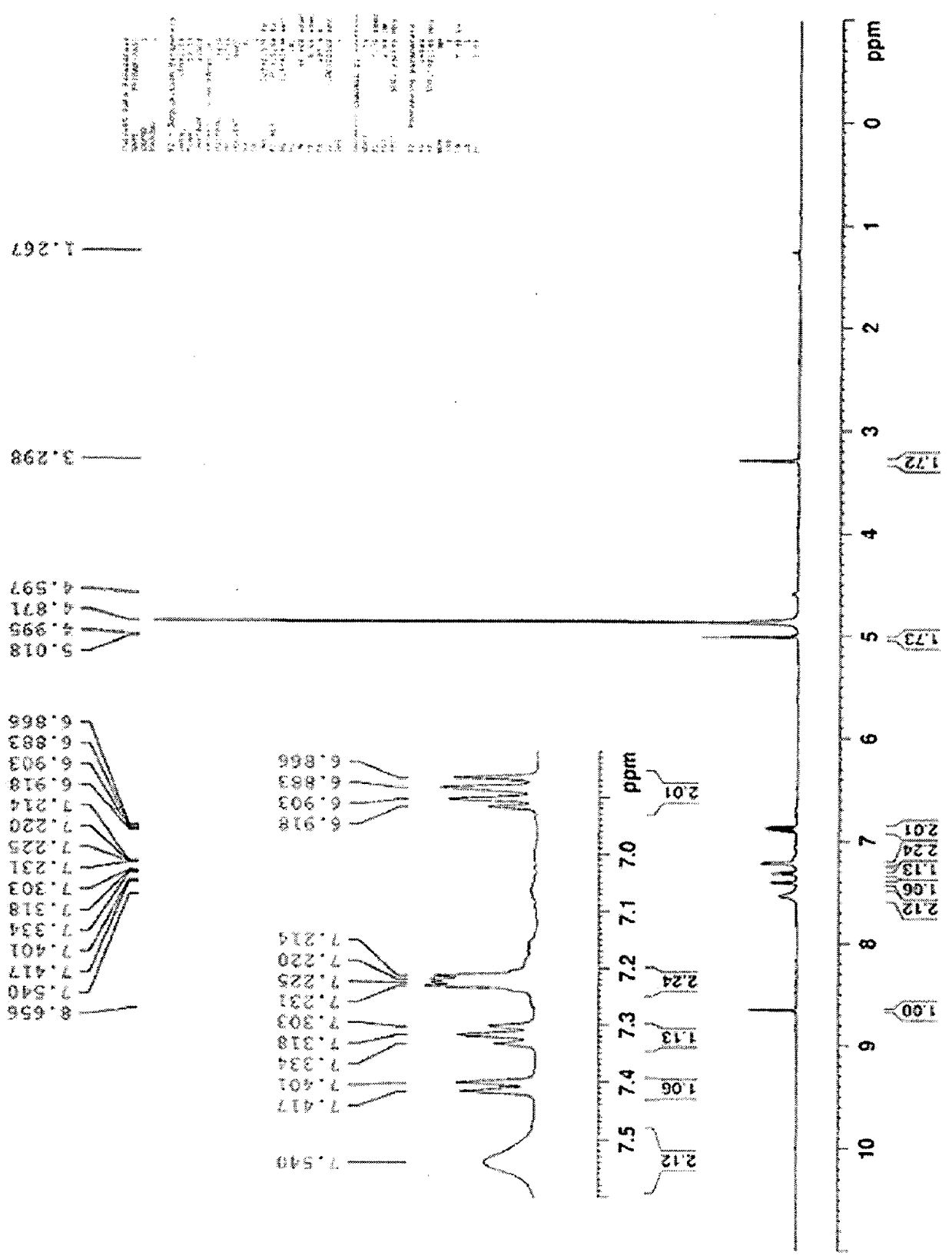
Figure 20: ^{1}H NMR of HSal-2-ambz
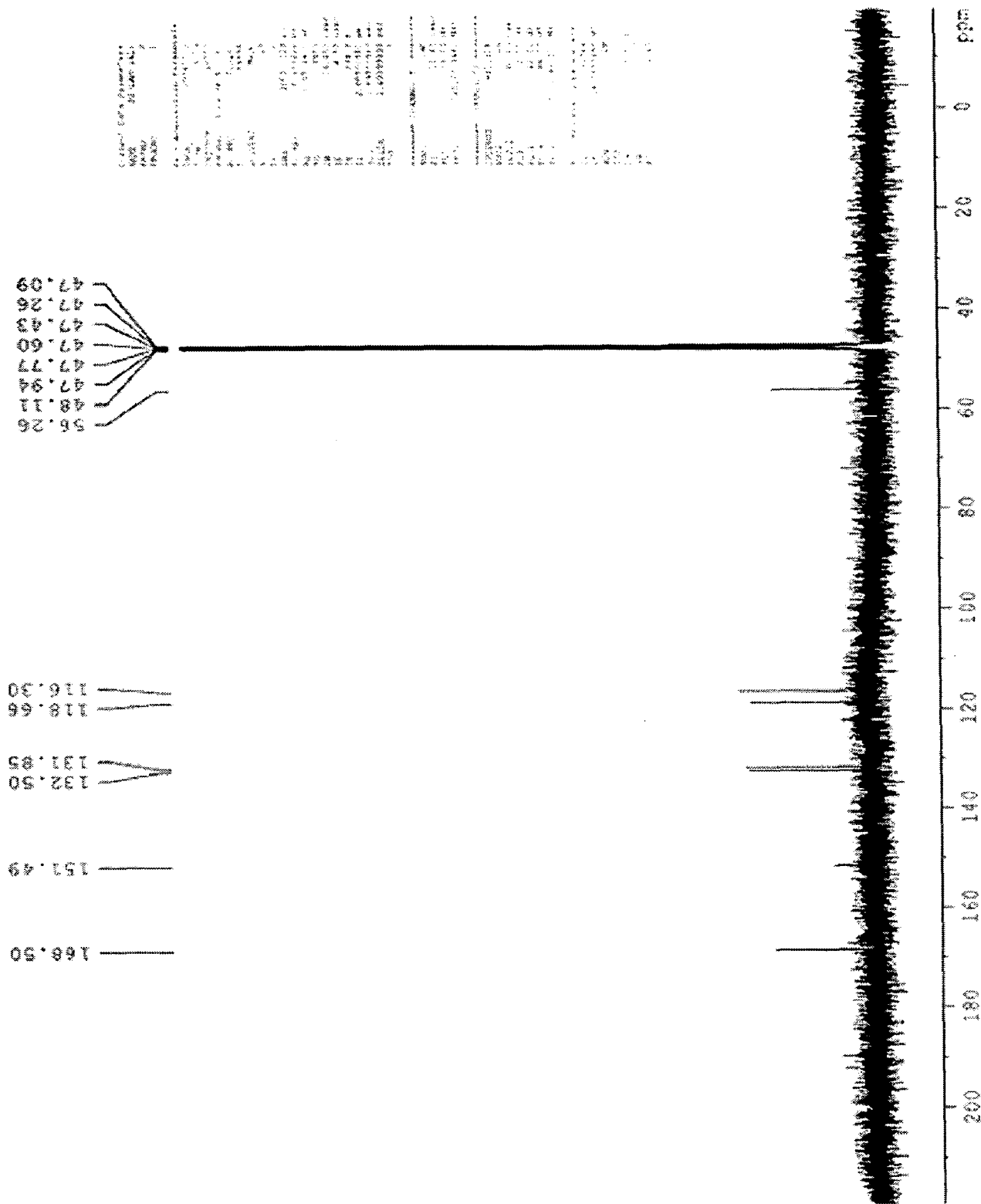
Figure 21: ^{13}C NMR of HSal-2-ambz

47.09
47.26
47.43
47.60
47.77
47.94
48.11
56.26

116.30
118.66

131.85
132.50

151.49

166.50

48

3.6.5 TG, DTG and DTA analysis

TG, DTG and DTA data of $Me_3Si(sal-2-ambz)$ and $Me_2Si(sal-2-ambz)_2$ are given in table 11 and presented in figure 22 and 23 respectively. The analysis is carried out under air atmosphere and at a heating rate of 10 °C /min. $Me_3Si(sal-2-ambz)$ complex shows four step decomposition in the temperature range 21–922 °C. The first step decomposition pattern shows one peak at 188 °C in DTG curve and at192 °C in DTA curve. The endothermic DTA peak with ΔH value of 85.9 mJ/mg corresponds to the removal of two methyl groups, inferred from closeness between observed and calculated weight loss. Step II reveals the loss of C_3H_6N moiety followed by the weight loss (62.54%)in the temperature range 299-567 °C and the peak at 549 °C in DTG and broad merged exothermic peaks at 510 °C and 562 °C in DTA with ΔH value of 4826 mJ/mg reveal decomposition of benezimidazole ring. In the temperature 567–922 °C, the sublimation of residue took place.

$Me_2Si(sal-2-ambz)_2$ complex shows three step decomposition in the temperature range 23–572 °C. The weight loss (8.03%) and the peaks at 107 °C and 190 °C in DTG in step I corresponds to loss of two methyl groups. Step II reveals the loss of C_2H_3N group, and a peak at 559 °C in DTG and a broad peak at 560 °C in DTA with ΔH value of 2454 mJ/mg and weight loss (55.36%), in the step III corresponds to decomposition of benezimidazole ring and giving a white residue (20.40%).

Table 11: TG, DTG and DTA data of di- and tri-methylsilicon complexes of Hsal-2-ambz

S. No	Compounds	Steps	TG Temp. range (°C)	DTG (°C)	DTA (°C)	ΔH mJ/mg	Wt. loss(%) obsd.(calcd.)	Species lost
1.	Me₃Si(sal-2-ambz)	I	21-194	188	192	85.9	10.8(9.3)	C_2H_6
		II	194-299	-	-	-	17.14(19.11)	C_3H_6N
		III	299-567	549	322 510,562	246 -4826	62.54(61.2)	$C_8H_9N_2$
		IV	567-922	609	-	-	-	Sublimed
2.	Me₂Si(sal-2-ambz)₂	I	23-200	107 190	-	-	8.03(9.7)	C_2H_6
		II	200-337	280 320	329	316	16.13(17.3)	C_2H_3N
		III	337-572	559	560	-2454	55.36(54.9)	$C_8H_7N_2$
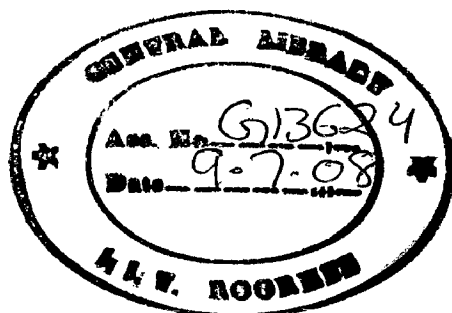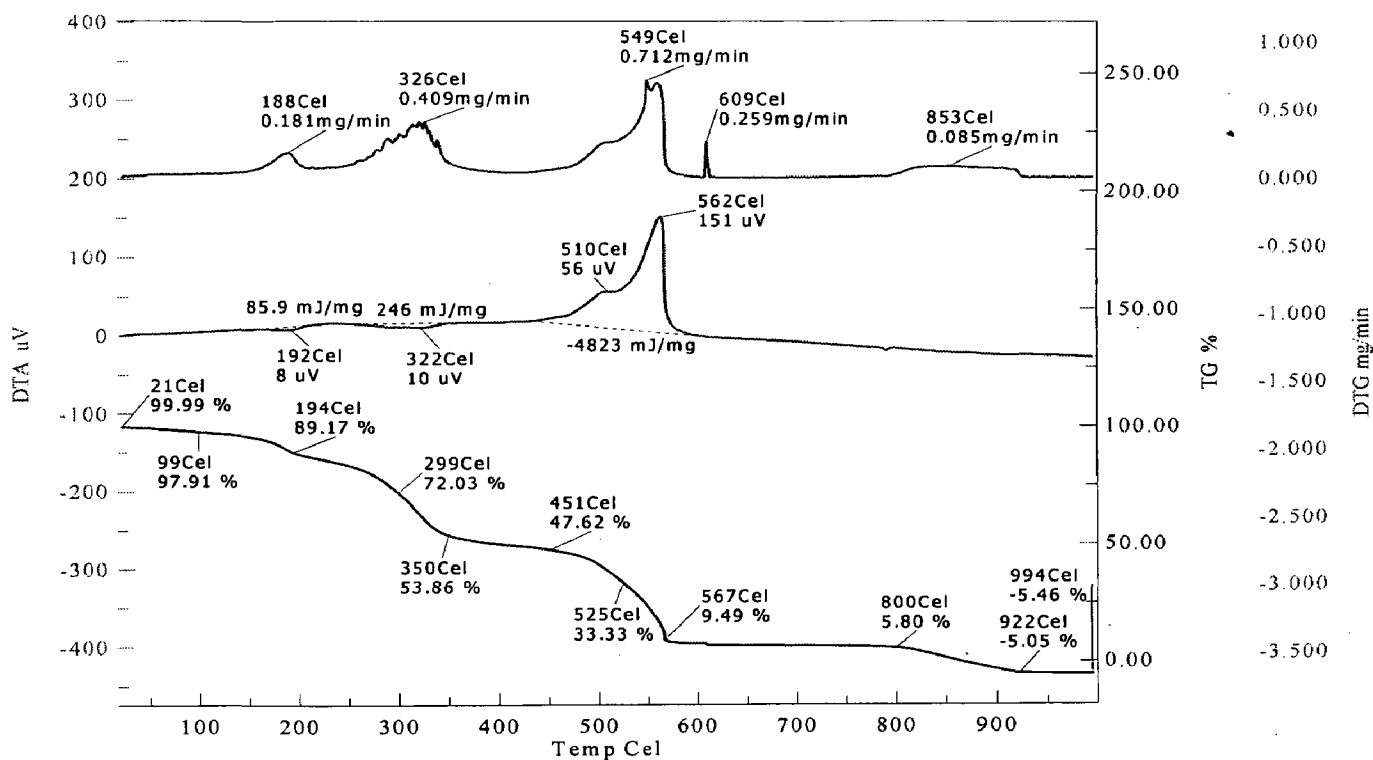
Figure 22: DTA –DTG –TG of Me₃Si(sal-2- ambz)
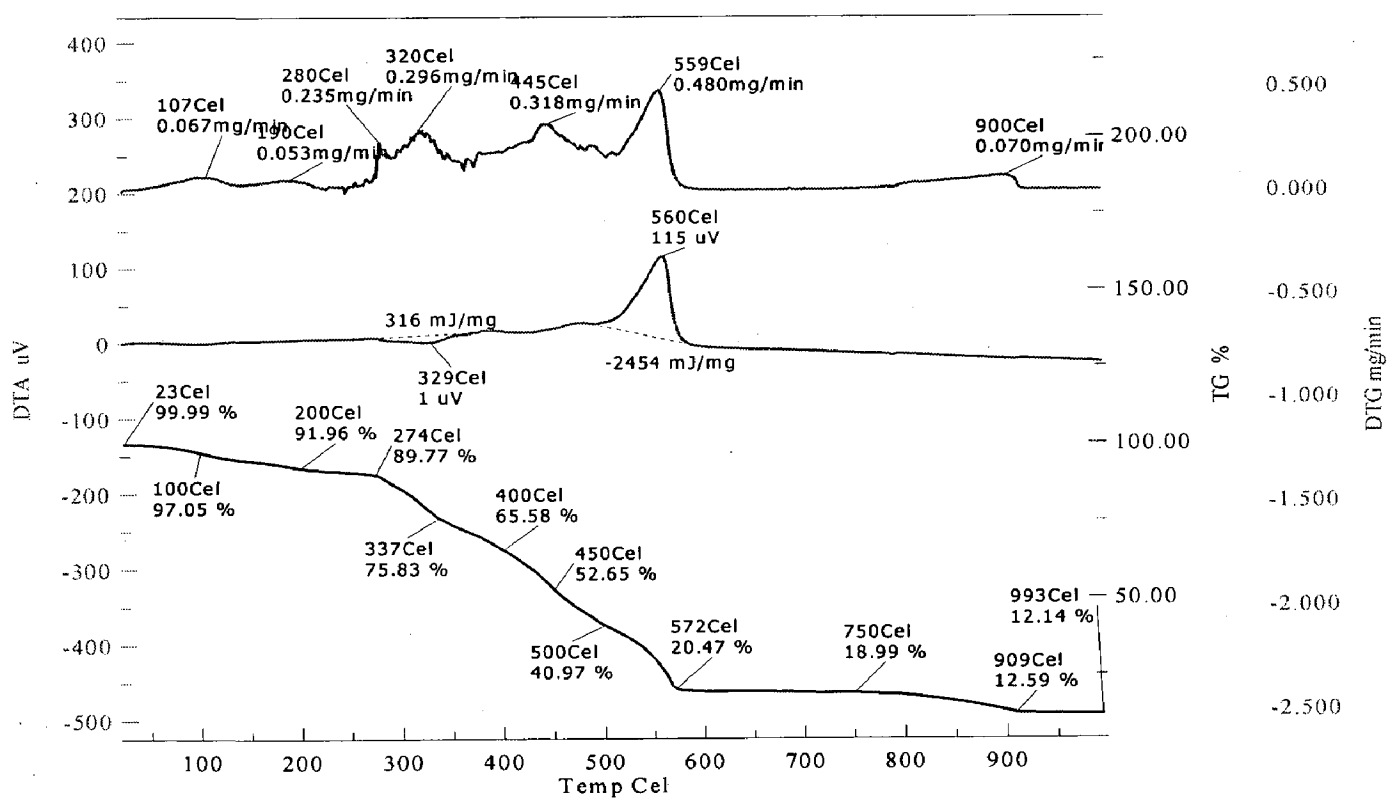
Figure 23: DTA –DTG –TG of Me₂Si(sal-2- ambz)₂

3.6.6 POWDER XRD RESULTS

On the basis of most prominent peak match programme, the table 12 for the residue obtained from $Me_3Si(sal-2-ambz)$ is given below. The data support the residue is SiO_2. Figure 24(a) Shows the XRD pattern for $Me_3Si(sal-2-ambz)$.

Table 12: d value and angle for residue obtained from $Me_3Si(sal-2-ambz)$

S.No.	Spacing(d)Å	Angle(2θ)	Intensities(counts)	Phase
1.	3.24	27.44^0	400	SiO
2.	2.81	31.76^0	3000	SiO_2
3.	1.99	45.50^0	1800	SiO_2
4.	1.62	56.54^0	500	SiO_2

The most prominent peak match programme support that the residue is SiO, which is obtained from $Me_2Si(sal-2-ambz)_2$ by pyrrolysis. The values are given in table 13 and shown in figure 24(b).

Table 13: d value and angle for residue obtained from $Me_2Si(sal-2-ambz)_2$

S.No.	Spacing(d)Å	Angle(2θ)	Intensities(counts)	Phase
1.	3.25	27.43^0	250	SiC
2.	2.81	31.78^0	1000	SiO
3.	1.99	45.50^0	400	SiO
4.	1.62	56.54^0	200	SiO

3.6.7: SEM RESULTS:

For residue obtained from $Me_3Si(sal-2-ambz)$

The figure 25(b) shows nanosize particle (68.79 nm and 195.13 nm) at different locations with globules structure [figure 25(c)] of nearly uniform size and dispersed in little area. The distribution of globules was found non-uniform [figure 25(a)].

For residue obtained from Me$_2$Si(sal-2-ambz)

The figure 26(b) shows nanosize particle (85.94 nm and 166.15 nm) at different locations with globules structure [fig. 26(a)] of rough surface. The figure 26(c) shows non-uniform distribution of particles.
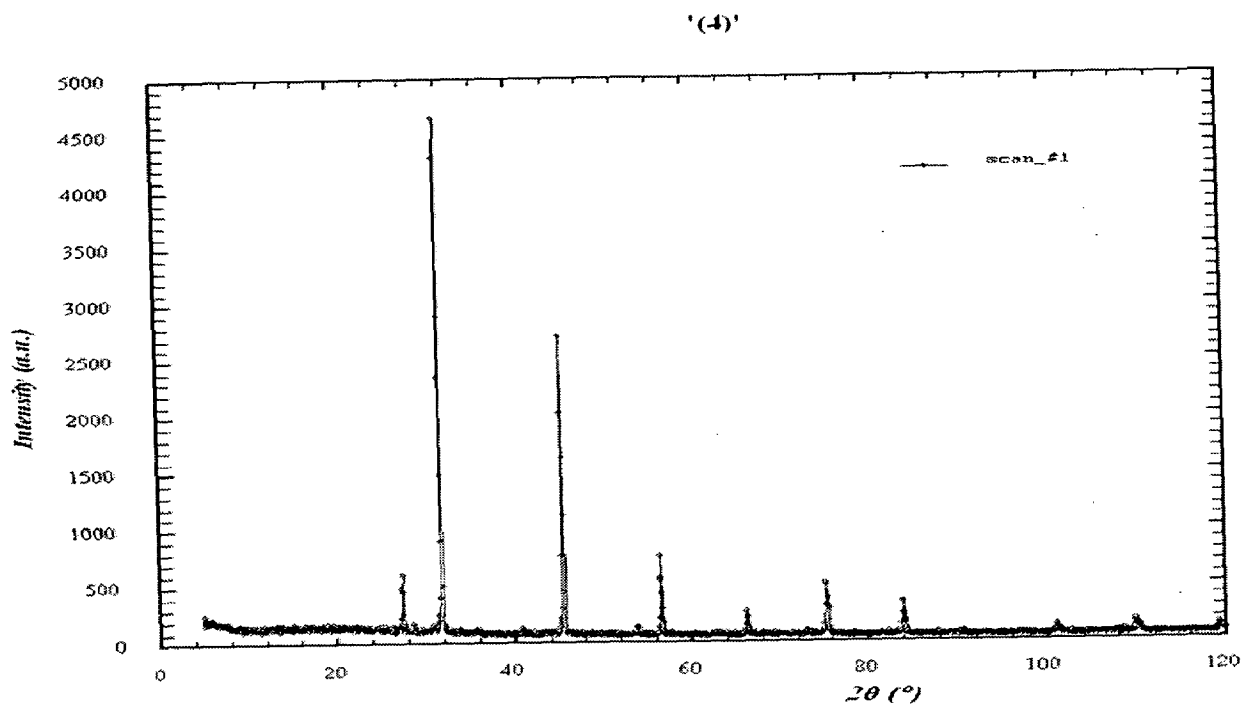
FIGURE 24(a): XRD pattern of residue obtained from Me₃Si(sal-2- ambz)
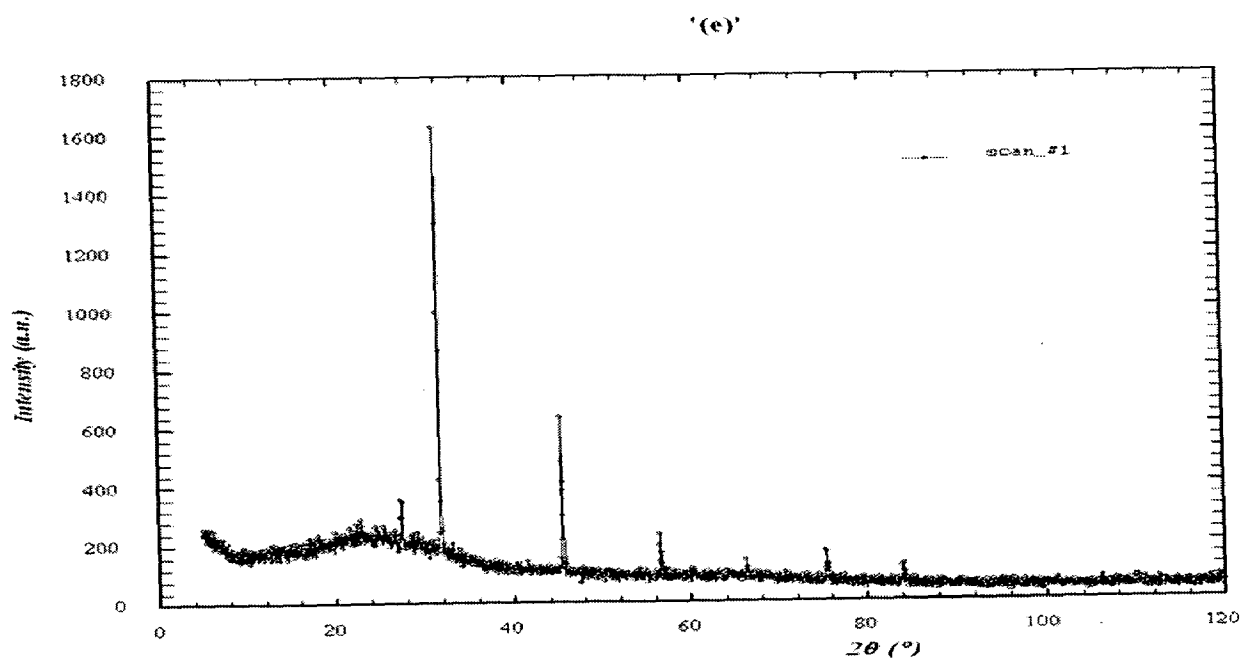
FIGURE 24(b): XRD pattern of residue obtained from Me₂Si(sal-2- ambz)₂
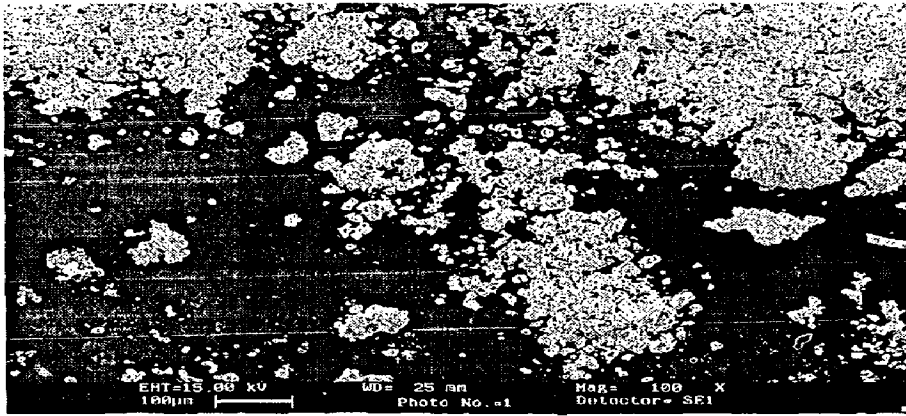
Figure 25(a): SEM image of residue obtained from Me₃Si(sal-2- ambz) Mag. =100 X
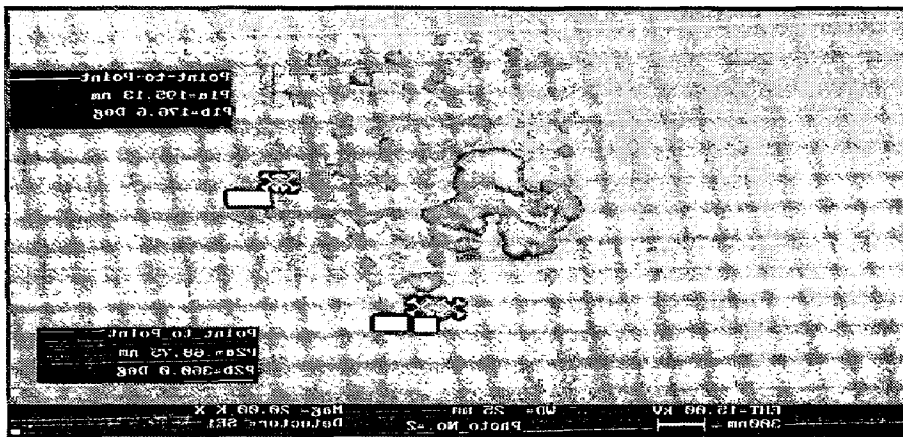
Figure 25(b): SEM image showing particle size
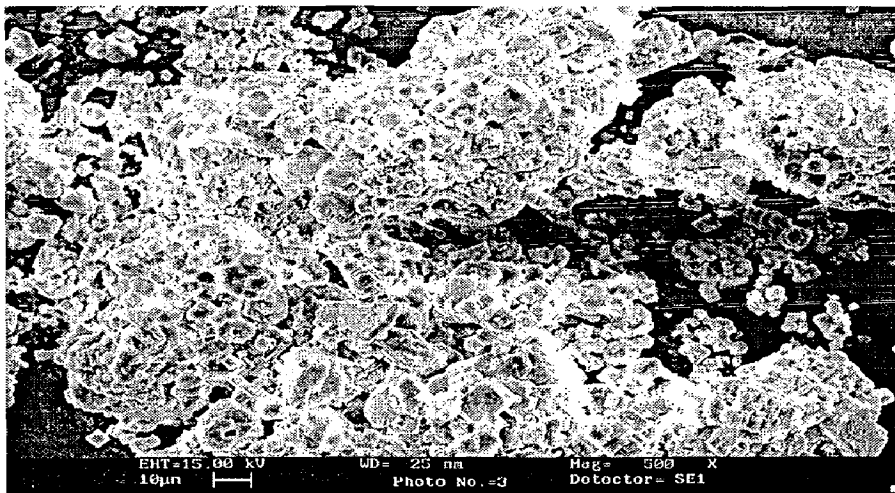
Figure 25(c): SEM image showing globules
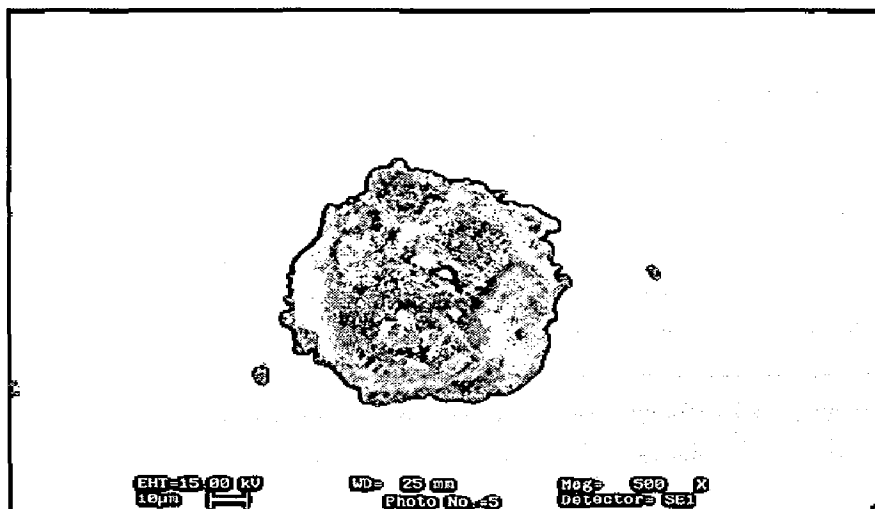
**Figure 26(a): SEM image of residue obtained from Me₂Si(sal-2- ambz)₂
Showing particle size at Mag. = 500 X**
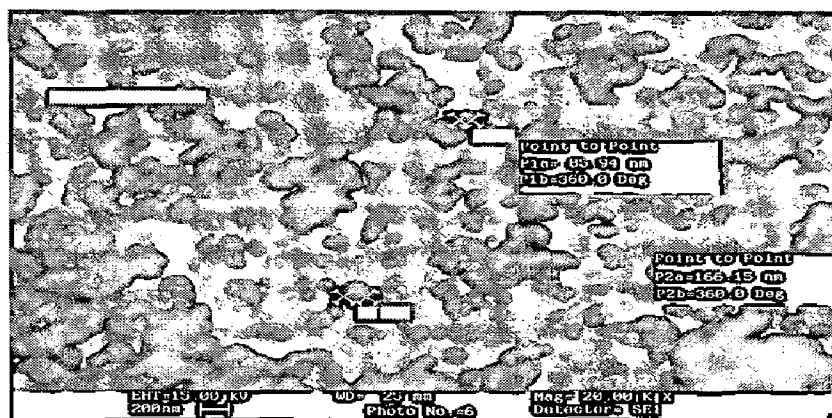
Figure 26(b): SEM image showing particle size at different region
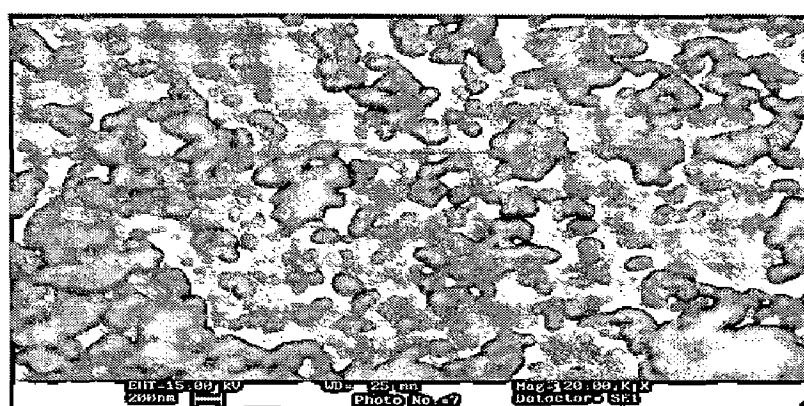
Figure 26(c): SEM image showing surface morphology

3.7. Dimethylsilicon Mixed Ligand (SB)-(RCOOH) Complexes

3.7.1 Physical characteristics

The physical characteristics of products obtained from reaction, are summarized below in the table14.

Table 14: Analytical data and physical characteristics of dimethyl mixed ligand (SB)-(RCOOH) complexes

S. No	Complexes (empirical formula)	m.p (^{0}C)	Yield (%)	M.wt (gm)	Color and physical state	%obsd. (calcd.)			Molar conductance ($\Omega^1 cm^2 mol$)
						C	H	N	
1	Me$_2$Si(SB) (Pal)	220	75	453	yellow solid	57.34 (60.90)	9.89 (11.95)	1.98 (3.09)	35.2
2	Me$_2$Si(SB) (Ste)	204	78	537	Dark orange solid	71.43 (72.90)	10.98 (12.16)	1.72 (2.61)	27.8
3	Me$_2$Si(SB) (Lau)	180	77	454	orange solid	66.97 (68.02)	10.78 (11.38)	2.4 (3.08)	31.5
4	Me$_2$Si(SB) (Mys)	198	80	481	yellow liquid	67.86 (70.22)	10.31 (11.7)	1.67 (2.91)	48.6

3.7.2: Electronic Spectra

The electronic spectral data of Me$_2$Si(SB)(Pal), Me$_2$Si(SB)(Lau), Me$_2$Si(SB)(Mys), and Me$_2$Si(SB)(Ste) are presented in table15 and spectra are shown in figure 27–30.

The spectra of first complex was taken in methanol while others in chloroform. A band at 334–340 nm, in all of the complexes, is due to n→π* transitions of azomethine (>C=N) group and at 260–270 nm is due to π→π* transition of the azomethine group. The band at 226–243 nm is due to n→π* transition of COO chromophore .

Table 15: Electronic spectral data of dimethylsilicon mixed ligand (SB)–(RCOOH) complexes

S.No.	Compounds	Transitions λ_{max} (nm); [abs.]		
		$\pi \rightarrow \pi^*$ (C=N)	$n \rightarrow \pi^*$ (C=N)	$n \rightarrow \pi^*$ (OCO)
1.	Me₂Si(SB)(Pal)	270 [1.3046]	334 [1.2689]	222 [2.0507]
2.	Me₂Si(SB)(Lau)	264 [1.0040]	340 [0.9515]	243 [0.8422]
3.	Me₂Si(SB)(Mys)	260 [1.3301]	336 [0.8514]	226 [0.2675]
4.	Me₂Si(SB)(Ste)	261 [0.9246]	337 [0.7230]	240 [0.8722]

3.7.3 Infrared spectroscopy

The IR spectra of all the four mixed ligand complexes are compared with those of the free ligands in order to determine the co-ordination sites that may involve in complexation. There are some guide peaks, in the spectra of the ligand, which are of good help for achieving this goal. The position and the intensities of these peaks are expected to be changed upon coordination.

The infrared spectral data of and of dimethylsilicon derivative of mixed ligands (SB) - (RCOOH) is given in table16 and presented in figure 31–34 respectively. The absorption band at 1618 cm⁻¹ is due to azomethine group of Schiff base. A shift in frequency (9–10 cm⁻¹) is observered in all of the four mixed ligand complexes. Further approximately 50–60 cm⁻¹ downward shift is observed in v_{as} (OCO) frequency from the parent carbonyl group present in the fatty acid. This indicates the coordination of azomethine and carboxylate groups, which are further confirmed by presence of new bands in the region 845-873 cm⁻¹ assignable to v_s(Si–O), 802–826 cm⁻¹ v_{as} (Si–O) and 1400 cm⁻¹ v(Si–C), in all of the complexes.

Table 16: Characteristics infrared frequencies (cm^{-1}) of dimethylsilicon mixed ligand (SB)–(RCOOH)

S.No.	Ligand/ complexes	ν(OH)	ν(C≡N)	ν_{asym}(OCO) ν_{sym}(OCO)	ν_{as}(Si–O) ν_s (Si–O)	ν(Si–C)	ν_{as}(Si–C) ν_s(Si–C)
1.	HPal	3412br	-	1703vs 1468s	-	-	-
2.	HSte	3421br	-	1713w 1466m			-
3.	HLau	3410br	-	1701vs 1466s			-
4.	HMys	3425br	-	1701vs 1468s			-
5.	SB	3452br	1618s	-	-	-	-
6.	Me$_2$Si(SB)-(Pal)	-	1607s	1648vs 1493ms	845w 684s	825s	1400m 1248s
7.	Me$_2$Si(SB)-(Ste)	-	1608s	1648vs 1477m	873s 684s	802w	1400m 1259s
8.	Me$_2$Si(SB)-(Lau)	-	1609s	1649vs 1494w	845w 685s	824w	1400w 1250m
9.	Me$_2$Si(SB)-(Mys)	-	1608s	1648vs 1478w	845w 685s	826s	1400w 1249s
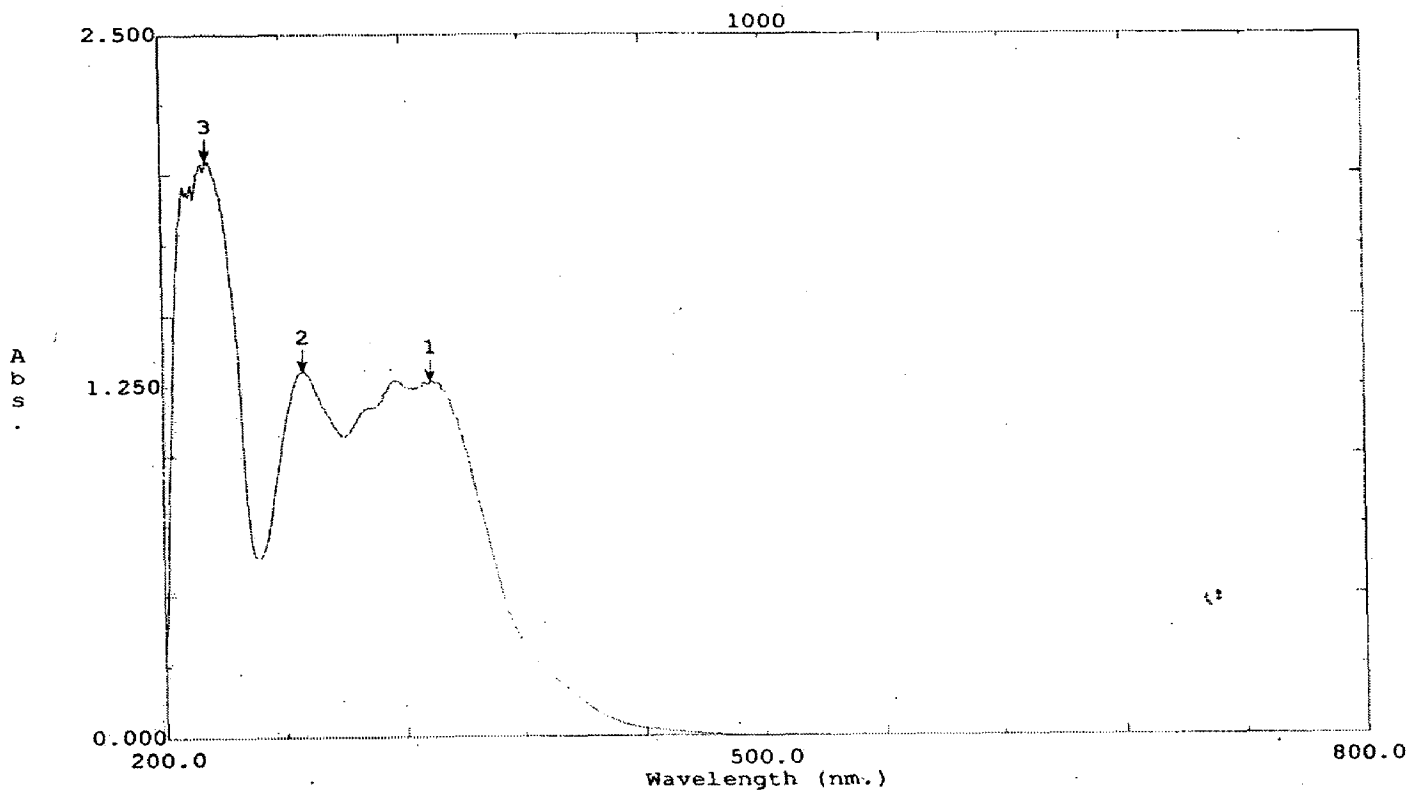
Figure 27: Electronic spectrum of Me₂Si(SB)(Pal)
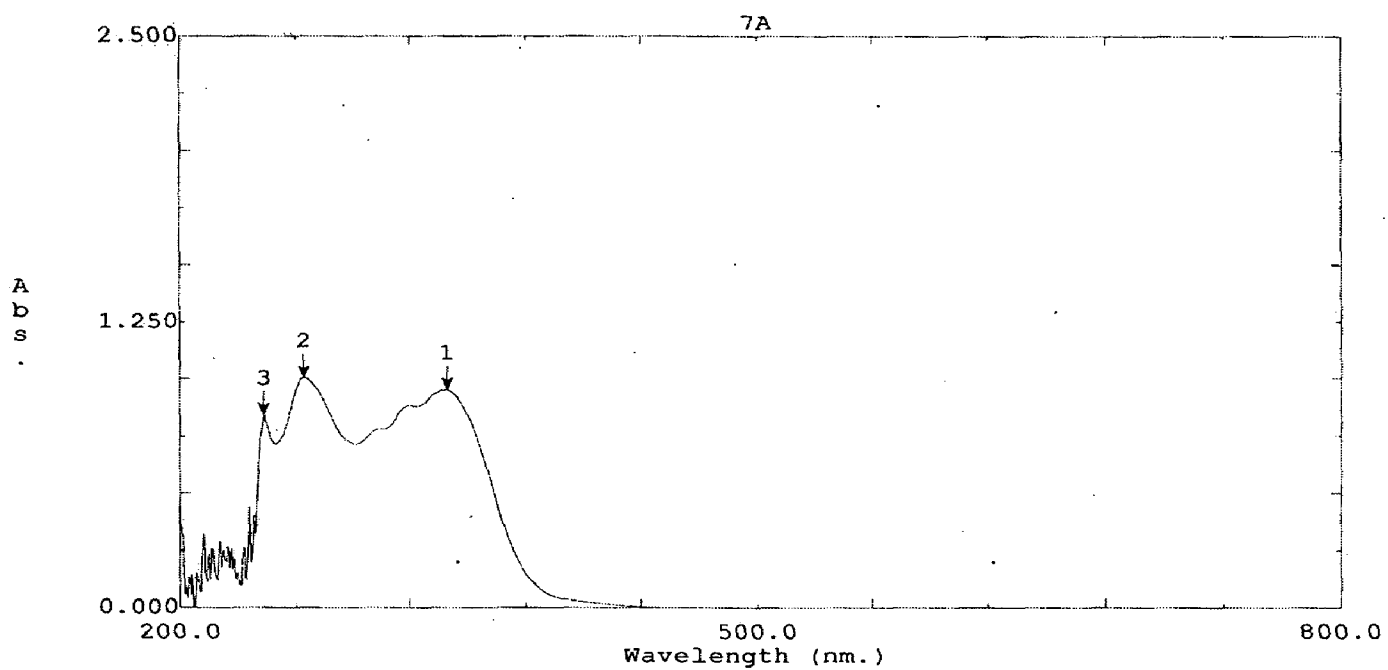
Figure 28: Electronic spectrum of Me₂Si(SB)(Lau)

60
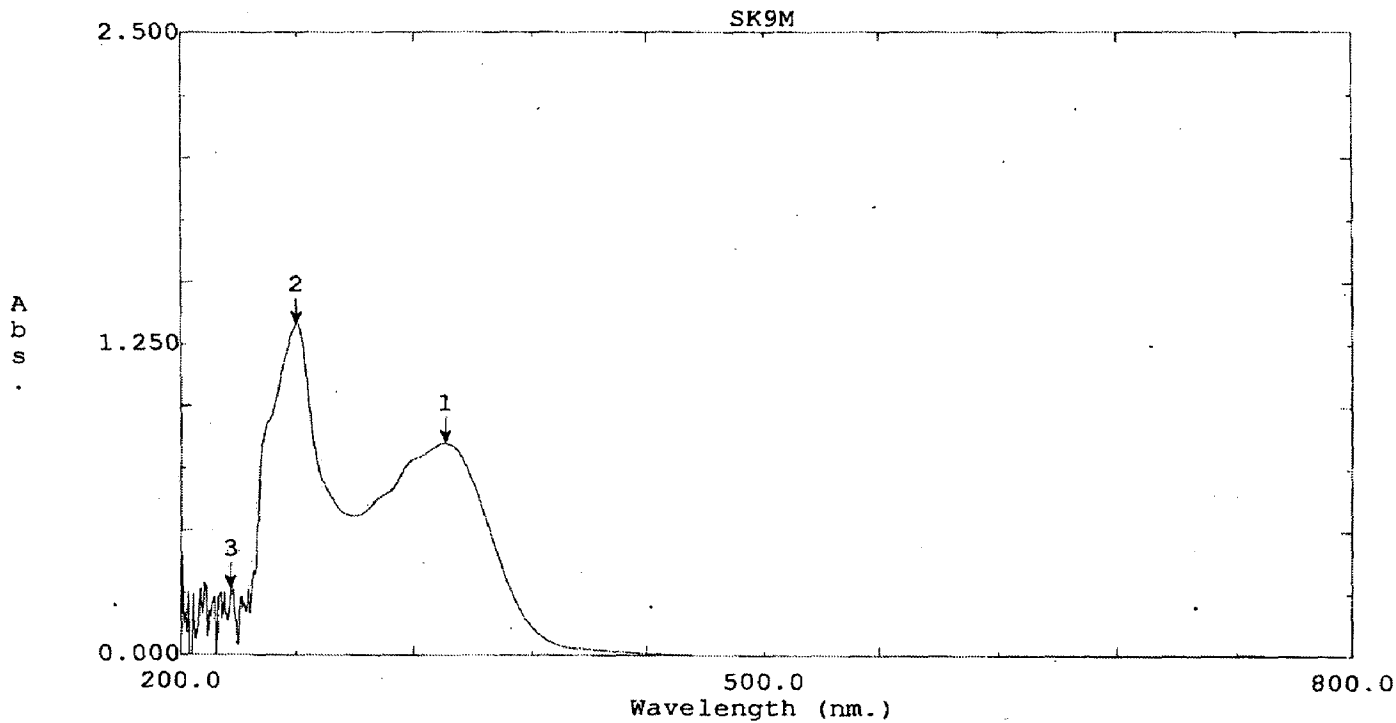
Figure 29: Electronic spectrum of Me₂Si(SB)(Mys)
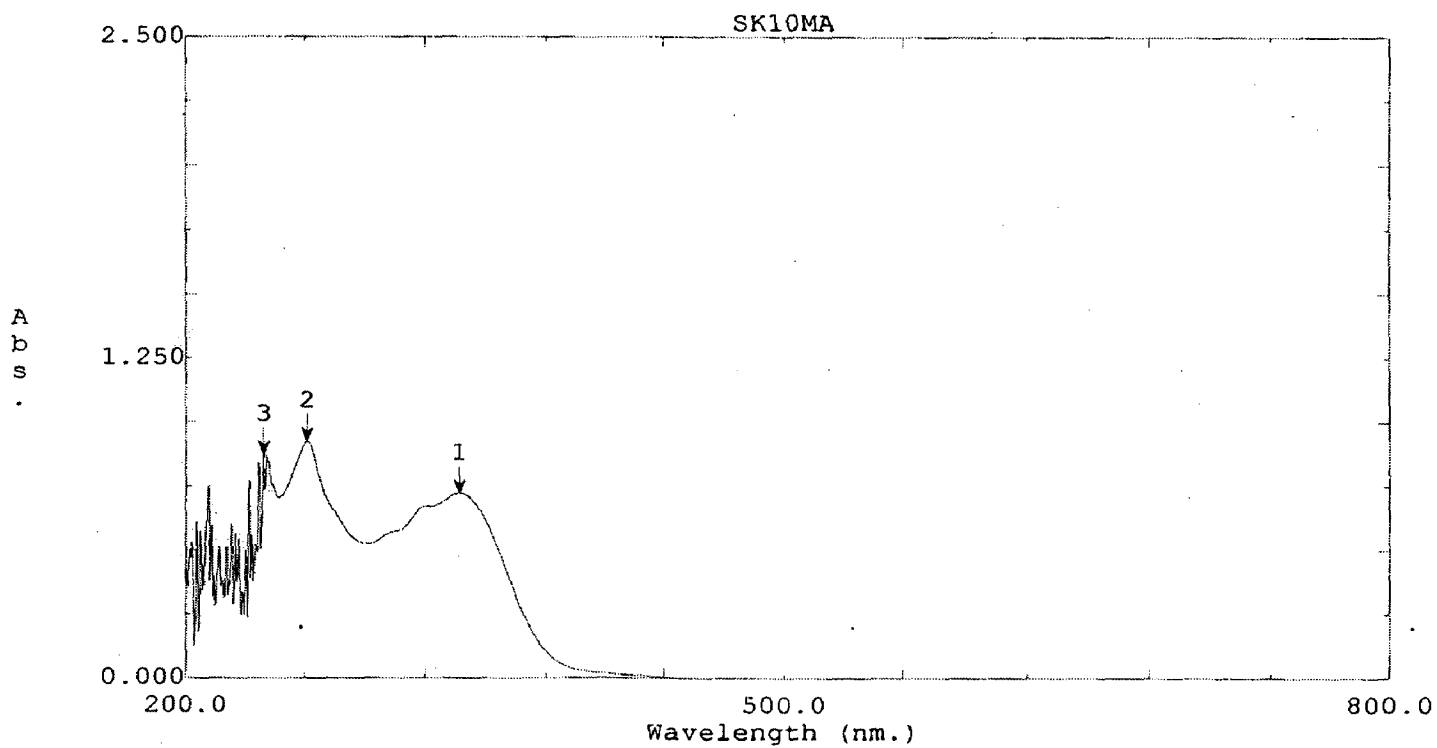
Figure 30: Electronic spectrum of Me₂Si(SB)(Ste)
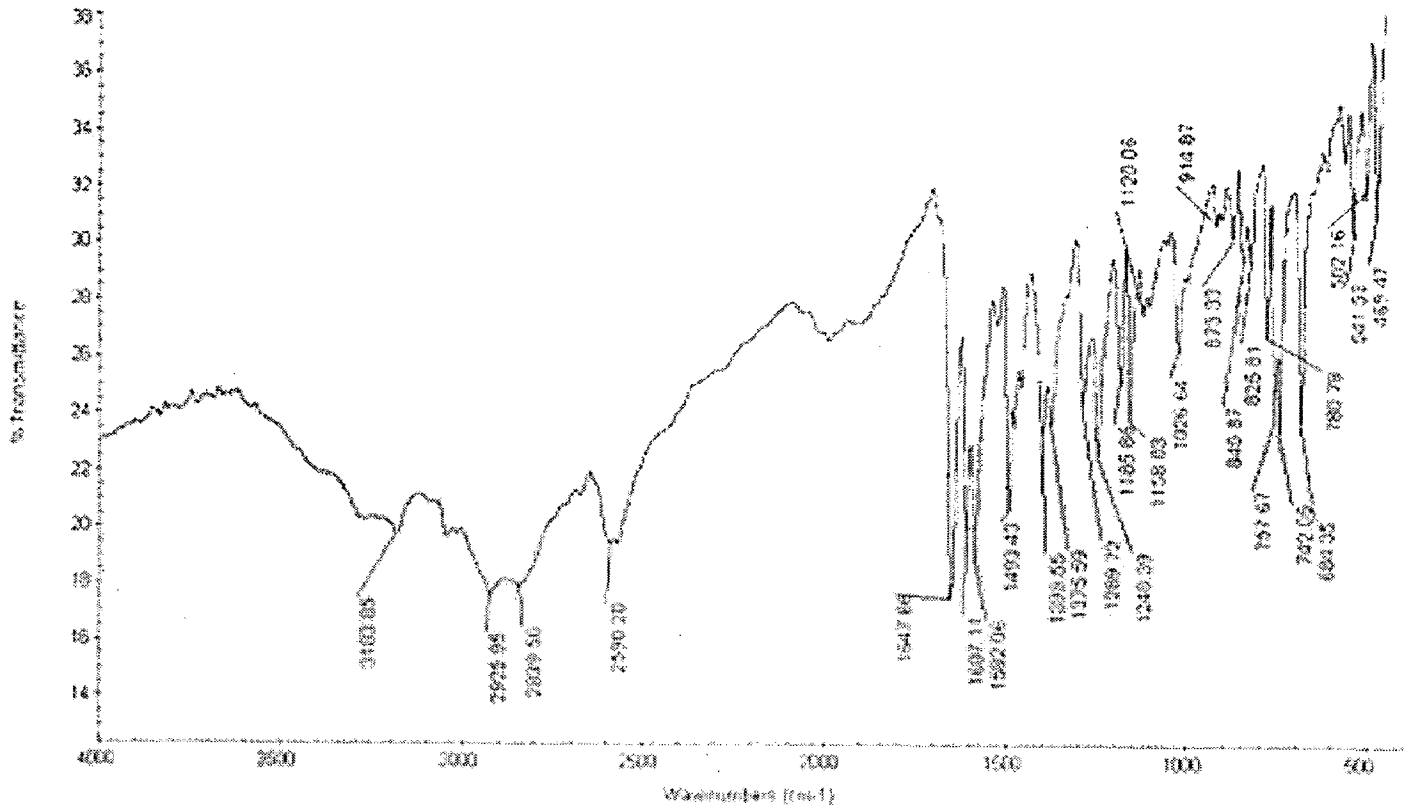
Figure 31: IR spectrum of Me₂Si(SB)(Pal)
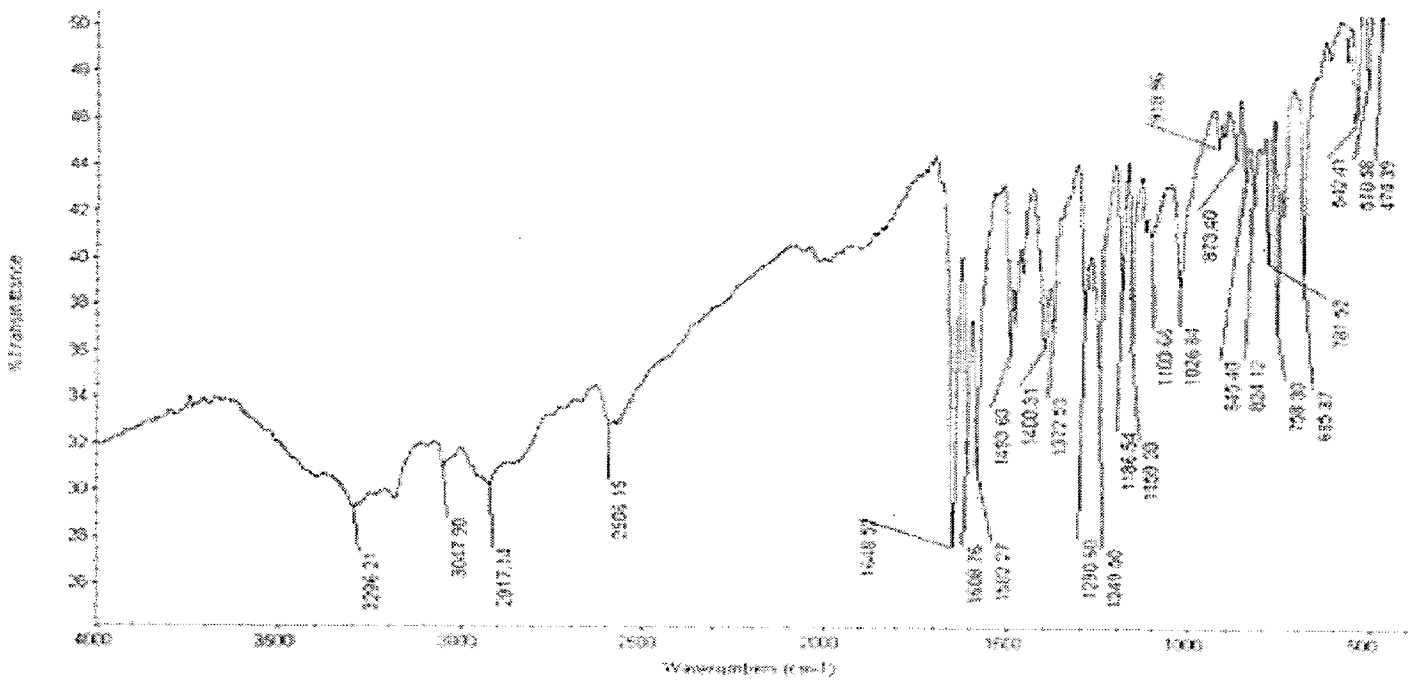
Figure 32: IR spectrum of Me₂Si(SB)(Lau)

62
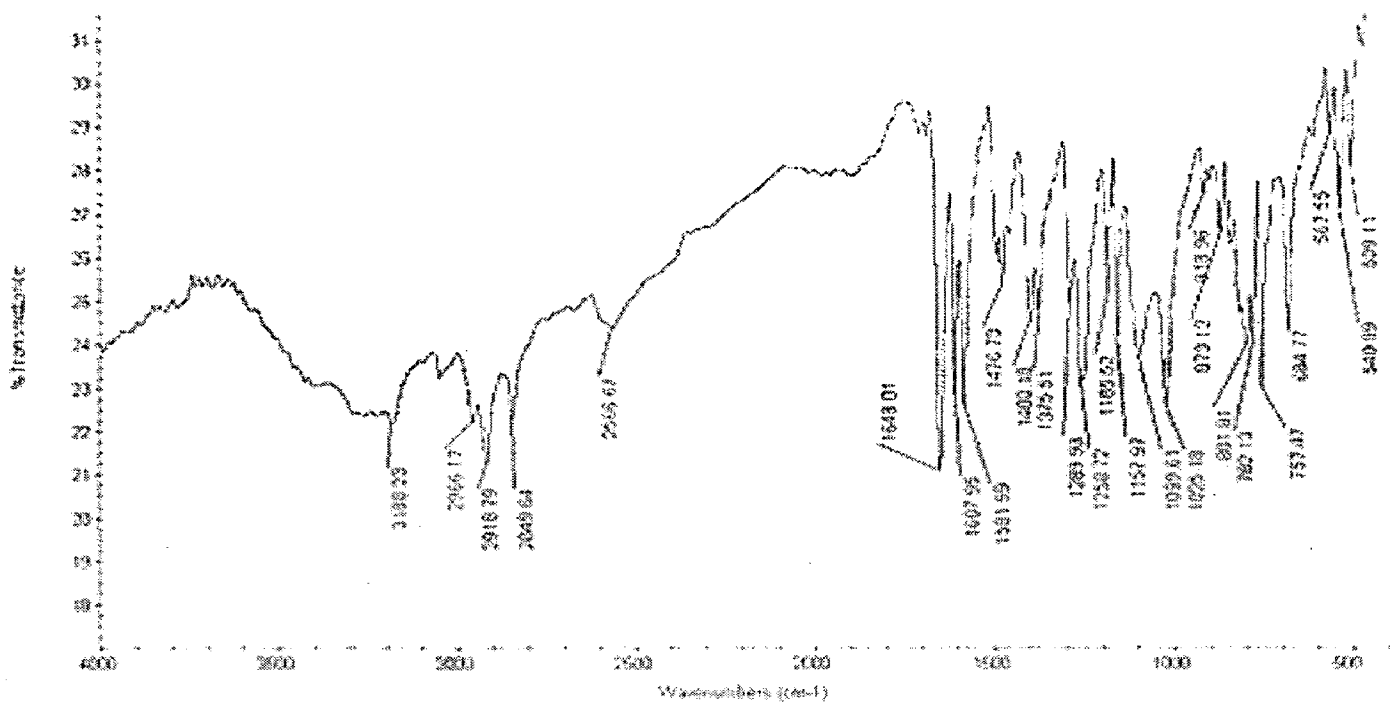
Figure 33: IR spectrum of Me₂Si(SB)(Mys)
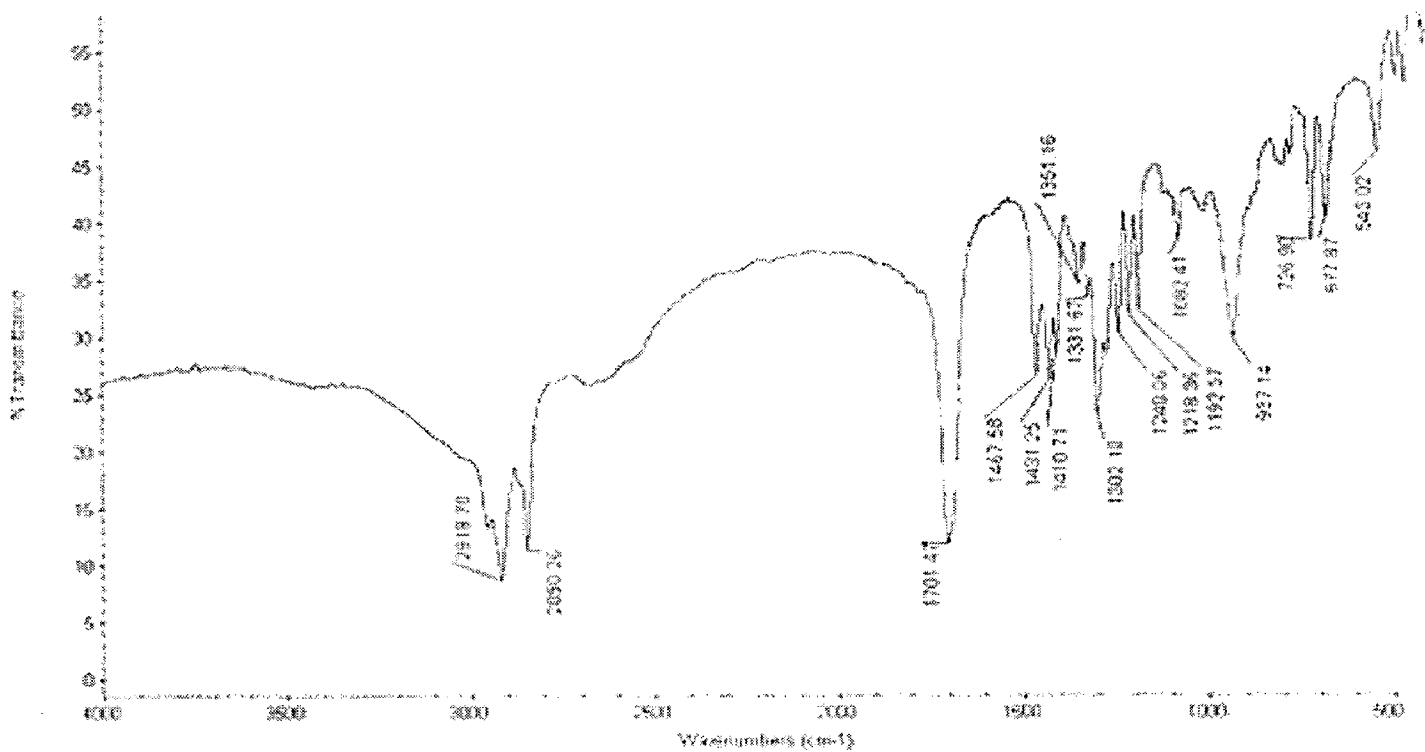
Figure 34: IR spectrum of Me₂Si(SB)(Ste)

3.7.4 ^{1}H and ^{13}C NMR Spectra

The chemical shift (δ ppm) for various protons and carbons are listed in the table17 below and given in figure 34(^{1}H) and 35(^{13}C)respectively.
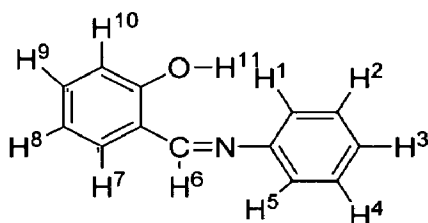
2-((phenylimino)methyl)phenol (SB)

Table 17: ^{1}H and ^{13}C values for SB

S.No.	Compounds	Analysis	δ(ppm)
1	2-((phenylimino)-methyl)phenol	^{1}H	8.82 (s, 1H) (for H^9), 7.56-6.96 (m, 9H) (for H^1-H^5 & H^7-H^{10}).
		^{13}C	163.75, 133.06, 132.47, 129.16, 122.44, 118.95, 116.44.

Figure 34: ^{1}H NMR spectrum of SB

Figure 35: ^{13}C NMR spectrum of SB

3.7.5 TG, DTG and DTA analysis

TG, DTG and DTA data of $Me_2Si(SB)(Mys)$, $Me_2Si(SB)(Lau)$, and $Me_2Si(SB)(Ste)$ are given in table 18. The analysis is carried out under air atmosphere and at temperature rate 10 °C/min. TG, DTG and DTA profile are shown in figure 36–38.

$Me_2Si(SB)(Mys)$ complex shows six step decomposition in the temperature range 26-963 °C. The first step decomposition pattern shows a peak at 88 °C in DTG curve and an endothermic heat at 92 °C in DTA curve with ΔH value 501 mJ/mg which corresponds to loss one methyl group (obsed. % loss 4.28; calcd. 3.01). In the step II, wt. loss of 8.31% indicates the oxidation of C_3H_8 group. In step III and IV, the weight loss and the peak at 170 °C and 226 °C in DTG and peaks at 166 °C and 232 °C in DTA, reveals decomposition of long fatty acid chain. Step V and VI corresponds to the decomposition and oxidation of Schiff base moiety leaving 8.18% residue.

$Me_2Si(SB)(Lau)$ complex shows five step decomposition in the temperature range 25—968 °C. The first step decomposition pattern shows one peak at 84 °C in DTG curve and at 86 °C in DTA curve, ΔH of (121mJ/mg) which corresponds to the loss of one methyl group, inferred from closeness between observed and calculated weight loss. Step II and III correspond to the decomposition of fatty acid chain, shown by endothermic large value of ΔH 110mJ/mg. Step IV and V show a large exothermic peak value with ΔH of 620 mJ/mg correspond to decomposition and oxidation of Schiff base moiety followed by rapid oxidation of the remaining organic group.

$Me_2Si(SB)(Ste)$ complex shows five step decomposition in the temperature range 25—878 °C. The first step shows a peak at 85 °C in DTG and endothermic peak at 90 °C in DTA with ΔH value of 127 mJ/mg. This is probably due to loss of one methyl group. Step II and III give information about decomposition andoxidation of fatty acid chain, shown by large weight loss 29.14% and 25.47%, respectively. Broad DTA peaks with ΔH value of 3245 mJ/mg show the decomposition of Schiff base moiety. The final step shows oxidation and sublimation of the remaining organic moiety of the compound.

Table 18: TG, DTG and DTA data of dimethylsilicon mixed ligand (SB) -(RCOOH) complexes

| S. No	Compounds	Steps	TG Temp. range (°C)	DTG (°C)	DTA (°C)	ΔH mJ/mg	Wt. loss(%) obsd.(calcd.)	Species lost
1.	$Me_2Si(SB)$-(Mys)	I	26-100	88	92	501	4.28(3.10)	CH_3
		II	100-150	-	-		8.31(8.15)	C_3H_8
		III	150-201	170	166		17.82(16.36)	C_5H_{10}
		IV	201-238	226	232		25.9(23.46)	C_6H_{12}
		V	238-451	441	443	-454	9.21(9.49)	C_2H_2
		VI	451-963	951	652 758	-12.8 68.8	26.3(26.2)	C_4H_3N
2.	$Me_2Si(SB)$-(Lau)	I	25-95	84	86	121	4.03(3.31)	CH_3
		II	95-176	172	172	110	17.9(16.44)	C_5H_{12}
		III	176-235	224	229	34.6	26.11(26.78)	C_7H_{14}
		IV	299-460	448	448	-620	4.77(4.85)	CH
		V	460-968	-	556 761	49.9 83.8	45.75(45.88)	$C_{12}H_7N_7$
3.	$Me_2Si(SB)$-(Ste)	I	25-88	85	90	127	3.7(2.80)	CH_3
		II	88-199	201	-	-	29.14(29.9)	$C_{11}H_{24}$
		III	199-398	258	-	-	25.47(26.76)	C_7H_{14}
		IV	398-601	507 590	476 507 592	-3245	22.64(24.3)	C_5H_5
		V	601-878	810	-	-	17.16(19.2)	C_2NH

68
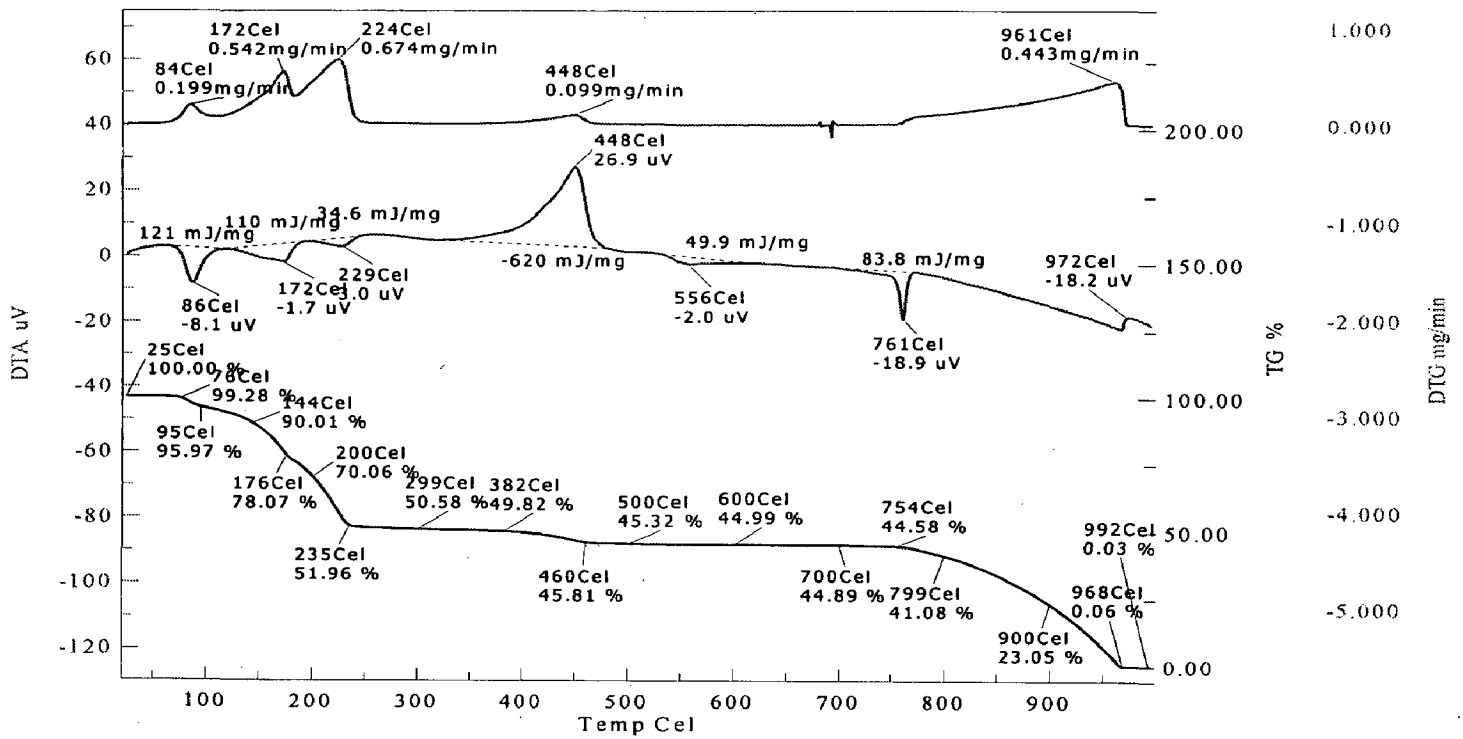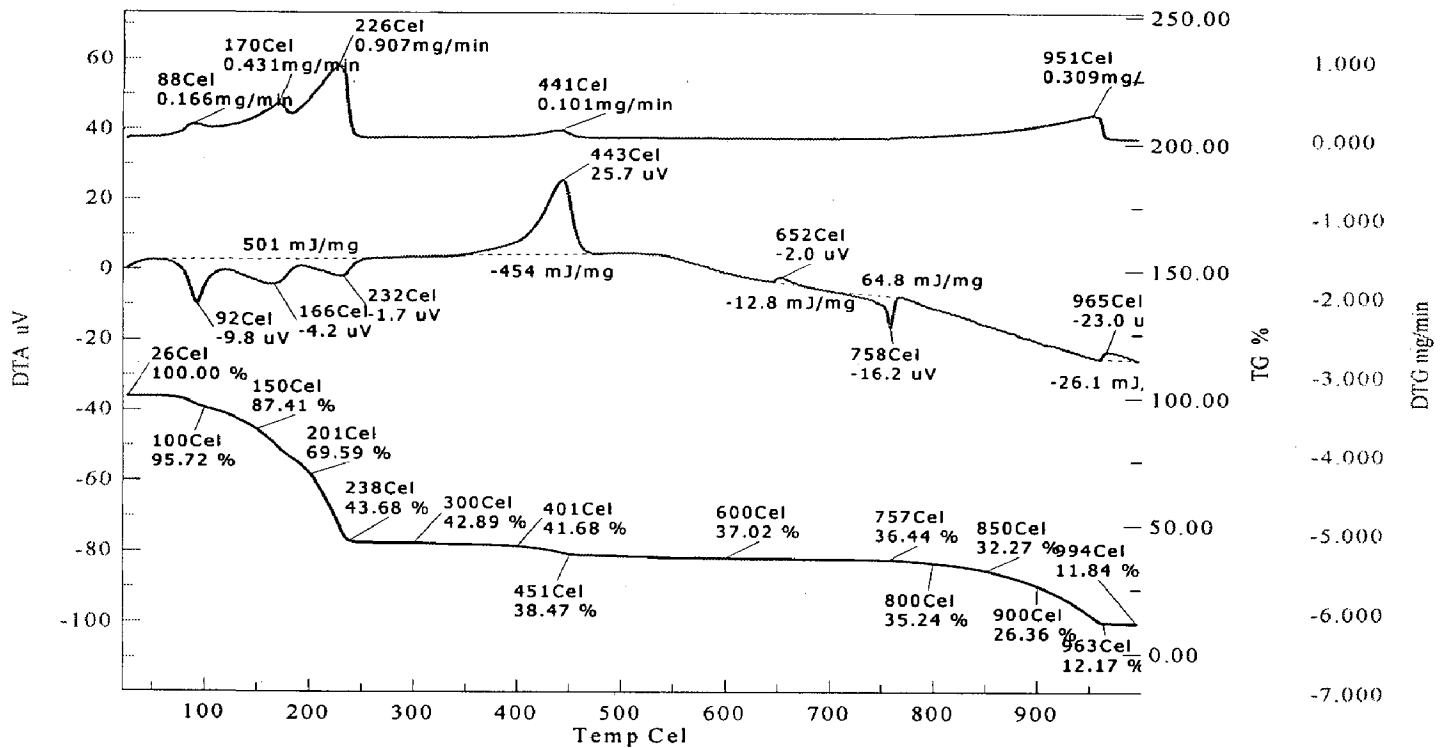
Figure 36: DTA –DTG –TG of Me₂Si(SB)(Lau)

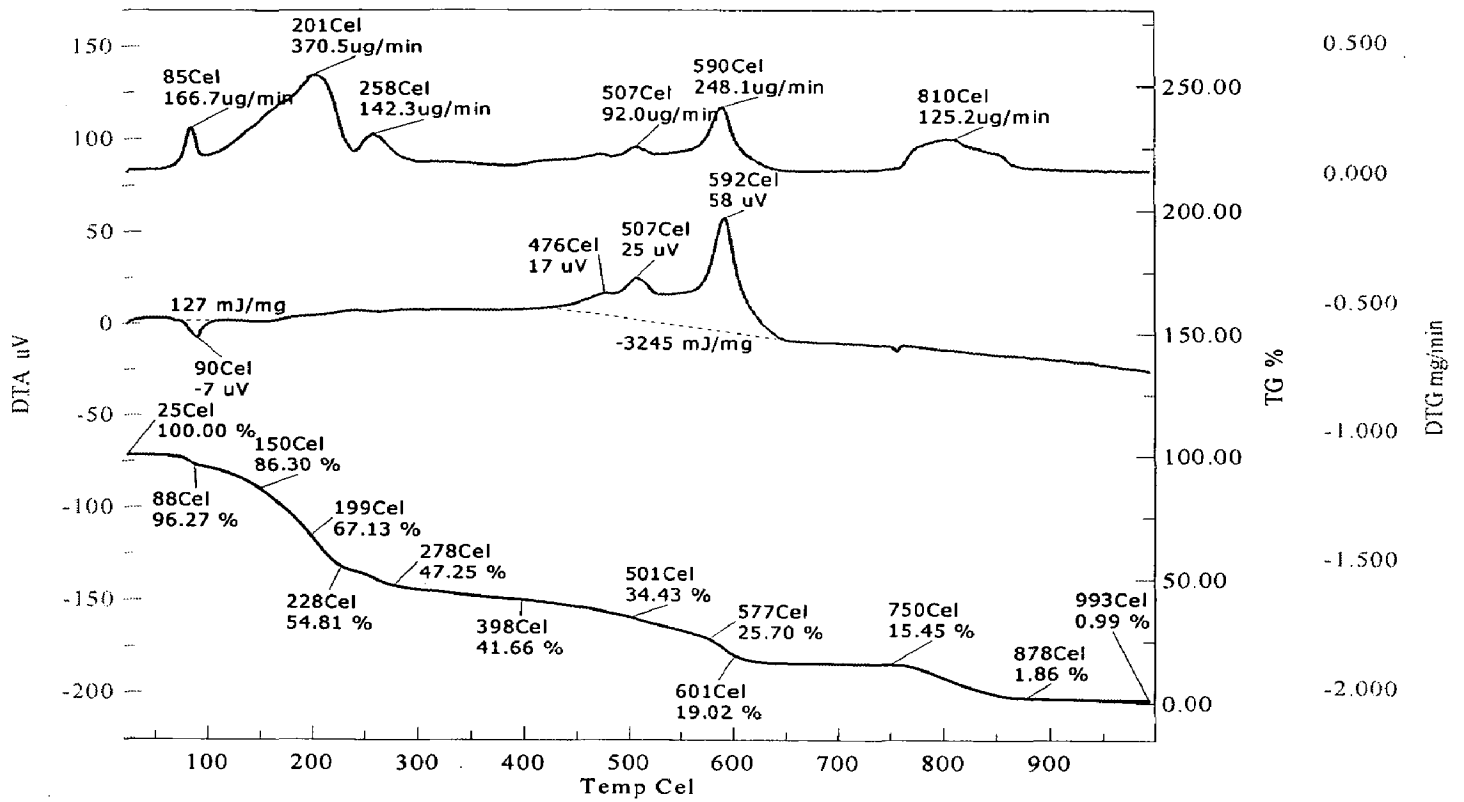**Figure 37: DTA –DTG –TG of Me₂Si(SB)(Mys)**

Figure 38: DTA –DTG –TG of Me₂Si(SB)(Ste)

CONCLUSIONS

CONCLUSIONS

The tetrahedral environment around silicon in all the organosilicon carboxlates is proposed on the basis of electronic, IR, ^{1}H NMR and ^{13}C NMR spectral studies, TGA/DTA and conductance measurements. All of the complexes are nonelectrolytes. The structure is given below:
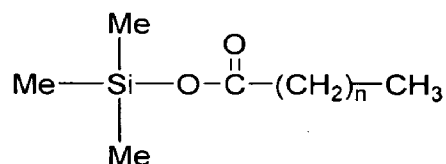
Organosilicon carboxylate

where, n = 10 for lauric acid; n = 12 for myristic acid;

n = 14 for palmitic acid; n = 16 for stearic acid.

The synthesized complexes, Me$_3$Si(sal-2-ambz)–I and Me$_2$Si(sal-2-ambz)$_2$–II, are characterized by IR, electronic, TGA/DTA studies. These data support the coordination of Schiff base through O and N to Si in the complexes. A trigonal bipyramidal geometry and an octahedral geometry for Me$_3$Si(sal-2-ambz) and Me$_2$Si(sal-2-ambz)$_2$ respectively have been tentatively proposed. The probable structures are given below:

(I)

(II)
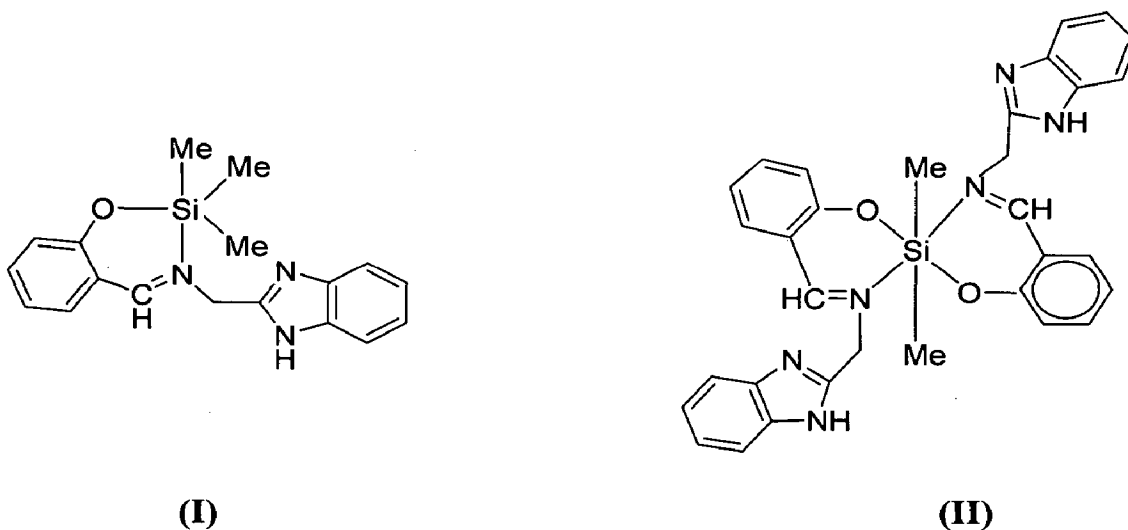
Organosilicon mixed ligand complexes are characterized by IR, electronic, and TGA/DTA studies.On the basis of spectral studies a penta-coordinate trigonal-bipyramidal structure has been suggested for all complexes. The probable structure is given below:
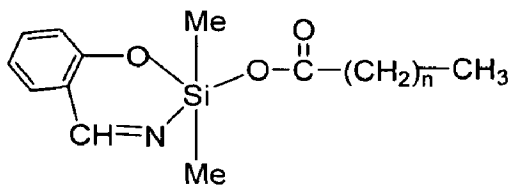
where, n = 10 for lauric acid; n = 12 for myristic acid;

n = 14 for palmitic acid; n = 16 for stearic acid.

REFERENCES

REFERENCES

1. F. A. Carey and R. J.Sundberg, 'Advanced Organic Chemistry', Kluwer Academic / Plenum Publishers, 4th edition, Part A, 2001.

2. R. Janoschek, J. Inorg. Org-Met. Polymers, 3 (1993) 4.

3. http://www.research.ibm.com/resources/press/strainedsilicon/

4. M. A. Brook, 'Silicon in Org., Org-met. and Polymer Chem'., J. Wiley, New York, 2000.

5. M. Zeldin, K. J.Wynne, and H. R. Allcock, 'Inorg. and Org-Met. Polymers: macromolecules Containing Silicon, Phosphorus and Other Inog. Elements', ACS, Washington, 1988.

6. B. Arkles, Chemtech. 13 (1983) 542.

7. J. E. Mark, H.R. Allcock, and R. West, 'Inorg. Polymers', Oxford University Press Inc., New York, NY, 2005 .

8. A. S. Chawla, Biomaterials, 2 (1981) 83.

9. J. Sakata, M. Yamamoto, and M. Hirai, J. Appl. Polym. Sci., 31 (1986) 1999.

10. P. K. Tien, Rev. Mod. Phy., 49 (1977) 361.

11. M. R. Wertheimer, and T.S. Ramu, U.S. Patent no. 4,599,578, 1986.

12. T. Wydeven, Appl. Opt., 16 (1977) 717.

13. A. Saxena and J. P. Tandon, Ind. J.Chem., 24A(5), (1985) 419.

14. N. N. Greenwood, and A. Earnshow, 'Chemistry of Elements', Pargamon Press, Oxford New York, 1995.

15. H. Schiff, Amm. Phy., 150 (1969) 193.

16. M. Moureau and S. Migoniac, Compt. Rand., 56 (1965) 1801.

17. D. N. Dhar and C. L. Taploo, J. Sci. Ind. Res., 41 (1972) 501.

18. Z. H. Chauhan and M. A. Farooq, Synth. React. Inorg. Met-Org. Chem., 31 (2001) 10.

19. Y. S. Cho and H. K. Kongop, Vichimbo, 12 (1972) 432.

20. S. G. Tech, S. H. Ang, S. B. Teo, K. L. Khew and C. W. Ong, J. Chem. Soc. Dalton Trans.,16 (1997) 46.

21. M. Tumar, M. Koksal, S. Serine and M. Digrak, Trans. Met. Chem., 13(1999)24.

22. B. Sun, J. Chen, and J. Hu, Chinesse chemical letters, 12(11) 2001 1043.

23. E. L. Mottaleb, A. Ramadan and N. Sawodny, J. Trans. Met. Chem., 22 (1995) 211.

24. F. L. Lee, E. G. Gabe and L. F. Khoo, Polyhedron, 9 (1990) 653.

25. I. M. Brown, D. Leopold and S. Mohite, Synth. Met. 72(3) (1995) 269

26. http://en.wikipedia.org/wiki/Fattyacid.

27. C. G. Soloman and J. E. Manson, Am. J. Clinic. Nutri., "Obesity and mortality: a review of the epidemiologic data", 66 (1997) 1044S.

28. A. A. Khandar and S. A. Zarei, Polyhedron, 26 (2006) 33.

29. S. A. Abdel-Latif, H. B. Hassib and Y. M. Issa., Spect. Chim. Acta Part A, 67 (2006) 950.

30. Leon Dyers, J. Steven, Y. Que, V. Donald and R. Xin. Inorg. Chem. Acta., 359 (1) (2006) 157.

31. A. A. Razaq, A. Eid, and M. Omar, Int. J. Chem. Sci., 3(2) 2005 253.

32. T. Akitsu and V. Einaga, Polyhedron, 4(12) (2005) 1368.

33. R. Gupta and B. Kirkan, Spect. Chim. Acta. Part A, 62(4) (2005) 1188.

34. S. M. Ben-Saber, A. A. Maihub, S. S. Hudere and M. M. El-ajaily., Mic.-Chem. J., 81 (2005) 191.

35. R.V. Singh, and P. Nagpal, Bioinorg. Chem. and Appl., 3(3-4) (2005) 255.

36. M. Nath and S. Goyal, Synth. React. Inorg. Met.- Org. Chem., 34(1) (2004) 187.

37. Shahina Khan, M. K Gupta, S Varshney and A. K. Varshney, J. Inst. Chem., 76(5) (2004) 146.

38. Mukta Jain, Shweta Gaur, S. C. Diwedi and S. C. Joshi, Phosphorus, Sulphur and Silicon and the Related Elements, 179 (2004) 1517.

39. A. T. Chaviara, P. J. Cox and K. H. Repana, J. Inorg. Biochem., 98 (2004) 1271.

40. M. M. Omar, M. Ahamed, and M. M. Hindy, Spect. Chim. Acta. Part A, 62(4) (2005) 1140.

41. X. W. Liu, N. Tang and Y.Change and M.Y. Tan, Tetrahedron, 15(8) (2004) 1269.

42. D. Sanz, A. Perona and R. M. Claramunt, Tetrahedron, 61 (2004) 145.

43. A. S. Al-Shihri, Spect. Chim. Acta. Part A, 60(5) (2003) 1189.

44. R. Karmakar, C. R. Chaudhary, G. Bravic and J. P. Sutter, Polyhedron, 23(6) (2003) 963.

45. K. Dravent, A. Bialonska and Z. Ciunik, Inorg. Chem. Commum., 7(2) (2003) 224.

46. B. K. Rai, J. Chem. Assy., 14 (2002) 3.

47. M. Nath and S. Goyal, Synth. React. Inorg. Met-Org. Chem., 32(7) (2002) 1205.

48. J. Wagner, U. Bohme,G. Roewer, Angewandte Chemie, 41(10) (2002) 1732.

49. M. Nath, S. Goyal, Phosphorus, Sulphur and Silicon and the Related Elements, 177(2) (2002) 447.

50. M. Nath and S. Goyal, Phosphorus, Sulphur and Silicon and the Related Elements, 177(4) (2002) 841.

51. M. Sharma , Phosphorus, Sulphur and Silicon and the Related Elements, 174 (2001) 239.

52. A. Phor, A. Chaudhary and M. Jain, Main Gr. Met. Chem., 24(7) (2001) 439.

53. M. Nath and S. Goyal, Synth. React. Inorg. Met-Org. Chem., 30(9) (2000) 1791.

54. M. S. Singh, and P. K. Singh, Main Gr. Met. Chem., 23(3) (2000) 183.

55. S. Belwal, R.V. Singh, and M.V. Voronkov, Russian J. Chem., 69(11) (1999) 1717.

56. M. S. Singh, and A. K. Singh, Ind. J. Chem. 38A (10) (1999) 1060.

57. M. Nath, S. Goyal, Synth. React. Inorg. and Met-Org. Chem., 28(5) (1998) 715.

58. S. Belwal, R. K. Saini, and R. V. Singh, Ind. J. Chem., 37A(3) (1998) 245.

59. R. Malhotra, S. Kumar, and K. D. Singh, Ind. J. Chem., 36A(4) (1997) 321.

60. R. K. Saini, and A. Kumar, J. Phy. Research, 10(1-2) (1997) 141.

61. D. Singh, R.V. Singh, and N. K. Jha, J. Inorg. Biochem. 62(1) (1996) 67.

62. M. A. Pujar, and K. Siddappa, National Academy Sci. Letters (India), 18(5&6) (1995) 99.

63. C. Saxena, and R.V. Singh, Synth. React. Inorg. and Met-Org. Chem., 22(8) (1992) 1061.

64. D. Singh, and R.V. Singh, Main Gr. Met. Chem., 13(5) (1990) 309.

65. M. R. Maurya , A. Kumar , M. Ebel and D. Rehder, Inorg. Chem. 45(15) (2006) 5924.